IMMUNOLOGICAL CHARACTERIZATION OF A PUTATIVE SERINE PROTEASE EXPRESSED IN ANTHERS OF *LILIUM LONGIFLORUM*

by

Andrew Alexander Taylor

A thesis submitted in conformity with the requirements
for the degree of Master of Science
Graduate Department of Botany
University of Toronto

© Copyright by Andrew Alexander Taylor 1997

National Library of Canada
Acquisitions and Bibliographic Services
395 Wellington Street
Ottawa ON K1A 0N4
Canada

Bibliothèque nationale du Canada
Acquisitions et services bibliographiques
395, rue Wellington
Ottawa ON K1A 0N4
Canada

Your file Votre référence

Our file Notre référence

The author has granted a non-exclusive licence allowing the National Library of Canada to reproduce, loan, distribute or sell copies of this thesis in microform, paper or electronic formats.

The author retains ownership of the copyright in this thesis. Neither the thesis nor substantial extracts from it may be printed or otherwise reproduced without the author's permission.

L'auteur a accordé une licence non exclusive permettant à la Bibliothèque nationale du Canada de reproduire, prêter, distribuer ou vendre des copies de cette thèse sous la forme de microfiche/film, de reproduction sur papier ou sur format électronique.

L'auteur conserve la propriété du droit d'auteur qui protège cette thèse. Ni la thèse ni des extraits substantiels de celle-ci ne doivent être imprimés ou autrement reproduits sans son autorisation.

0-612-28737-8

Canada

Immunological characterization of a putative serine protease expressed in anthers of *Lilium longiflorum*

by

Andrew Alexander Taylor

Master of Science, 1997
Graduate Department of Botany,
University of Toronto

An antiserum was generated which specifically recognizes the product of LIM9, an anther-specific gene from *Lilium longiflorum*. Immunoblotting and immunocytochemistry experiments indicate that the LIM9 protein appears during the late zygotene stage of microsporogenesis and accumulates until tetrad dissolution. Although it occurs within the microsporocytes and microspores, it is expressed predominantly within the cells of the surrounding tapetum. The mature protein is secreted into the locule where it coats the microspore tetrads.

Immunoblotting experiments suggest that the LIM9 gene encodes an 84kDa preproprotein which is posttranslationally modified to yield an 82kDa glycoprotein possessing complex glycans. Sequence homologies suggest that the mature LIM9 glycoprotein is a member of the subtilisin-like family of serine proteases. Preliminary electrophoretic functional assays provide empirical evidence supporting the LIM9 protein's identity as a protease.

Acknowledgments:

I would like to extend my sincere gratitude to my supervisor, Dr. C.D. Riggs for his guidance, trust and patience. I am also indebted to Dr. C.A. Hasenkampf and Dr. R. Dengler for their assistance with immunocytochemistry and tissue fixation, the use of their laboratory equipment, and their helpful suggestions.

The LIM9 cDNA and the xylose antiserum were generously donated by Dr. Satoshi Tabata and Dr. Arnd Sturm respectively. I would also like to acknowledge two years of financial support provided by a University of Toronto Open Fellowship.

I would like to thank my friends and colleagues Michelle Dookheran, Duane Mendis, Pat Manzerra, Lakshmi Tirupathipanayam, Hania Quraishi, and Scott Walsh. In particular, I wish to thank Annette Rzepczyk for her comments and, most importantly, for her encouragement and friendship.

I am especially grateful to my parents, Ronald and Jean Taylor, for their support through difficult times and their unending patience and understanding. It is to my parents that I dedicate this thesis.

Table of Contents:

List of Figures:

Abbreviations:

aa(s)	amino acid(s)
APS	ammonium persulphate
BCIP	5-Bromo-4-chloro-3-indoly-phosphate p-toluidine salt
bp(s)	base pair(s)
BSA	bovine serum albumin
β-SH	2-mercaptoethanol
°C	degrees Celcius
CCC	central cell cluster
cDNA	complementary DNA
DB	denaturation buffer
DIW	deionized water
DNA	deoxyribonucleic acid
EDTA	ethylenediaminetetraacetic acid
Endo H	endoglycosidase H
ER	endoplasmic reticulum
EtOH	ethanol
Fuc	fucose
g	grams/gravity
Glc	glucose
GlcNac	N-acetylglucosamine
G-phase	gap-phase
GTP	guanosine triphosphate
IgG(s)	γ-class immunoglobulin(s)
IMAC	immobilized metal affinity chromatography
HEPES	N-hydroxyethylpiperazine-N'-2 ethane sulfonic acid
kDa	kiloDalton
M	molarity
Man	mannose
µg	microgram
µl	microlitre

µm	micrometre
mg	milligrams
ml	millilitre
mm	millimetre
mM	millimolar
mRNA	messenger RNA
MW	molecular weight
MWCO	molecular weight cut off
NBT	nitroblue tetrazolium chloride
nm	nanometre
PEG	polyethylene glycol
PBS	phosphate buffered saline
poly(A) RNA	poly adenylated RNA
PMC(s)	pollen mother cell(s)
RNA	ribonucleic acid
rpm	revolutions per minute
rRNA	ribosomal RNA
SC	synaptonemal complex
SDS	sodium dodecyl sulphate
SDS-PAGE	SDS-polyacrylamide gel electrophoresis
SI	self-incompatibility
S-phase	DNA-synthesis phase
SRP	signal recognition particle
TBA	tertiary butyl alcohol
TEMED	N,N,N^1,N^1, tetra-methylenediamine
TM	trade mark
tRNA	transfer RNA
TTBS	Tween/Tris buffered saline
Tween 20	polyoxyethylenesorbitan monolaurate
V	volts
Xyl	xylose

Introduction:

I Meiosis and the Alternation of Generations:

Natural selection, the driving force of Darwinian evolution, is fueled by the diversity of form and behavior inherent to a population. Genetic exchange, by generating novel recombinations of genes from two parents, may increase phenotypic diversity within a population and thereby enhance its ability to adapt and evolve. In sexually reproducing organisms, these genetic recombinations occur during a special type of nuclear division known as meiosis. In contrast to the conservative nature of an asexual mitotic division, the two divisions of meiosis generate four genetically unique haploid cells from a single diploid parent cell. This halving of the chromosome number is a necessary prerequisite of syngamy or fertilization. At fertilization the fusion of two haploid sex cells or gametes restores the diploid state in the zygote, thereby conserving the chromosome number passed from parent to offspring.

The lifecycles of all sexually reproducing organisms consist of an alternation between the diploid and haploid state. Multicellularity can occur in one or both of these phases by the addition of mitotic divisions. In animals, multicellularity occurs only in the diploid phase. The gametes of animals are formed directly by the meiotic division of specialized diploid cells which are set aside as a germ line during embryogenesis. In contrast, meiosis in plants generates haploid spores which, through one to several mitotic divisions, become multicellular individuals known as gametophytes. Additional mitotic divisions within the gametophyte generate one or more gametes. This cycle of a diploid spore-producing (sporophytic) generation followed by a haploid gamete-

producing (gametophytic) generation is appropriately termed "the alternation of generations".

The life cycle of the seed plants is dominated by the sporophytic generation (Goldberg, 1988). The gametophytes are not free-living, but instead are housed and nourished within sporophytic structures termed sporangia (Esau, 1977). Perhaps the best documented evolutionary trend in terrestrial plants, this suppression of the gametophyte generation is most pronounced within the angiosperms, or flowering plants (Blackmore and Knox, 1990). The product of only two or three mitotic divisions of the haploid spore, the angiosperm gametophyte is dependent upon the sporophyte to the extent that it may be considered a "parasitic plantlet" (Dickinson, 1987). As in all seed plants, the sporophyte not only generates the reduced gametophytes, but is also the site of fertilization and embryogenesis. In angiosperms, each of these events occurs within a highly specialized structure termed the flower. Comprising more than 90% of the 275 000 known plant species (Raven *et al.*, 1986), the angiosperms may owe their success to this unique reproductive structure.

II Angiosperm Reproduction:

A The Angiosperm Flower:

The angiosperm flower is a modified shoot comprised of whorls of sterile and reproductive organs (each a modified leaf) borne on a shortened axis termed the receptacle. A flower is said to be complete if it consists of four whorls, as follows (Greyson, 1994). The outermost whorl, or calyx, is a collection of leaf-like sepals. Inward from this is a whorl of petals collectively termed the corolla. (When indistinguishable from one another, the sepals and petals are termed tepals). Together these sterile structures make up the perianth of the plant. An

essential component of the angiosperm flower, the perianth of most angiosperms has evolved elaborate forms and diverse patterns of pigmentation to attract animal pollinators (Weberling, 1989)

Enclosed within the perianth are the reproductive organs (sporophylls) of the flower. Angiosperms produce sexually dimorphic spores and are thus said to be heterosporous. Small microspores ultimately develop into microgametophytes (male gametophytes), while the larger megaspores develop into megagametophytes (female gametophytes). Hermaphroditic or "perfect" flowers generate both spore types. Microspores are produced in a whorl of stamens (microsporophylls) immediately interior to the petals. Collectively, the stamens form the androecium of the flower (Greyson, 1994). Each stamen consists of a lobed anther comprised of two or four sporangia (microsporangia) which is connected to the receptacle of the flower by a long thin stalk termed the filament. Megaspores are produced within the innermost whorl (gynoecium) of the flower in structures termed carpels (megasporophylls). Each sporangium (megasporangium) is encased by an integument to form a structure termed an ovule (Bold *et al.*, 1987). One or more ovules are contained within the base or ovary of each carpel. The tip of the carpel, termed the stigma, forms a receptive surface for microgametophytes. A columnar structure termed the style extends between the stigma and the ovary. In many angiosperms, the carpels fuse along their entire length to form a single structure termed a compound pistil or syncarpous gynoecium (Esau, 1977).

B The Angiosperm Life Cycle:

The megagametophyte or embryo sac of most angiosperms is comprised of seven cells (Jenson, 1973). The haploid egg cell (the female gamete) and two adjacent synergids form the "egg apparatus" at the micropylar end of the embryo

sac while at the opposite (chalazal) end of the embryo sac are three antipodal cells. These two groups of cells are separated by a large binucleate cell termed the central cell. The two "polar nuclei" of the central cell may fuse prior to fertilization, forming a single "secondary endosperm nucleus" (Esau, 1977). In the majority of angiosperms the megametophyte is monosporic in origin (Bold *et al.*, 1987). That is, the meiotic division of a megaspore mother cell or megasporocyte produces a chain of four haploid megaspores, all but one of which degenerate. The surviving megaspore undergoes three free-nuclear mitotic divisions to generate eight haploid nuclei which are then partitioned into seven cells (Bold *et al.*, 1987; Esau, 1977). In *Lilium* and *Fritillaria* however, the meiotic division of the megasporocyte nucleus is not accompanied by cytokinesis. The four haploid megaspore nuclei, contained within a common cytoplasm, collectively contribute to the formation of the megasporangium, which is thus said to be tetrasporic in origin. Following the fusion of three of these nuclei, three rounds of mitosis generate four triploid nuclei and four haploid nuclei. Cell wall formation produces an embryo sac comprised of three triploid antipodal cells, two haploid synergids, a haploid egg cell, and a central cell containing one haploid nucleus and one triploid nucleus (Bold *et al.*, 1987; Esau, 1977). [Other variations also occur, such as the embryo sac of *Allium* which is bisporic in origin (Maheshwari, 1950)].

Within the anther, numerous microsporocytes or pollen mother cells (PMCs) divide meiotically to generate tetrads of haploid microspores. Following their release from the tetrads, each of the microspores undergoes an asymmetric mitotic division which yields a generative cell completely enclosed within a vegetative cell (Jenson, 1973). The microgametophyte or pollen grain is typically shed from the anther at this two-celled stage. During its short autonomous existence, the microgametophyte serves as a vehicle for the transport of sperm

cells to the sessile megagametophyte, the site of fertilization and embryogenesis. The transfer of pollen to the gynoecium (pollination) is accomplished by wind or animal pollinators. Contact with the stigma of a compatible flower stimulates the growth of a pollen tube from an aperture in the pollen wall. The pollen tube, containing the generative cell and vegetative cell nucleus, penetrates between cells of the stigma and elongates through the style until it reaches the embryo sac. Prior to reaching the embryo sac, the generative cell divides mitotically into two sperm cells (male gametes). [While this second division usually occurs within the pollen tube, in approximately 30% of angiosperm species it can occur prior to the pollen's release from the anther (Brewbaker, 1967)].

The pollen tube enters the embryo sac, usually through an opening termed the micropyle (Jenson, 1973), and its contents are discharged. While the vegetative cell nucleus degenerates, the sperm cells participate in a process unique to the angiosperms. Termed "double fertilization", one of the sperm cells fuses with the haploid egg cell to produce a diploid zygote while the nucleus of the second sperm cell fuses with the polar nuclei or secondary endosperm nucleus of the central cell to form a triploid (most species) or pentaploid (*Lilium* and *Fritillaria*) primary endosperm nucleus (Esau, 1977). The zygote develops into a histologically complex embryo possessing the axial meristems and rudimentary body plan of the adult sporophyte (Sussex, 1989). Mitotic divisions of the primary endosperm nucleus generate a nutritive polyploid tissue, the endosperm, surrounding the embryo. (The other cells of the megagametophyte rapidly degenerate). The integument of the ovule develops into a durable seed coat, while surrounding tissues of the ovary form the fruit. Safely packaged, the embryo may remain dormant for an extended period of time. When environmental conditions are favorable, the embryo will develop into an independent sporophyte and complete the life cycle.

III An Introduction to the Anther:

Of all floral organs, the anther has attracted the greatest scientific interest and is the best studied component of the flower (Greyson, 1994). Androgenesis in the flowering plants has been investigated for more than 30 years by classical techniques of cytology, cytochemistry, and (to a lesser extent) biochemistry (Scott *et al.*, 1991). Beyond its agricultural significance, pollen development within the anther is a relatively simple system in which many fundamental biological processes can be studied with relative ease. These include: cell differentiation; meiosis; cell communication; and the establishment and maintenance of cellular domains leading to the polarization of cells (Bedinger, 1992). The recent application of molecular biological techniques to the study of microsporogenesis is likely to make far-reaching contributions to the field of biology as a whole.

A Phylogeny and Morphology:

The microsporophyll or stamen is comprised of a fertile anther supported and nourished by a sterile filament. Evolutionary reduction produced the thin single-veined stamen from a wider three-veined leaf-like sporophyll still present in some primitive dicotyledons today (Esau, 1977). The anther evolved through the fusion of sporangia on the surface of this leaf-like archetype. The anthers of most angiosperms are tetrasporangiate. They consist of two lobes, or thecae, each in turn comprised of two pollen sacs (microsporangia). Each pollen sac consists of several concentric wall layers surrounding a central fluid-filled cavity termed the locule (Esau, 1977). The locules contain sporogenous cells which will ultimately give rise to mature pollen grains.

B Histology:

The anther consists of six functionally distinct sterile tissues (Goldberg *et*

al, 1993). The sterile tissues protect and nourish the developing microgametophytes and coordinate anther dehiscence (the spontaneous release of the mature pollen). At the centre of the anther is the connective tissue. Comprised of undifferentiated parenchyma cells, this tissue forms the "intersporangial septum" between adjacent pollen sacs of the same theca and binds the thecae to the filament (Bonner and Dickinson, 1989). Within each septum, specialized cells may form what is termed a circular cell cluster (CCC) (Goldberg *et al*, 1993). Centered within the connective tissue is a single vascular bundle. The xylem and phloem of this bundle are continuous with that of the filament and serve to transport water and nutrients into the anther.

The epidermis, endothecium, middle layer(s), and tapetum constitute the wall of the microsporangium. The epidermis or exothecium is the outermost wall layer of the anther. The cuticle, a waxy covering on the outer surface of these cells, protects the anther from desiccation. Two columns of small isodiametric epidermal cells termed stomial cells may run the length of the anther overlying the intersporangial septae. The stomial cells, the endothecium (immediately beneath the epidermis), and the CCCs cooperate to form the stomium, a slit-like opening through which the mature pollen is shed from each theca (see below). Beneath the endothecium are one or more seemingly unspecialized cell layers, collectively termed the middle layers. These wall layers are compressed by adjacent tissues as the anther matures and may completely degenerate prior to dehiscense.

The tapetum forms the lining of the locule and is the only sterile tissue in direct contact with the sporogenous cells. This highly specialized secretory layer may take one of three forms. A secretory or glandular tapetum consisting of a continuous layer of cells lining the locule, is the most common form among angiosperms. Tapetal cells of this type remain associated with the wall of the

anther throughout its development. Alternatively, an amoeboidal tapetum may occur during sporogenesis with amoeboid tapetal cells migrating into the locule and penetrating between the developing microspores. A plasmodial tapetum results if the walls of these amoeboid cells disintegrate (Weberling, 1989).

IV Anther Development:

The development of the diverse sterile tissues of the anther is intimately linked with the development of the male gametophyte. Goldberg *et al* (1993) suggest that anther development can be conveniently divided into two phases. The first phase consists of a "histospecification program" in which tissue differentiation is completed and meiosis within the sporogenous tissue generates haploid microspores. A "cell degeneration and dehiscence program" follows in which microspores undergo mitosis to yield pollen grains which are shed by the coordinated breakdown or desiccation of sterile anther tissues. Mitotic divisions accompany the growth of the anther during the first phase of development, while anther growth during the second phase is simply the result of cell enlargement. The maturation and dehiscence of the anther is depicted in Figure 1.

A Phase I: Anther Histogenesis and Microsporogenesis:

i) Anther Histogenesis:

In response to environmental or developmental stimuli, flower evocation initiates a program of "coordinately executed morphological changes" that generates the highly complex structure of the flower from the simple vegetative shoot apex (Scott *et al.*, 1991). The vegetative meristem ceases its indeterminate reiterative leaf forming activity and, as a floral meristem, generates a limited

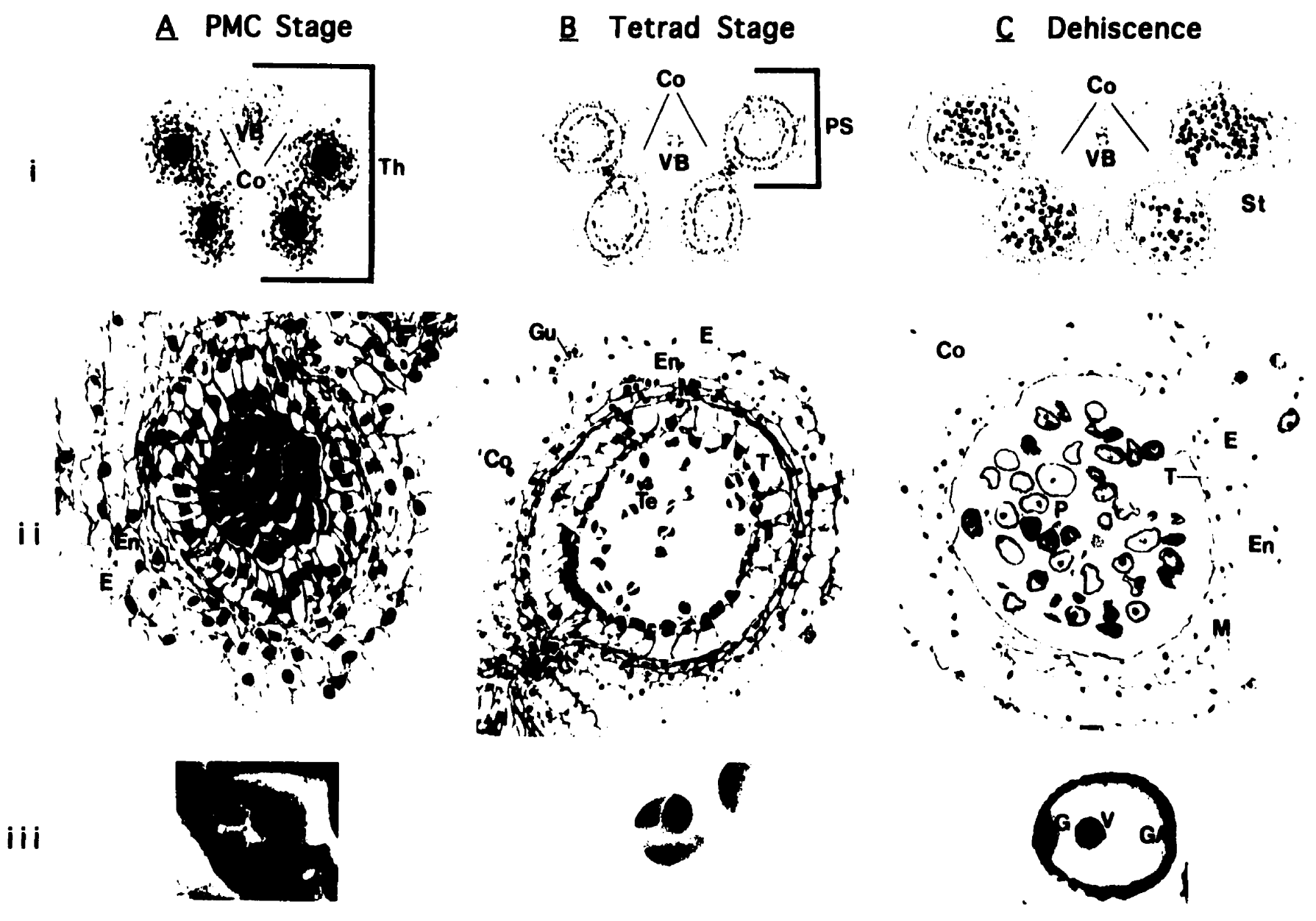
A PMC Stage
B Tetrad Stage
C Dehiscence
i
ii
iii
VB
Co
Th
PS
St
Gu
E
En
M
T
Te
P
G
V

Figure 1 **Anther maturation in *Lilium longiflorum* (var. Enchantment).** The morphology of the anther (i), the histology of the pollen sac (ii), and the cytology of the microsporocytes, microspores, and pollen (iii) are shown in transverse sections of anthers from three developmental stages (stained with Toluidine Blue). Following anther histogenesis, microsporocytes (pollen mother cells) develop from the sporogenous tissue. Prior to the initiation of meiosis, the microsporocytes contain several nucleoli and their metabolically active cytoplasm stains darkly (**A**). Each microsporocyte undergoes meiosis to yield a tetrad of haploid microspores surrounded by callose (**B**). At this stage the tapetum and endothecium are prominent components of the anther wall. By dehiscence (**C**), the tapetum has degenerated and the microspores have undergone mitosis to yield two-celled pollen grains. Sporopollenin (green) lines the remnants of the tapetum and comprises the exine of the pollen. The exine layer is thin or absent at germinal apertures, where the pollen tube will emerge upon germination. The cells of the epidermis have expanded between adjacent pollen sacs, but have degenerated elsewhere. Mature pollen grains are shed from each theca through the stomium, an opening produced by the enzymatic degradation of cells within the intersporangial septum and mechanical forces generated within the anther wall. **Co**, connective; **CCC**, circular cell cluster; **E**, epidermis; **En**, endothecium; **G**, generative cell; **GA**, germinal aperture; **M**, middle wall layers; **P**, two-celled pollen grain; **PMC**, pollen mother cells (microsporocytes); **PS**, pollen sac (microsporangium); **Gu**, guard cell of stoma; **St**, stomium; **T**, tapetum; **Te**, tetrad of microspores; **Th**, theca; **V**, vegetative cell nucleus; **VB**, vascular bundle.

sequence of morphologically and functionally distinct floral organs (Sussex, 1989). The stamen primordia make their appearance as a circle of small bumps initiated by the elongation and periclinal division of subepidermal cells. The initial longitudinal growth of the stamen primordia proceeds from a subapical initial cell. Rows of submarginal initial cells then differentiate on the lateral faces of the primordia, taking over its lateral growth and defining the anther and filament compartments (Weberling, 1989). Although the filament differentiates early during stamen development, it remains short during anther development and often does not reach its full length until after the flower has opened (Weberling, 1989).

The shoot apical and floral meristems of higher plants are comprised of three superimposed 'germ' layers: a superficial L1 layer; a subsurface L2 layer; and a deeper L3 layer (Satina *et al.*, 1940) (Figure 2 and Figure 3). The lineage of each of the anther's various tissues has been traced to these three layers through the study of genetic chimeras in which one of the initial layers is polyploid or albino (e.g. Satina and Blakeslee, 1941). The differentiation of cells from these layers appears to be position dependent and not lineage dependent. Cells displaced from one 'germ' layer into another layer inherit this second layer's developmental future (Sussex, 1989). Although cell commitment does not occur until late in development (Sussex, 1989), unique and precisely timed histodifferentiation events appear to occur within specific regions established early in anther development (Goldberg *et al.*, 1993).

Cells from the L1 layer or protoderm come to form the epidermis of the anther. In some anthers, stomial cells form between adjacent pollen sacs to demarcate where the anther will open during dehiscence (Bonner and Dickinson, 1989). As epidermal divisions are restricted to the anticlinal plane, the morphology of the anther is the product of differential mitosis and cell

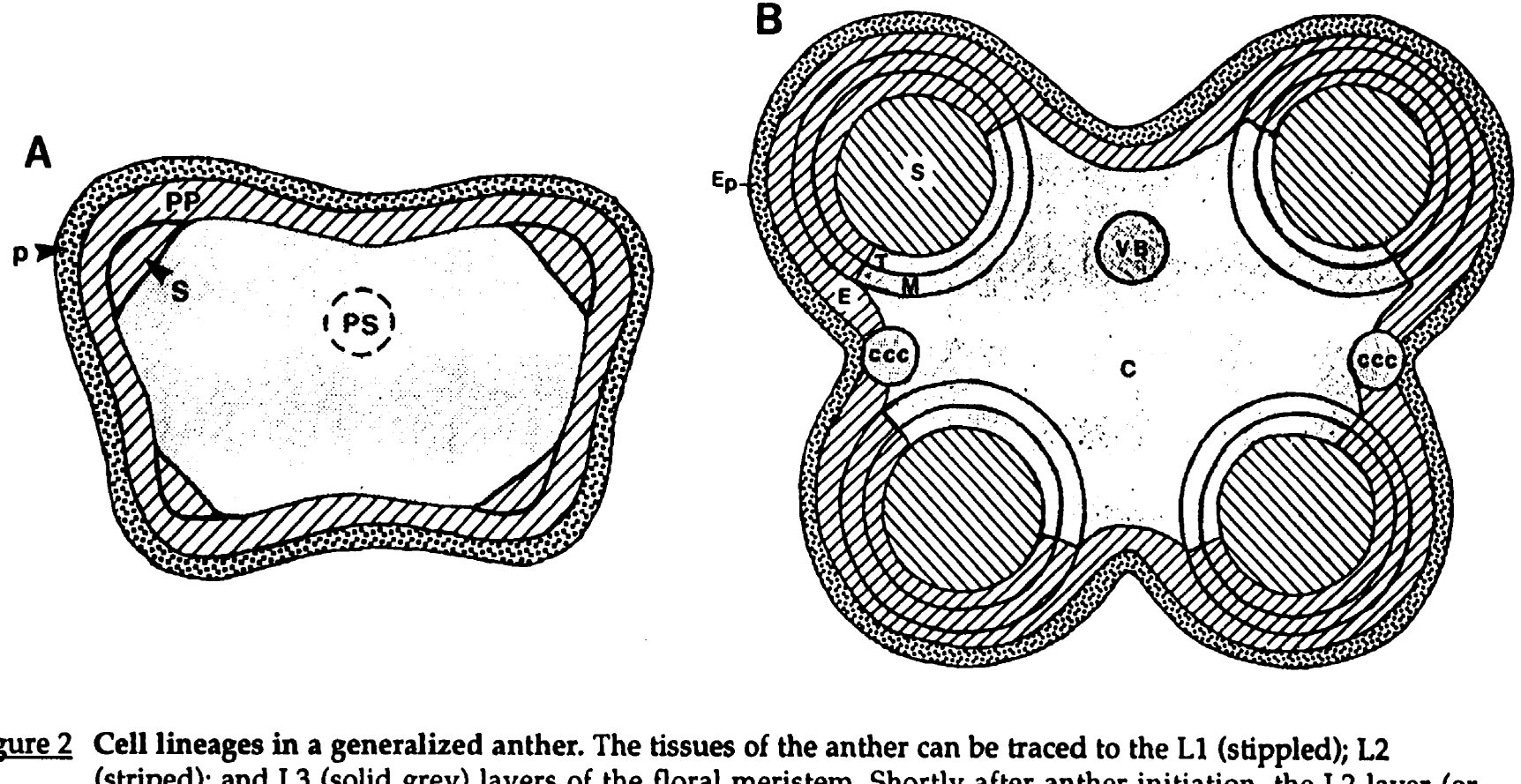

Figure 2 **Cell lineages in a generalized anther.** The tissues of the anther can be traced to the L1 (stippled); L2 (striped); and L3 (solid grey) layers of the floral meristem. Shortly after anther initiation, the L2 layer (or hypoderm) gives rise to a column of one or more archesporial cells within each corner of the anther. These divide periclinally to generate an outer primary parietal layer and an inner sporogenous layer (cross-section **A**). Derivatives of the primary parietal layer form the outer portion of the anther wall in the mature anther (**B**) while the sporogenous tissue gives rise to the microsporocytes (pollen mother cells). The inner portion of the anther wall, the CCCs, the connective tissue, and the tissues of the vascular bundle are derived from the L3 layer. The epidermis is derived from the L1 layer (or protoderm). **C**, connective; **CCC**, circular cell cluster; **E**, endothecium; **Ep**, epidermis; **M**, middle layers; **p**, protoderm; **PP**, primary parietal layer; **PS**, procambial strand; **S**, sporogenous layer/tissue; **T**, tapetum; **VB**, vascular bundle.

Figure 3 **Anther histogenesis in monocotyledonous plants.** The tissues of the anther are derived from three cell layers (L1, L2, and L3) present in the anther primordia. The innermost portions (towards the vasculature) of the tapetum and middle wall layers are derived from the L3 layer while the outermost portions of these tissues are derived from the L2 layer. All other tissues are derived from a single 'germ' layer. Many of the anther's tissues ultimately degenerate as part of the dehiscence program. The stomial cells define the longitudinal slit (stomium) through which the pollen grains are shed. The middle wall layers may be crushed, or (as in *Lilium*) remain intact at dehiscence (modified from Goldberg *et al.*, 1993).

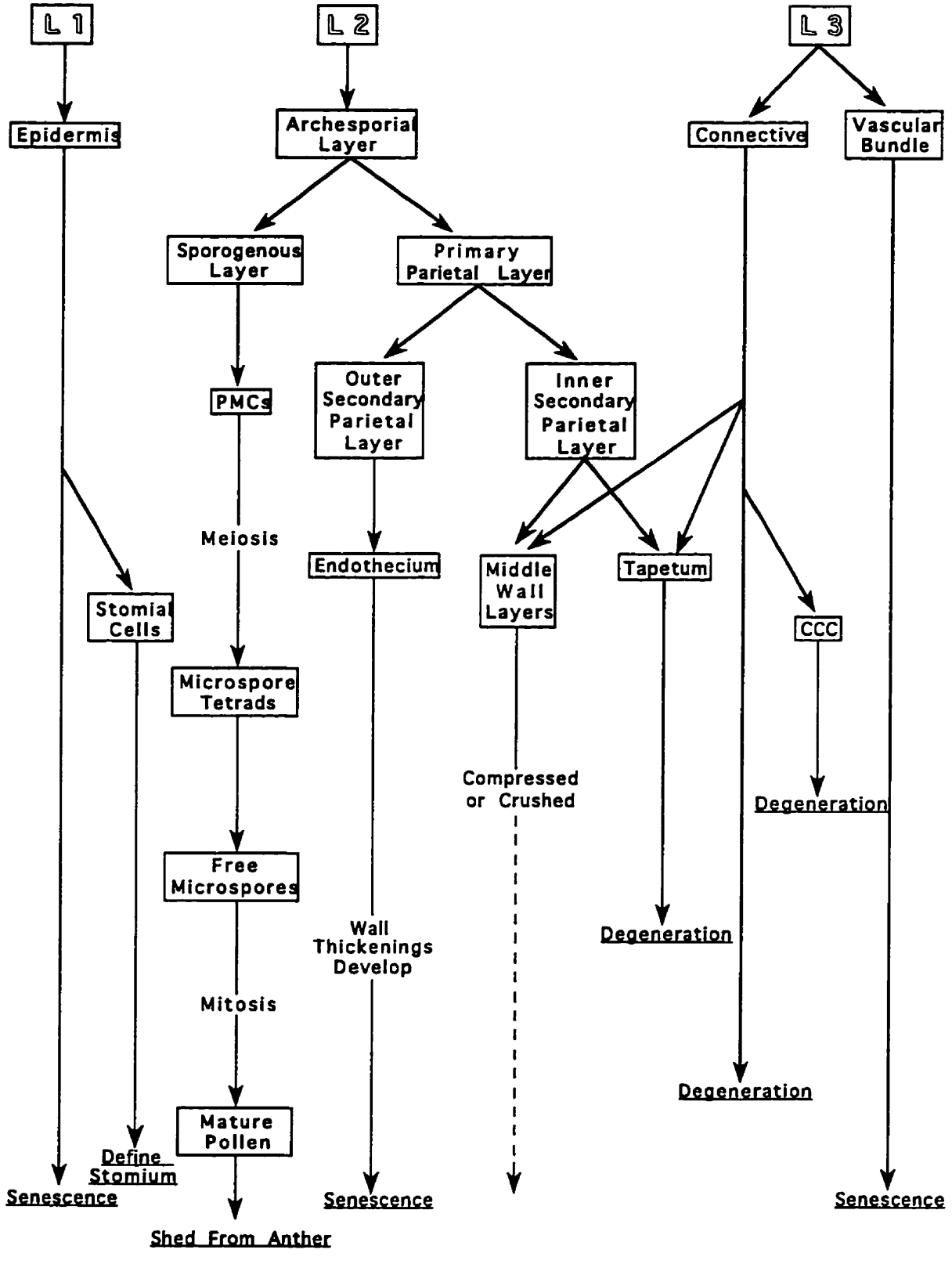
L 1
L 2
L 3
Epidermis
Archesporial Layer
Connective
Vascular Bundle
Sporogenous Layer
Primary Parietal Layer
PMCs
Outer Secondary Parietal Layer
Inner Secondary Parietal Layer
Meiosis
Endothecium
Middle Wall Layers
Tapetum
Stomial Cells
CCC
Microspore Tetrads
Compressed or Crushed
Degeneration
Free Microspores
Wall Thickenings Develop
Degeneration
Mitosis
Degeneration
Mature Pollen
Define Stomium
Senescence
Senescence
Senescence
Shed From Anther

enlargement within the hypodermal layers (Raghavan, 1988).

Within each of the four corners of the anther primordium, cells of the L2 layer (hypoderm) differentiate to form a column of archesporial initials (Raghavan, 1988; Scott, 1993). These initials divide periclinally to produce a primary parietal layer directly beneath the epidermis and a deeper primary sporogenous layer. The primary parietal layer divides again to form two secondary parietal layers between the epidermis and the primary sporogenous layer (Esau, 1977). In the dicotyledons, the outermost of these two layers divides to form the endothecium and one or more middle layers while the inner secondary parietal layer becomes the outer tapetum. In the monocotyledons, the outer secondary parietal layer becomes the endothecium directly while the middle layer(s) and the tapetum are derived from a division of the inner secondary parietal layer (Davis, 1966). The archesporial cells of the primary sporogenous layer undergo several asynchronous rounds of mitosis, the completion of which yields microporocytes (PMCs) (Scott, 1993). Meiosis follows and generates four microspores from each of these cells (see below).

The L3 layer gives rise to the connective and vascular tissues of the anther as well as the circular cell clusters. The L3 layer also forms the inner portions (towards the vasculature) of the middle wall layers and the tapetum. The differentiation of the middle layers and the tapetum from two separate 'germ' layers is likely orchestrated by precise cell-to-cell communications (Goldberg *et al.*, 1993). The cytology of the inner and outer tapetal cells, however, may differ appreciably as a result of their different histories (Polowick and Sawhney, 1993).

ii) Microsporogenesis:

Sporogenous cells exhibit peculiarities several divisions prior to the onset of meiosis. A progressive prolongation of mitotic S-phase, for example, has been observed in *Triticum* (Bennett *et al.*, 1973) and *Lilium* (Stern and Hotta, 1967). In

many angiosperms, meiosis is initiated synchronously throughout the thousands of microsporocytes within the separate locules and anthers of a floral bud or floret (Heslop-Harrison, 1966a). This synchrony is imposed by a developmental hold that accumulates the sporogenous cells at G_1 of the interphase immediately preceding meiosis (Bennett *et al.*, 1973). The factors responsible for this developmental hold also appear to act on the tapetal cells, causing them to become synchronized at G_1 of (mitotic) interphase within a few hours of the sporogenous cells (Scott *et al.*, 1991). The tapetal and sporogenous cells are released from G_1 and initiate DNA synthesis simultaneously (Scott *et al.*, 1991).

Potential microsporocytes and tapetal cells are in direct contact with one another and presumably share programs of gene expression. The controlling elements determining whether a cell will enter meiosis or mitosis must therefore be extremely precise and rigidly controlled. Experiments in which microsporocytes were explanted from *Lilium* anthers at different stages of development and cultured *in vitro*, suggest that by premeiotic G_2 the microsporocytes are irreversibly committed to meiosis (Stern and Hotta, 1967; Ito and Takegami, 1982). As S-phase commences, both the tapetal cells and microsporocytes develop enlarged nuclei with conspicuous regions of condensed chromatin (Dickinson, 1987). However, nuclear vacuoles (caused by the invagination of the inner membrane of the nuclear envelope) appear only within the microsporocytes and are the first structural features distinguishing these cells from the cells of the tapetum (Sheffield *et al.*, 1979).

The chromosomes of the microsporocytes condense dramatically as the first division of meiosis (meiosis I) is initiated. Recombination and many of the other events unique to meiosis occur during the five substages of this division's prolonged prophase. During leptotene, the first substage of prophase I, the ends

of the chromosomes, or telomeres, attach to the nuclear envelope. The chromosomes condense further and the telomeres are drawn together into a single region of the nuclear envelope producing a so-called "bouquet structure" of chromosomes during the second substage, zygotene. Homologous chromosomes become tightly bound (synapsed) along their entire length by a structure termed the synaptonemal complex (SC). The bouquet formation dissolves at the close of zygotene and the homologue pairs (bivalents) disperse over the nuclear surface (Dickinson, 1987). During pachytene (substage 3), recombination occurs as homologues exchange segments and generate new combinations of alleles. As the cells enter the fourth substage, diplotene, the SC begins to disintegrate. It remains intact in the regions at which recombination occurred, however, possibly contributing to chiasmata formation. Through diplotene and diakinesis (the final substage of prophase I) the chromatin condenses further. Diakinesis ends as the nuclear envelope disintegrates.

Metaphase I of meiosis begins as fibers of the spindle invade the region formerly occupied by the nucleus and bind to the centromeres of the chromosomes. The bivalents are aligned along the metaphase plates with their homologous chromosomes attached to spindle fibres originating at opposite poles. Homologous chromosomes separate and are pulled to opposite poles during anaphase I. In some cases, the chromosomes decondense completely and become temporarily surrounded by new nuclear membranes during telophase. A cell wall may form resulting in a dyad of two diploid cells. A brief interphase may follow, but DNA replication does not occur. The second division of meiosis (meiosis II) resembles a mitotic division and generates a tetrahedral or tetragonal tetrad of haploid microspores (Esau, 1977).

Prior to the onset of meiosis, plasmodesmata connect the compactly arranged microsporocytes to one another and to the cells of the tapetum. These

connections are severed early in prophase I of meiosis as the microsporocytes deposit a wall of callose (a β-1,3-glucan polymer) between their plasma membrane and their original cellulosoic wall. The original cell walls are degraded and the sporocytes remain encapsulated by a thick layer of callose throughout meiosis. Although direct connections with the tapetum are lost, the microsporocytes remain connected to one another by cytoplasmic bridges (cytoplasmic or cytomictic connections) 1.0 to 1.5μm in diameter (Heslop-Harrison, 1966a,b), large enough to permit the passage of organelles (Polowick and Sawhney, 1992). Electrophysiological techniques have revealed these connections to be low-resistance junctions (e.g., Spitzer, 1970). By allowing the rapid transport of nutrients and growth substances, this cytoplasmic continuity is thought to maintain the synchrony of meiosis (Esau, 1977). The cytoplasmic connections between microsporocytes remain until metaphase I. Cytokinesis and the deposition of additional callose then completely isolates these cells from one another. By the completion of meiosis, the entire tetrad and each of its individual microspores is enveloped in callose.

Callose deposition occurs in all angiosperm anthers and appears to be a critical aspect of microsporogenesis, although its precise role remains unclear (Scott *et al.*, 1991). Several theories have been advanced, including that the callose wall may act as a mould for exine formation (see below); callose production provides a mechanism for generating separate cells following meiosis (Larson and Lewis, 1962); callose acts as a barrier or 'molecular filter' (Heslop-Harrison, 1966b); and the hygroscopic nature of callose may protect the sporocytes from drought stress (Bhandari, 1984). The callose wall may even act as a barrier preventing the transmittance of viruses from the sporophytic generation to the gametophytic generation (Heslop-Harrison, 1980).

B Phase II: Pollen Maturation and Anther Dehiscence:

i) Maturation of the Pollen Protoplast:

Following telophase of meiosis II, the microspores are released from the tetrads by the action of callase (a β-1,3 endo- and exo-glycosidase complex) secreted by the tapetum (Stieglitz, 1977). The microspores (now termed "free microspores") grow rapidly at first (in *Lilium*, the spores increase three-fold in volume within 24 hours of release; Mascarenhas, 1975). Growth slows as autophagic vacuoles significantly reduce the volume of cytoplasm in the microspores during the ensuing 'vacuolate stage'. New cytoplasm is generated and numerous plastids differentiate into amyloplasts to store newly synthesized starch. Much of this starch is hydrolysed during the formation of the pollen wall (see below) (Pacini, 1990). The free microspore stage of pollen development draws to a close as the growth of a large central vacuole partitions the majority of the microspore's organelles into what will become the cytoplasm of the vegetative cell.

The asymmetric mitotic division of the microspore to generate a small generative cell and a larger vegetative cell is a determinative division as it yields two cells with very different fates (Horvitz and Herskowitz, 1992). The spindle-shaped generative cell nucleus is initially displaced toward the pollen wall and, along with its small volume of cytoplasm, is separated from the vegetative cell by the establishment of a hemispherical cell wall. The cell wall lengthens to encircle the generative cell which detaches from the pollen wall and becomes completely surrounded by the cytoplasm of the vegetative cell. The generative cell wall (with plasmodesmata) persists in some species but is lost in others. In species in which the cell wall disappears, the generative cell is delimited only by two plasma membranes (Esau, 1977). As occurred in the microspore, vacuolation of the vegetative cell consumes about 50% of its cytoplasm. New cytoplasm is

again generated and a second amylogenesis occurs. In some species this starch is entirely consumed during the final maturation or "ripening" of the pollen, while in others (e.g. *Lilium*) some of this starch remains at dehiscence (Pacini, 1990). The pollen grain is shed from the anther in a highly dehydrated state and remains metabolically inactive until rehydrated on the stigmatic surface.

ii) Assembly of the Pollen Wall:

Perhaps the most distinctive feature of the pollen grain is its complex and remarkably durable wall. This unique structure typically consists of two layers, an inner intine and an outer exine. The intine is largely pectocellusoic (Knox, 1984) while the exine is composed mainly of sporopollenin, a chemically resistant substance formed by the oxidative polymerization of carotenoids and carotenoid esters (Shaw, 1971). The exine can be further divided into an inner nexine and an outer sexine. The sexine may be sculpted into elaborate species-specific patterns. In localized regions termed germinal apertures, the entire exine layer is thin or absent. These apertures permit the passage of the pollen tube during pollen germination and also permit the pollen grain to expand or contract in response to changes in humidity (Walker, 1974).

The formation of the pollen wall is initiated while the microspores are still enclosed by callose within the tetrads. A fibrillar matrix termed the primexine (glycocalyx) is deposited by the microsporocyte protoplast on the outer surface of the plasma membrane (Heslop-Harrison, 1971; Rowley, 1973). The primexine appears to provide a matrix of receptors for the deposition of the exine. The distribution of these primexine elements on the plasma membrane may ultimately coordinate the species-specific surface patterning seen on the mature pollen grain. During the deposition of the primexine, stacks of endoplasmic reticulum (ER) cisternae occur immediately beneath the plasma membrane at the future sites of pore formation. The presence of the cisternae

may inhibit the production of a primexine in these regions and thus prevent the deposition of an exine layer (Blackmore and Barnes, 1990). [These domains may be established as early as meiosis as they often correlate with the position of the meiotic spindle poles (Bedinger, 1992)]. When released from the tetrads, the microspores possess a minimal exine constructed using precursor molecules derived solely from the microspore protoplast. The majority of exine deposition, however, occurs during the ensuing free-microspore stage using precursor molecules contributed mainly by the tapetum (McCormick, 1993) (see below).

Construction of the intine does not commence until deposition of the exine is well underway. The last wall layer to be completed, the intine may not attain its final thickness until after the first mitotic division of the pollen grain (Scott *et al.*, 1991). The intine is assembled between the exine and plasma membrane by the microspore protoplast (likely by the fusion of Golgi-derived vesicles with the plasma membrane) and consists of microfibrils of cellulose held together by a matrix of pectic materials and hemicelluloses (Mascarenhas, 1975).

In addition to structural components, the microspore and tapetum also contribute proteins to the pollen wall. Acid phosphatases, ribonucleases, esterases, amylases and proteases are among the hydrolytic enzymes contributed to the matrix of the intine by the microspore. These enzymes are especially concentrated in the region of the germinal apertures, where they are easily solubilized and released during rehydration of the pollen grain (Knox and Heslop-Harrison, 1970). Proteins contributed by the tapetum occur within cavities of the sexine or as a component of the "pollen coat" (see below).

iii) Anther Dehiscence:

The "dehiscence program", a sequential destruction of specific anther cell types, is initiated after the formation of microspore tetrads and is coordinated temporally with the process of pollen differentiation (Goldberg *et al.*, 1993). The

coordinated breakdown of the anther ultimately effects the release of the mature pollen grains. Although some anthers shed their pollen through discrete pores (poricidal dehiscence), the majority dehisce by splitting lengthwise and are said to possess a longitudinal mode of dehiscence (Weberling, 1989). Longitudinal dehiscence is preceded by the degeneration of the intersporangial septae and the subsequent fusion of adjacent locules within each theca. The contents of each theca are then emptied through the stoma, a slit-like opening produced by mechanical forces generated within the epidermis and endothecium.

The fusion of adjacent locules is accomplished by the enzymatic degradation of the circular cell clusters. In tomato (Bonner and Dickinson, 1989) and tobacco (Goldberg *et al.*, 1993) the cells of the CCC have each acquired a single large calcium oxalate (druse) crystal by the completion of microsporogenesis. The accumulation of calcium oxalate in the cells may trigger the activation of hydrolytic enzymes (Bonner and Dickinson, 1989). Alternatively, the crystals may provide an indirect means of osmoregulation (Raven and Smith, 1976) or of maintaining an optimal pH for enzymatic activity (Bonner and Dickinson, 1989). However regulated, enzymatic activity dissolves the middle lamellae between adjacent cell walls, causing the cells of the CCC to dissociate from one another (Keijzer, 1987a). The cells become devoid of cytoplasm and their walls thin dramatically (Bonner and Dickinson, 1989). The circular cell clusters may completely degenerate to form a large lacuna within each septum or, as in *Lilium*, the degraded cells may simply form a line of weakness at which the septum will eventually rupture (Keijzer, 1987a). If a lacuna forms, the swelling of the locule contents as the pollen expands may be sufficient to break the degenerated tapetum and middle wall layers and cause the fusion of adjacent pollen sacs. In anthers which do not develop intersporangial lacunae, these cell

layers are ruptured just prior to dehiscence as the anther wall bends inwards (Keijzer, 1987a; see below).

The progressive breakdown of the intersporangial septae is accompanied by dramatic changes in the anther wall. The epidermis may desiccate and degenerate completely. In *Lilium* and others, the cells of the epidermis expand immediately surrounding the stomial cells despite degeneration elsewhere. The cells of the endothecium develop conspicuous U-shaped secondary wall thickenings along their inner tangential walls (giving the endothecium its alternate name of fibrous layer). These large cells may comprise the majority of the anther wall at maturity. Prior to anthesis (i.e. the opening of the flower), the cells of the endothecium (and epidermis if present) swell tangentially (Keijzer, 1987a). The reinforced inner walls of the endothecium resist the expansion, however, causing the anther wall to bend inward. The wall ruptures between the small stomial cells, forming the stomium. Following anthesis, the wall dehydrates, causing the cells of the epidermis and endothecium to contract. The strengthened inner walls of the endothecium contract to a lesser extent than the outer walls causing the entire anther wall to peel back from the stomium and expose the mature pollen grains (Keijzer, 1987a).

V The Role of the Tapetum in Pollen Development:

The tapetum is a consistent feature of the anthers of higher plants (Scott *et al.*, 1991). Its development and degeneration appear to be precisely coordinated with many events of microsporogenesis and pollen development (Figure 4). Mariani *et al.* (1990) expressed a cytotoxic gene specifically within the tapetum of transgenic *Brassica* anthers and found that the resultant premature destruction of this layer arrested pollen development. Likewise, several natural mutations

Figure 4 **Pollen generation and the development of the tapetum.** Mitotic divisions of the sporogenous cells generate diploid microsporocytes or PMCs (**a**). The walls of these cells are replaced by a layer of callose (grey) as meiosis commences (**b**). Callose deposition severs plasmodesmata between the microsporocytes and the cells of the surrounding tapetal layer. However, plasmodesmata continue to interconnect the tapetal cells, which may become multinucleate at this stage (**i**). Meiosis in the microspocytes generates tetrads of haploid microspores invested by a thick layer of callose (**c**). The tapetal cells become highly vacuolate and large openings develop in their radial walls, turning the cell layer into a syncytium (**ii**). Callase secreted by the tapetum causes the breakup of the tetrads. The free microspores (**d**), possess a rudimentary exine layer (asterisks) and develop autophagic vacuoles within their cytoplasm. Orbicules form beneath the inner tangential and radial walls of the tapetal cell (**iii**) and are released into the locule by the breakdown of the tapetal cell walls. Sporopollenin secreted by the tapetum forms the majority of the mature sculpted exine (black) of the pollen wall (**e**). Germinal apertures occur where the exine layer is thin or absent. The complete degeneration of the tapetum (**iv**) releases stored substances (pollenkitt) into the locule. Pollenkitt and tapetal cell debris (tryphine) coat each pollen grain, forming the pollen coat. The mature two-celled pollen grain is released from the anther. Upon landing on a receptive stigma, the pollen grain germinates. A pollen tube, enclosed by an extension of the intine (grey), grows from the germinal aperture. Within the pollen tube, the generative cell divides to form two sperm cells. This final division generates the mature three-celled male gametophyte (**f**).

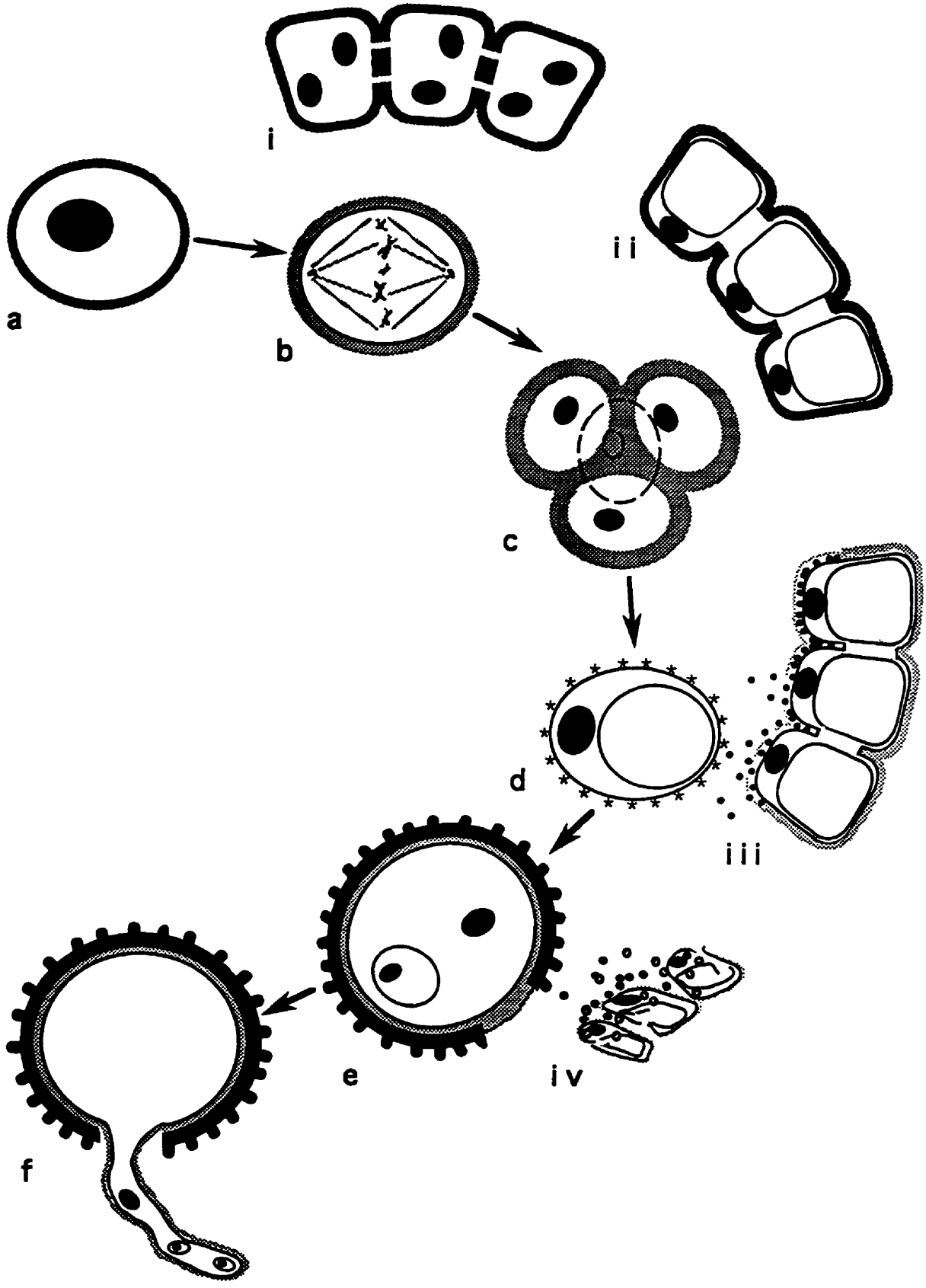
i
ii
a
b
c
d
iii
e
iv
f

affecting tapetal cell metabolism have been found to cause male-sterility (e.g. Graybosch and Palmer, 1988; Kaul, 1988). While these observations suggest an important role for the tapetum in microsporogenesis, very few precise functions of the tapetum have been identified (Scott *et al.*, 1991).

During meiosis in the microsporocytes, mitotic divisions unaccompanied by cytokinesis may generate tapetal cells which are binucleate or multinucleate. In some species, endoreplication within the tapetal cells may raise the ploidy number as high as 32n (Chapman, 1987). The resultant replication of gene sites likely serves to increase the number of transcripts sent to the cytoplasm. Abundant rough ER, dictyosomes and vesicles suggest that the cytoplasm of the tapetal cells is highly synthetic or ergastoplasmic (Chapman, 1987). Indeed, the tapetum is known to synthesize all major classes of organic compounds (Mascarenhas, 1990a).

The cells of the tapetum are highly polarized, often by the development of a large vacuole which displaces the cytoplasm and nucleus towards the locule (e.g. Wang *et al.*, 1992a). Secretory vesicles accumulate along the locular wall and their contents are emptied into the locule. Secretion peaks shortly after the break-up of the microspore tetrads (Schrauwen *et al.*, 1996), at which time the cellulose matrix of the locular walls may loosen or dissolve completely to facilitate the release of materials (e.g. Polowick and Sawhney, 1993). The nature of the compounds secreted into the locule by the tapetum has implicated this cell layer in many important aspects of microsporogenesis.

A Nutrition of the Sporogenous Tissue:

The tapetum is the only sporophytic tissue in direct contact with the sporogenous tissue. While connected to the microsporocytes by plasmodesmata, the tapetal cells may nourish the meiocytes in a manner analogous to that of

mammalian nurse cells (Bedinger, 1992). The tapetum may also generate or process the factors which initiate the synchronous meiosis of the microsporocytes. Microsporocytes extracted from the anther after the leptotene-zygotene phase (about the time that the tapetal-microsporocyte plasmodesmata are severed), however, can successfully complete meiosis *in vitro* (Scott *et al.*, 1991; Takegami *et al.*, 1981). This suggests that beyond this point the sporophyte does not contribute unique or essential meiotic factors to the microsporocyte.

As meiosis proceeds, the microsporocytes separate from one another and become suspended within a fluid secreted and maintained by the tapetum. The tapetal cells often become connected to one another by large fenestrae, turning the entire layer into a syncytium. The resultant synchronization of tapetal activities around the locule ensures that the locular fluid remains homogeneous (Rowley, 1993). The tapetum elaborates the locular fluid with metabolites which are taken up by the developing microspores. Low molecular weight polysaccharides, for example, are secreted by tapetal cells and absorbed by the microspores (Pacini and Franchi, 1983). Similarly, Reznickova and Dickinson (1982) have observed the release of lipids from the tapetum and their subsequent uptake by young pollen grains, presumably to serve as metabolites for the final stages of pollen development.

While the tapetum is likely involved in the passage of reducing sugars and simple metabolites to the developing pollen grains, it remains uncertain how many of these simply pass through from surrounding tissues in an unaltered state. Clement *et al.* (1994; 1996) demonstrated that sugars are stored within the cells of the outer wall and connective tissue of *Lilium* anthers and mobilized at specific times during pollen maturation. Plasmodesmata allow these sugars to travel a symplastic pathway from the phloem cells of the vascular bundle to the cells of the middle wall layers. Plasmodesmata are lacking,

however, between the cells of the innermost middle wall layer and the cells of the tapetum (Clement and Audran, 1995). To enter the tapetal cells, sugars and metabolites must be actively transported across the membrane, an event which could be precisely regulated in response to microspore requirements.

B Callase Synthesis:

Callase is the only anther-specific enzyme yet identified that is synthesized by the tapetum and and has been shown to play a direct and essential role in pollen development (Scott *et al.*, 1991). In *Lilium*, callase activity appears during meiosis I, peaks just prior to tetrad dissolution and then declines rapidly (Stieglitz and Stern, 1973). The precise timing of peak callase activity appears to be coordinated by changes in the locule pH. For example, in anthers of *Petunia hybrida*, callase is inactive above a pH of 6.3. Callase is activated when the locule pH drops precipitously from its value at meiosis of 6.8-7.0 to a value of 5.9-6.2 at the tetrad stage (Izhar and Frankel, 1971).

Male-sterile mutants of *P. hybrida* have been identified in which a premature drop in pH appears to cause a premature release of the microspores from the tetrads (Izhar and Frankel, 1971). Worral *et al* (1992) observed that microspores which were released from tetrads early developed abnormal exine layers which often ruptured prior to maturation. The callose wall may thus be required as a framework for early exine deposition. Alternatively, microspores may have to attain a certain developmental stage before their release from the tetrad. The events responsible for the developmental precision of callase activity may be coordinated by the early synchronization of the tapetal and sporogenous cells or by direct communication between these two tissues (Scott *et al.*, 1991).

C Sporopollenin Synthesis:

The breakdown of the microspore callose wall coincides closely with the synthesis and release of sporopollenin precursors by the tapetum. These precursors appear to become polymerized soon after crossing the tapetal cell membrane (Pacini, 1990). Sporopollenin-containing orbicules (Ubisch bodies) 0.1-0.8μm in diameter accumulate between the plasma membrane and inner tangential and radial walls of the tapetal cells during the tetrad stage of pollen development (Pacini, 1990). The breakdown of the tapetal cell walls at the time of tetrad dissolution releases the orbicules into the locule where they are transported to the surface of the microspores (Chapman, 1987; Keijzer, 1987b). The assembly of sporopollenin into the mature exine is likely accomplished by enzymatic machinery contained within the microspore protoplasts (Scott *et al.*, 1991).

D Formation of the Pollen Coat:

Not until after its disintegration does the tapetum make its final contribution to pollen maturation. The breakdown of the tapetum releases a complex mixture of stored compounds and cellular debris into the locule. Stored compounds are released as pollenkitt, a hydrophobic mixture of lipids, carotenoids, and a small quantity of protein. In lily, these compounds are formed at the time of tetrad dissolution and stored in the cytoplasm of the tapetum as highly osmophilic globules. As the pollen grains dehydrate, the pollenkitt fills recesses in the exine and forms a hydrophobic coating (Heslop-Harrison, 1968). The cellular debris forms a substance known as tryphine, a mixture of hydrophobic and hydrophilic substances frequently containing remnants of degenerating organelles. Tryphine is the final addition to the surface of the pollen grains.

Pollenkitt and tryphine together form a sticky pigmented coating termed the pollencoat on the pollen grains of most insect-pollinated angiosperms. The pollencoat is thought to cause pollen to clump together and adhere to insects, thereby aiding in pollen dispersal. Pigments within the pollencoat may serve as a visual attractant for insects (Heslop-Harrison, 1968). The assembly of some of these pigments (e.g. flavanoids and cinnamic acid derivatives) is catalyzed within the locule or exine cavities by enzymes synthesized within the tapetum just prior to its disintegration (Scott *et al.*, 1991).

E Provision of Self-Incompatibility Recognition Proteins:

In more than one half of all angiosperm species, outbreeding is encouraged by a mechanism termed self-incompatibility (SI). First discussed by Darwin (1877), this phenomenon may have been one of the most important factors leading to the evolutionary success of the angiosperms (Whitehouse, 1951; Newbigin *et al.*, 1993). The self-incompatibility response occurs within tissues of the stigma and style and arrests the growth of pollen tubes from microgametophytes generated by the same individual. This genetically controlled phenomenon is usually under the control of a single locus (the S-locus) which possesses several alleles. The SI phenotype of the pollen may be determined by its own haploid S genotype (gametophytic SI), or by the diploid S genotype of the pollen producing plant (sporophytic SI).

Proteins responsible for gametophytic SI appear to be contained within the intine of the pollen wall while those responsible for sporophytic SI are components of the sexine (Mascarenhas, 1975). As the pollen grain is rehydrated on the surface of the stigma, the sexine-held recognition proteins are rapidly released (within seconds), while intine-held proteins are released more slowly (after approximately 5 minutes) through the germinal pores (Mascarenhas, 1975).

While gametophytic SI typically does not arrest pollen tube growth until the tube has penetrated deeply into the style, sporophytic SI occurs at the pollen-stigma interface (Nasrallah and Nasrallah, 1993).

Pandey (1958) suggested that sporophytic SI is generated by S genes which are expressed within the microsporocytes prior to meiosis. However, a self-incompatibility response to compatible pollen has been generated in pistils of *Iberis* with tapetal tissue dissected from anthers of the same flower (Heslop-Harrison *et al.*, 1974). Sporophytic SI may therefore be the result of S gene-products expressed in the tapetum and incorporated into the matrix of the pollen wall during sexine formation (Knox, 1984), or incorporated into sexine cavities as a component of the pollen coat. Allergens may be among the recognition proteins contributed by the tapetum (Greyson, 1994).

VI Molecular Aspects of Microsporogenesis and Pollen Maturation:

The alternation of diploid and haploid generations is accomplished by dramatic changes in gene expression. Although a very simple organism, the microgametophyte undergoes a series of discrete differentiation events requiring the expression of a large pool of genes contained both within its own haploid genome and the diploid genome of the sporophyte. Kamalay and Goldberg (1980; 1984) suggest that in anthers of tobacco, 10 000 of the 25 000 genes being expressed at the free microspore stage are specific to the anther. The expression of some of these genes occurs within the connective and outer wall layers and appears to be linked to the dehiscence of the anther [for example, the TA56 gene encodes a thiol endopeptidase within the CCC of tobacco (Goldberg et al., 1993)]. However, the majority of the anther-specific genes identified appear to be expressed within the developing gametophytes and the tapetum, where they likely play a direct

role in microsporogenesis and pollen maturation. As in other organs, the expression of anther-specific genes is likely regulated by a combination of general and tissue-specific factors and cis-acting elements.

A Gametophytic Gene Expression:

i) Transcription of mRNAs:

Approximately 20 000 mRNAs occur in mature pollen. This is 60% as many as are expressed within the many different cell types of the much more complex shoot (Mascarenhas, 1990a,b). Evidence from colony hybridization experiments suggests that 10-20% of these genes are pollen-specific and are not expressed elsewhere during the angiosperm lifecycle (Stinson *et al.*,1987; Mascarenhas, 1989). RNA blot hybridization experiments suggest that the genes expressed in pollen can be grouped into two distinct sets based upon the timing of their transcription (Mascarenhas, 1990a,b). The first, or "early", set become active shortly after meiosis. Their mRNAs accumulate to reach peak levels just prior to the first pollen mitosis and disappear completely by anthesis, suggesting a role in pollen mitosis and pollen maturation. Among the products of these genes are cytoskeletal proteins and proteins required for wall synthesis and starch deposition. Transcription of genes of the second or, "late", set commences following the first mitotic division of the microspore and continues until the dehydration of the pollen just prior to dehiscence. Many of the transcripts are not simultaneously translated, but instead accumulate within the pollen. At anthesis, the pollen contains a large store of mRNAs and some protein. The "late" pollen genes which have been tentatively identified with respect to function are all involved in the degradation of the middle lamella, presumably to facilitate the elongation of the pollen tube through the tissues of the stigma and style (Mascarenhas, 1989).

The vegetative cell possesses a highly synthetic cytoplasm and has been implicated by many *in situ* hybridization experiments as the transcription site of the "late" pollen genes (e.g. Hanson *et al.*, 1989; Ursin *et al.*, 1989; Twell, 1992). The cytology of the vegetative cell contrasts markedly with that of the small generative and sperm cells. The cytoplasm of these greatly reduced cells contains few mitochondria and little endoplasmic reticulum while their small nuclei possess few nuclear pores and contain condensed chromatin (Wagner *et al.*, 1990). Despite these characteristics, the generative and sperm cells are capable of expressing a small number of genes (Blomstedt *et al.*, 1996; Zang *et al.*, 1993). The majority of the proteins these encode do not occur within the vegetative cell (Blomstedt *et al.*, 1996) and are thus likely specific to aspects of fertilization. The drastic divergence of the generative and vegetative cells appears to occur as a result of the asymmetry of the division from which they arose. If a symmetrical mitotic division is induced in cultured microspores by exposure to cold or colchicine, the gametophytic pathway of development is abandoned and the two-celled 'microspore' develops into a haploid plant (McCormick, 1991; 1993).

ii) Meiotic purging and the transcription of rRNAs:

Ribosome and RNA populations are known to decrease dramatically in the microsporocytes of *Lilium* and *Trillium* during prophase I of meiosis. Termed "meiotic purging", the active degradation of these components may relieve the cytoplasm of the sporophytic translation machinery (and perhaps RNA viruses) and allow for the rapid differentiation of the gametophyte (Mackenzie *et al.*, 1967). Ribosomal RNAs (rRNAs) are actively transcribed from the haploid genome of the microspore in *Lilium* and *Trandescantia* prior to the first microspore mitosis. After this division, there is a sharp drop in the transcription of these genes. By anthesis, the rRNA genes have become transcriptionally inactive and the sites of rRNA transciption (the nucleoli) are

extremely reduced or absent (Tupy *et al.*, 1983). A similar pattern of transcription is observed for the transfer RNAs (tRNAs) (Peddada and Mascarenhas, 1975). Ribosome assembly peaks following microspore mitosis and stops prior to pollen maturation. At anthesis the pollen grain thus contains a large store of ribosomes and tRNAs in addition to its store of mRNAs.

iii) Protein Synthesis in Germinating Pollen Grains

Pollen tubes may grow along and between the cells of the style at a rate of 1-2μm/s (Heslop-Harrison, 1987). Growth activities occur at or near the tip and involve the metabolically active cytoplasm of the vegetative cell (Greyson, 1994). Rapid germination and tube growth is facilitated by the large store of ribosomes, tRNA, mRNA and protein present in the mature pollen grain (Bedinger, 1992; Mascarenhas, 1990a and b). Frankis and Mascarenhas (1980) observed a 50% decrease in the quantity of poly(a) mRNA within pollen grains during the first 30 minutes following their rehydration.

B Sporophytic Gene Expression:

i) Overlap of Sporophytic and Gametophytic Gene Expression:

An extensive overlap exists between genes expressed in the male gametophyte and the vegetative tissues of the sporophyte. Tanksley *et al.* (1981), for example, found that 60% of the structural genes coding for isozymes in the sporophyte were also expressed in pollen. In the pollen grain, these genes are likely linked to germination and the growth of the pollen tube. As pollen grains must compete to reach and fertilize one of a limited number of megagametophytes, alleles which enhance the rapidity of germination and pollen tube growth will be strongly favoured by natural selection. By simultaneously enhancing the selective pressures acting on a large pool of sporophytic genes, selection for pollen traits may have contributed to the rapid rate at which the

angiosperms have evolved (Mulcahy and Mulcahy, 1987).

ii) Gene Expression in the Tapetum:

The recessive nature of most male-sterile mutations suggests that the expression of these genes occurs within the diploid cells of the sporophyte (McCormick, 1991). As the only direct link between the sporophyte and its developing gametophytes, the tapetum participates directly in many processes which are essential to microsporogenesis. Not surprisingly, many of the mutations causing male sterility have been linked to this single layer of cells.

Differential screening of cDNA libraries and subtractive hybridization experiments have identified numerous anther-specific mRNAs which occur solely within the tapetum. The expression of tapetum-specific genes is tightly regulated in time, suggesting that they are not involved in general metabolic activities within the tapetal cells. Instead, the vast majority appear to encode products which are secreted into the locule where they are proposed to participate directly in microsporogenesis and pollen maturation (for review see Schrauwen *et al.*, 1996). With the exception of the callases, the precise function of each product remains uncertain.

Some tapetum-specific genes are transcribed shortly after the differentiation of the tapetum (e.g. the tap1 and tap2 genes of *Antirrhinum majus;* Nacken *et al.*, 1991) and may play a role in the regulation of microsporocyte meiosis. Callose genes such as the A6 genes of *Brassica* (Scott *et al.*, 1991; Hird *et al.*, 1993) and *Arabidopsis* (Hird *et al.*, 1993; Roberts *et al.*, 1993) are expressed during microsporocyte meiosis and accumulate within the locule. The tapetum may simultaneously express callose inhibitors such as the putative inhibitor TOMA5B protein of tomato (Smith *et al.*, 1990). Schrauwen *et al.* (1996) suggest that at the completion of meiosis, the microspores may generate a signal which deactivates callase inhibitors and thereby effects their release from the

tetrads. Numerous tapetum-specific genes continue to be expressed following meiosis; the majority of these are speculated to be involved in the degeneration of the tapetum, or the construction of the pollen wall or pollen coat [e.g. the LLA-15 glycoprotein of *Lilium* (Wang *et al.*, 1991b)]. The products of the satap 35 and satap 44 genes of mustard have been directly implicated by immunocyto-chemistry in the construction of the pollen exine layer (Staiger and Apel, 1993; Staiger *et al.*, 1994; see Discussion). Based on their deduced amino acid sequences and the presence of two hydrophobic regions, other tapetum-specific proteins have been proposed to carry sporopollenin precursors to the pollen exine where they may also participate in its oxidative polymerization (e.g. the tobacco TA29 gene product, Koltunow *et al.*, 1990).

Despite the large number of tapetum-specific transcripts which have been studied by *in situ* RNA hybridization, very few of the proteins these encode have been subjected to biochemical characterization or immunolocalization. Instead, functions have been proposed for the majority of these proteins based solely on their deduced amino acid sequences and the time course of their expression (Schrauwen *et al.*, 1996). Presented in this thesis is perhaps the only example of a tapetum-expressed protein other than callase which has been localized temporally and spatially within the anther and for which sequence homology and preliminary functional assays strongly indicate a specific biochemical function.

VII The Identification of LIM9, An Anther-Specific Gene from *Lilium*:

The angiosperm anther provides a valuable means of investigating meiosis and sporogenesis. Unlike megagametophytes, microspores are produced in large numbers and are easily extracted from the flower. *Lilium* (lily) is an

especially valuable system as its large anthers and naturally synchronous meiosis allow stage-specific meiotic cells to be collected in quantities sufficient for biochemical studies.

In an attempt to identify meiotic regulatory proteins, Riggs and Horsch (1995) generated an antiserum directed against putative meiotic DNA-binding proteins by "subtractive immunoscreening". A total protein extract was prepared from *Lilium* microsporocyte nuclei at meiotic prophase. The extract was subjected to DNA cellulose chromatography and the bound fraction was used to generate an antiserum. The rabbit antiserum recognized three proteins expressed only in the anther and thus likely specific to aspects of microsporogenesis (Figure 5). Among these is an 82kDa protein which first appears during the pachytene stage of microspore meiosis. The concentration of this protein increases as microsporogenesis continues and appears to peak at the tetrad stage. A sufficient amount of the protein was purified to perform N-terminal protein sequencing. A database search revealed that the N-terminal sequence matched perfectly with that of a recently described cDNA from *Lilium* named LIM9 (Lily messages Induced at Meiosis, clone #9, Kobayashi *et al.*, 1994; GenBank accession number D21815). The deduced amino acid sequence of the LIM9 product suggests it is a preproprotein exhibiting homology to several recently described serine proteases.

VIII Research Goals:

The objective of this Master's project was to generate an antiserum specific to the LIM9 protein and to use this to investigate the protein's intracellular maturation pathway and its spatial and temporal patterns of expression within the anther. An appropriate antigen was generated by expressing a portion of the LIM9 cDNA in the bacteria *Escherichia coli*. The antiserum generated to this

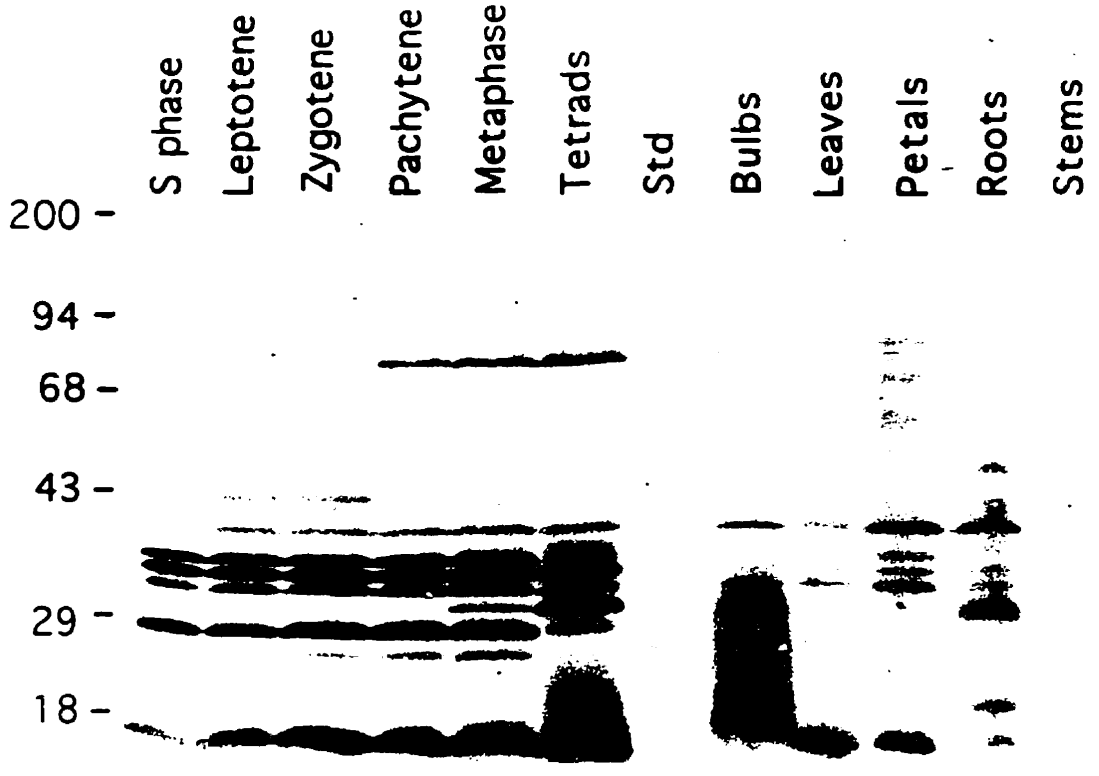

Figure 5 **An antiserum to DNA cellulose-binding microsporocyte proteins identifies the LIM9 protein.** A protein extract was made from the nuclei of *Lilium* microsporocytes in prophase I of meiosis and subjected to DNA cellulose chromatography. The bound fraction was used to generate an antiserum. On the above immunoblot of anther and vegetative protein extracts, the antiserum has recognized three proteins (with apparent molecular weights of 190kDa, 82kDa, and 29kDa) which appear to be specific to microsporogenesis. The 82kDa protein was first apparent during pachytene and accumulated until the tetrad stage. A small quantity of this protein was purified, subjected to N-terminal sequencing, and identified as the product of the LIM9 gene isolated by Kobayashi *et al.*, 1994. (Each lane of the immunoblot contains approximately 20μg of protein; Riggs and Horsch, unpublished).

protein consistently identified an 82kDa band, an 84kDa band and a 92kDa band on immunoblots of *Lilium* anther protein extracts. These bands were shown to represent stages in the posttranslational modification of the LIM9 protein consistent with the hypothesis that LIM9 encodes a preproprotein which acquires complex-glycans. Immunocytochemistry experiments indicate that the protein is expressed primarily in the tapetum and is secreted into the locule where it appears to encircle the microsporocytes. Drawing from the immuno-cytochemistry findings and the functions of homologous proteins, the LIM9 protein is proposed to be a serine protease which may play a role in the assembly of the pollen wall or pollen coat, perhaps by acting as a protein convertase.

Materials and Methods

I General Molecular Techniques:

A Acetone Precipitation of Proteins:

Protein extracts were mixed with 5 volumes of 100% acetone and proteins were precipitated out of solution overnight at -20°C. Proteins from small samples (less than 250µl) were precipitated in an Eppendorf tube and were pelleted by a 5 minute, 12 000rpm spin in an Eppendorf 5414 centrifuge (Brinkmann Instruments, Mississauga, ON) at 4°C. Proteins from larger samples were precipitated in a 30ml Corex™ tube and pelleted by a 25 minute spin at 10 000rpm in a Sorvall HB4 rotor (DuPont, Wilmington, DW) at 4°C. The supernatant was decanted and salts were washed from the pellet by gently vortexing it in 90% acetone. The tube was spun as before, the supernatant was discarded, and the pellet was vacuum-dried for approximately 5 minutes in a SVC 100 SpeedVac™ (Savant, Farmingdale, NY).

B Estimation of Protein Concentration by the Micro-Lowry Technique:

Protein concentrations were estimated by the method of Lowry *et al.* (1951). A small quantity of the sample was mixed with sufficient deionized water (DIW) to bring the volume to 100µl. Proteins were then acetone precipitated as described above. Subsequent steps were performed at room temperature (approximately 25°C) with occasional vortexing of the samples. The dried protein pellet was dissolved in 0.5ml of reagent #1 (2% Na_2CO_3 in 0.1M NaOH). After 30 minutes, 0.5ml of reagent #2 ($2x10^{-3}$% potassium tartarate and $1x10^{-3}$% $CuSO_4$ in reagent #1, prepared 10 minutes prior to use) was added.

Samples were then left 10 minutes prior to the addition of 100µl of Folin-Ciocalteu phenol reagent (Sigma, St. Louis, MO). After an additional 30 minutes, optical densities were measured for each sample at a wavelength of 700nm using a Ultraspec™ II 4050 spectrophotometer (LKB Biochrom, Cambridge, England). The spectophotometer was calibrated to a 'blank' sample consisting of 0.5ml of reagent #1 which was treated identically to the samples. The protein concentration of each sample was then deduced from a standard absorbance/concentration curve for bovine serum albumin (BSA).

C SDS-PAGE:

SDS-polyacrylamide gel electrophoresis (SDS-PAGE) was performed using a discontinuous Laemmli buffer system (Laemmli, 1970) consisting of a 10-15% polyacrylamide resolving gel and a 4.5% polyacrylamide stacking gel. The resolving gel solution [10-15% acrylamide (ICN Biomedicals, Inc., Aurora, OH), 0.05-0.075% N,N^1-Methylene-bisacrylamide (Gibco-BRL, Gathersburg, MD), 0.1% SDS, 375mM Tris pH 8.8] was vacuum degassed for 15 minutes. To this solution, 5µl/ml of 10% ammonium persulfate (APS) (Gibco-BRL) and 0.5µl/ml of N,N,N^1,N^1, tetramethylethylene-diamine (TEMED) (Schwarz/Mann Biotech, Cleveland, OH) was added. The solution was poured between glass plates (spaced 1mm apart) and carefully overlaid with DIW using a syringe. After at least one hour, the water was removed and the stacking gel (4.5% acrylamide, 0.12% N,N^1-Methylene-bisacrylamide, 0.1% SDS, 125mM Tris pH 6.8, 3µl/ml of APS, 1µl/ml of TEMED) was similarly degassed and cast. A teflon comb was inserted between the plates to form wells and the gel was left to polymerize for one hour.

Prior to loading, samples were adjusted to denaturation buffer [1% SDS, 0.33% 2-Mercaptoethanol (β-SH) (Kodak, Rochester, NY), 20mM Tris pH 8.6,

8.3% glycerol] and heated at 95°C for 5 minutes. The denatured samples were mixed with 1/3 volume of protein dye (10% glycerol, 1.0% bromophenol blue) and loaded into the wells of the stacking gel with a Hamilton 50µl syringe. Electrophoresis was performed at 100V for 1.5 to 2 hours in SDS running buffer (0.1% SDS, 25mM Tris, 192mM glycine) using a Mini Protean™ II system (Bio-Rad, Mississauga, ON). Gels were then transferred to nitrocellulose (see below) or fixed for approximately 15 minutes in 25% methanol/9% acetic acid. During this, and all subsequent steps, the gels were rocked gently at room temperature. Fixed gels were stained in 0.25% Coomassie Brilliant Blue R250 (Sigma) in 25% methanol/9% acetic acid for one hour and then destained in 25% methanol/9% acetic acid overnight. A 60 minute wash in DIW (with 3 changes) followed. The gels were dehydrated by a 30 minute soak in Gel-Dry™ (Novex, San Diego, CA) and permanently sealed between DryEase™ (Novex) mini-cellophanes.

II Purification of a LIM9 Polypeptide Expressed in *E. coli*:

A Bacterial Expression of a LIM9 Polypeptide:

The native LIM9 protein could not be purified in quantities sufficient to serve as an antigen for the production of an antiserum. Instead, the LIM9 cDNA, supplied by Dr. Satoshi Tabata (see Kobayashi *et al.*, 1994), was used to generate a suitable antigen. A 900bp fragment predicted to encode 300 amino acids of the carboxyl terminus of the LIM9 protein was excised with *Hin*dIII (Gibco-BRL), inserted in frame into an RSET™ expression vector (Invitrogen, San Diego, CA) and expressed in the *E. coli* strain BL21(DE3)lysS (Gibco-BRL) by C. D. Riggs. Cells were sedimented from the LIM9 expressing culture by centrifugation at 5 000 rpm for 5 minutes in a Sorvall HB-4 rotor and resuspended in 10 ml of 37°C 6M guanidium buffer (6M Guanidine Hydro-

chloride, 20mM sodium phosphate, 500mM NaCl, pH 7.8). The solution was rocked slowly at room temperature for 15 minutes to ensure thorough cell lysis. DNA and RNA were sheared by sonicating the cell lysate with three 5 second high intensity pulses using a Biosonik™ III sonicator (Bronwill Scientific, Rochester, NY). The cell lysate was stored at -20°C.

B IMAC Purification of the Expressed Protein:

i) Overview:

A preliminary purification of the RSET™ expressed protein was achieved by immobilized metal affinity chromatography (IMAC) using ProBond™ resin (Invitrogen). The RSET™ vector possesses a nucleotide sequence that encodes a polyhistidine metal binding domain expressed as an N-terminal fusion to the expressed protein. This domain gives the expressed protein a high affinity for the nickel ions of ProBond™ resin. The expressed protein is preferentially retained within a column of ProBond™ resin and contaminating host cell proteins can be removed by a stepwise decrease in pH. A final rinse at a much lower pH elutes the expressed protein.

ii) Column Preparation:

An Invitrogen spin column was loaded with 5ml of ProBond™ resin and centrifuged at 800 rpm for one minute in a Sorvall H400 rotor to gently compact the resin. The buffer was carefully aspirated with an inverted pipette and replaced with 7ml of DIW. The resin was gently resuspended by tapping and repeatedly inverting the closed column. The column was again centrifuged, the water was aspirated and the wash process was repeated two additional times. The column was then washed (as just described) three times with denaturing binding buffer (8M urea, 20mM sodium phosphate, 500mM NaCl, pH 7.8). The buffer was aspirated and 3-5ml of the expressing cell lysate was added to the

column. The volume in the column was brought up to 9ml with denaturing binding buffer and the resin was resuspended by gently inverting the column. The column was supported in a vertical position and the resin was allowed to settle by gravity for 20-30 minutes.

iii) Column Washes:

The resin was washed 5 times with denaturing binding buffer to remove contaminating bacterial proteins which possessed a low affinity for the resin. Bacterial proteins with a stronger affinity for ProBond™ resin were removed by washing the resin 5 times with denaturing wash buffer (8M urea, 20mM sodium phosphate, 500mM NaCl, pH 6.0). The bottom of the column was then removed and 8ml of denaturing wash buffer was loaded and allowed to flow slowly through the column by gravity (care was taken not to allow the resin to dry).

iv) Elution of the Target Protein:

The immobilized protein was eluted from the resin by passing 1ml fractions of denaturing elution buffer (8M urea, 20mM sodium phosphate, 500mM NaCl, pH 4.0) through the column. The protein concentration of each fraction was assessed by measuring the optical density of the eluted sample at a wavelength of 280nm. Bound proteins were typically eluted entirely within the third, fourth and fifth fractions. These fractions were pooled together and placed in 3 500 kDa molecular weight cut off (MWCO) Spectra/Por™ dialysis tubing (Spectrum Medical Industries, Houston, TX) held closed at both ends with dialysis clamps. The solution was then dialysed to remove excess urea and salts.

C Dialysis of the ProBond™ Column Eluate:

Urea was removed from the eluted protein by dialysing it at 4°C in 2 litres of 20mM sodium phosphate and 500mM NaCl for a minimum of 32 hours (solution was changed periodically). A white precipitate typically formed in the

tubing during this dialysis. The dialysis was continued in 2 litres of 10mM sodium phosphate, 250mM NaCl and 2.5% Polyethylene glycol 8 000 (PEG 8 000) (BDH, Toronto, ON) followed by a final dialysis in 2 liters of 5mM sodium phosphate, 125mM NaCl and 5.0% PEG 8 000 pH 7.0. Each of these dialyses was performed at 4°C for at least 24 hours with periodic changes of the dialysing solutions. The volume of the elution was further reduced to less than 1 ml by placing the dialysis tubing in solid PEG 8 000 at 4°C for approximately 2 hours. The solution (including precipitate) was transferred to a 30ml Corex™ tube and proteins were acetone precipitated. The washed protein pellet was air dried for approximately one hour and resuspended in approximately 250µl of denaturation buffer.

D SDS-PAGE Purification of the Expressed Protein:

A small volume of the dialysed and denatured solution was run on an SDS-polyacrylamide gel. In addition to the desired target protein of 35kDa, the solution contained a small quantity of contaminating bacterial proteins. These contaminants, however, had molecular weights sufficiently different from that of the target protein to permit their removal by electrophoresis followed by band excision and electroelution.

The remainder of the preparation (approximately 235µl) was loaded into the large slot well of a 15% polyacrylamide gel and electrophoresed as previously described. Proteins were visualized as white bands by staining the gel with 0.25M KCl at 4°C for approximately 30 minutes. The 35kDa band was excised with a razor and rinsed in room temperature DIW for 40 minutes with gentle rocking (DIW was changed after 20 minutes). The gel slice was then equilibrated to electroelution buffer (2.5mM Tris, 19.2 mM glycine, 0.1% SDS) at room temperature for 20 minutes with gentle rocking (buffer was changed after 10

minutes). The gel slice was cut into small squares and placed into the porous polyethylene funnel of a gel electroelution apparatus filled with electroelution buffer. The protein was electroeluted overnight at a voltage of 350V into a length of 6-8 000kDa MWCO dialysis tubing (Spectra/Por^{TM}) knotted at its far end. The current was then reversed for 30 seconds to recover protein bound to the dialysis membrane. The lower liquid phase containing the protein was collected with a pasteur pipette and transferred to a 30ml Corex^{TM} tube. The protein was acetone precipitated and the washed pellet was air dried for approximately one hour and resuspended in phosphate buffered saline (PBS) (7mM Na_2HPO_4, 3mM NaH_2PO_4, 130mM NaCl, pH 7.4) and 0.1% SDS.

III Generation of a LIM9 Antiserum:

A small quantity of blood was collected from the ear of a New Zealand white rabbit (*Oryctolagus cuniculus*) for use as a preimmune serum. This serum did not exhibit cross-reactivity on immunoblots of early and late whole anther total protein preparations (see below) from lily (*Lilium longiflorum*) and tomato (*Lycopersicon esculentum*).

Approximately 150µg of the purified 35kDa protein was emulsified with an equal volume (300µl) of Freund's complete adjuvant (85% paraffin oil, 15% mannide monocleate, 1mg/ml of heat-killed and dried *Mycobacterium tuberculosis*) (Sigma) using a double-canula microemulsifying needle. This preparation was injected subcutaneously at multiple sites on the rabbit's back. Two booster injections followed at three week intervals. The booster injections consisted of approximately 150µg of the protein emulsified in an equal volume (150µl) of Freund's incomplete adjuvant (85% paraffin oil, 15% mannide monocleate) (Sigma). Blood samples were periodically drawn and tested by

immunoblotting for the presence of a LIM9 antibody. A high titer of LIM9 antibody was attained two months after the initial injection and the rabbit was sacrificed to obtain a large volume of antiserum. The blood was allowed to clot in several glass centrifuge tubes overnight at 4°C. The tubes were then centrifuged at 1 500g (3 000rpm) for 10 minutes in a Sorvall H400 rotor at room temperature to pellet the clots. The supernatant (antiserum) was then decanted from the tubes and adjusted to 0.05% NaN_3. Aliquots of the antiserum were stored at both -20°C and -70°C.

IV Collection and Staging of *Lilium* Anthers:

A Anther Collection:

Plants of the *Lilium longiflorum* cultivar Enchantment, were grown from bulbs in the Scarborough Campus greenhouse under natural lighting conditions. Additional plants were field grown within the Highland Creek valley. Floral buds were carefully measured from stalk to tip. Those suspected to be of the appropriate developmental stage (based on measurements from previous harvests) were wrapped in wet paper towels and transported on ice to the laboratory. The buds were carefully dissected and the 6 anthers were removed intact (unhealthy or damaged anthers were discarded). One of these anthers was used to assess the stage of microsporocyte development by the squash technique (see below). While the squash was performed, the remaining anthers were kept in an Eppendorf tube on ice (if for use in protein preparations) or submerged in 2ml of fixative.

B Anther Squash Preparations:

The developmental stage of the microsporocytes within an anther was

determined using the squash technique. As the anthers within a single *Lilium* floral bud are synchronized in their development (Heslop-Harrison, 1966b), the staging of a single anther provided an accurate estimate of the developmental stage of the microsporocytes within the entire bud.

The tip of the anther was removed with a lance and the contents of the four locules were gently squeezed onto a glass slide. From anthers in which meiosis was still occurring, the microsporocytes were extruded as four thin white filaments. A single drop of iron acetocarmine [45% acetic acid, 1% carmine, filtered and saturated with $Fe(OH)_2$] was placed on the slide followed by one drop of 2.2% orcein in glacial acetic acid. The process was repeated and the pool of solution was gently mixed with a lance. The slide was left at room temperature with occasional mixing for approximately 15 minutes. A coverslip was added and tapped gently with a small brass rod to spread the cells into a monolayer. Excess solution was blotted from the slide and the coverslip was sealed in place using nail enamel. The slides were examined using a Zeiss Standard 25 binocular microscope. The developmental stage of the microsporocytes was determined based on cell and chromosome morphology.

V Localization of the LIM9 Protein within the Developing Anther:

A Preparation of Anther Sections:

i) Anther Fixation:

A method of fixation which preserved both the morphology and immunogenicity of the anther's tissues was required. To achieve this goal, two fixation procedures were evaluated. In one method, anthers from each bud were prefixed in 2ml of a 4% solution of paraformaldehyde in DIW (pH 7.4) for 2 hours. During this period, the vials containing the anthers were placed in a

vacuum of 500-600mm of mercury for 15-30 minutes (until anthers sank) to displace interstitial air from the tissue and facilitate the infiltration of the fixative. The paraformaldehyde solution was then replaced with modified Carnoy's solution (60.2% ethanol, 30% chloroform, 6% glacial acetic acid, 1.8% formaldehyde; Hasenkampf *et al.*, 1992). The solution was changed after 10 minutes and the vials were again vacuum infiltrated for 30 minutes as before. After a total of 3 hours in modified Carnoy's solution, the fixative was replaced with 70% ethanol.

Alternatively, the anthers were placed directly into (unmodified) Carnoy's solution (75% ethanol, 25% glacial acetic acid) and fixed in this solution for 3.5 hours. During this period the Carnoy's solution was changed 3 times and the vials were vacuum aspirated as previously described. The fixative was then replaced with 70% ethanol.

ii) Dehydration and Paraffin Embedding of Anthers:

Once in 70% ethanol, anthers from both fixation treatments were dehydrated through the same sequence of alcohol solutions. The anthers were left in 70% ethanol for 90 minutes (changed 3 times) to completely remove the fixative. The anthers were then dehydrated through the following sequence of solutions: 56% ethanol/20% 2-Methylopropan-2-ol (Tertiary Butyl Alcohol or TBA); 55.25% ethanol/35% TBA; 42.75% ethanol/55% TBA; 25% ethanol/75% TBA (absolute alcohols were completely dehydrated using molecular sieves). The anthers were left in each solution for a total of 2.5 hours. Solutions were changed using pasteur pipettes. To ease the transition between solutions, only 2/3 of the solution was changed initially. After the anthers had been in a solution for one hour, the solution was changed completely (taking care not to expose the anthers to the air). Following dehydration, the anthers were placed in 100% TBA for 3 hours (during which the solution was changed completely

three times). Absolute TBA solutions were kept at approximately 30°C to prevent solidification.

The anthers were transferred, along with approximately 3ml of 100% TBA, to open shell vials containing about 3ml of solidified Tissue Prep™ (Fisher Scientific, Fair Lawn, NJ). The vials were placed in a Fisher Isotemp™ oven at 63°C overnight to slowly melt the paraffin and evaporate the TBA. The paraffin was replaced with fresh molten paraffin and the vials were left in the oven for two additional days to ensure complete infiltration of the anther tissues (the paraffin was replaced at approximately 12 hour intervals). The anthers were then placed in small ceramic trays of molten Tissue Prep™ and cooled on ice. Anthers were stored at room temperature in these solidified tablets. When required for sectioning, an anther was 'thawed' by an immersion in molten Tissue Prep™. The anther was then embedded in Tissue Prep™ in a small metal mould mounted on a plastic embedding frame. The mould was cooled and removed and the block was trimmed to give a trapezoidal cutting surface for sectioning.

iii) Anther Sectioning and Section Staining:

Ribbons of 10 μm-thick sections were cut using an AO 820 microtome (American Optical Instrument Company, Buffalo, NY). A scalpel was used to cut the ribbons into segments consisting of 2-3 sections which were then floated on 45°C distilled water for approximately 5 minutes to relieve creasing. The sections were lifted onto slides which had been cleaned (first with detergent and then with 95% ethanol) and coated with a 0.5% gelatin solution. Excess water was blotted from the slides and the slides were placed on a 37°C slide warmer for 12 to 36 hours.

Slides were placed into a vertical slide rack and dewaxed through two 10 minute immersions in 100% Histo-Clear™ (National Diagnostics, Atlanta, GA).

The slides were then rehydrated through the following sequence (slides were immersed for 2 minutes in each solution): 50% Histo-Clear™/50% ethanol; 100% ethanol; 95% ethanol; 80% ethanol; 70% ethanol; 50% ethanol; and 30% ethanol. Following a three minute immersion in distilled water (water was changed three times), the sections were completely rehydrated and ready for either immunostaining (see next section) or staining with dyes. To assess anther morphology and cytology, sections were stained with Ehrlich's hematoxylin (33.3% glycerol, 32% ethanol, 3.3% acetic acid, 22mM hematoxylin, 22mM aluminum ammonium sulfate, 6.8mM sodium iodate, 'ripened' by exposure to air in a cotton-plugged bottle for several weeks with frequent mixing) for 30 seconds. Alternatively, sections were stained with a 0.5% solution of Toluidine Blue (Fisher Scientific) in DIW for 60 seconds. Following a 5 minute rinse in distilled water (with 4 changes), the stained slides were dehydrated through the following sequence of solutions: 30% ethanol for 30 seconds; 70% ethanol for 30 seconds; 95% ethanol for 120 seconds (changed after 60 seconds); 100% ethanol for 120 seconds (changed after 60 seconds); 50% ethanol/50% Histo-Clear™ for 60 seconds: and 100% Histo-Clear™ for 3 minutes. Excess Histo-Clear™ was drained from the slides and coverslips were permanently mounted over the sections using a drop of Permount™ (Fisher Scientific).

B Immunocytochemistry:

Immunocytochemistry experiments were performed using the technique of Hasenkampf *et al.*, 1992 (with slight modifications). Anthers were selected for immunocytochemistry based on tissue morphology, particularly the preservation of the delicate tapetum. Anthers were chosen from six developmental stages to construct a developmental series. Three slides, each with two 10μm thick sections, were prepared from consecutive sections for each

anther. One of the three slides was immunostained with the LIM9 antiserum while the other two provided a positive control and a negative control (see below).

Following rehydration, the slides were removed individually from the distilled water and dried with blotting paper except for a small droplet of water covering the sections (extreme care was taken to keep the sections wet at all times). The water droplet was encircled with a ring of molten paraffin approximately 15mm in diameter. This wax ring would serve as a reservoir for incubation solutions.

As each wax ring was completed, the slides were immediately placed in a horizontal slide rack submerged in fresh distilled water. Once all of the wax rings had been prepared, the slides were transferred to phosphate-buffered saline (PBS) (130mM NaCl, 10mM sodium phosphate, pH 7.4). Following three 5 minute immersions in PBS, the slides were individually removed from the slide rack. The wax reservoir was kept filled with PBS while the remainder of the slide was blotted dry. When this step had been completed for all the slides, the PBS within the reservoirs was blotted away and immediately replaced with 150µl of blocking solution [130mM NaCl, 10mM sodium phosphate, 5% goat serum (Sigma), 0.16% BSA (Gibco-BRL), 0.4mM NaN_3, pH 7.4]. After 30 minutes, the blocking solution was replaced with 150µl of a dilution of the primary antibody in incubation buffer (130mM NaCl, 10mM sodium phosphate, 0.08% BSA, 0.2mM NaN_3, pH 7.4). The LIM9 antiserum was used at a dilution of 1:2 000. Negative controls were performed by incubating sections in a 1:2 000 dilution of LIM9 preimmune serum while positive control slides were prepared using an anti-histone H1 antiserum (411 serum, see Riggs, 1994) at a dilution of 1:350. Each of the three primary incubations was 1 hour in duration. The solutions were changed after the first 5 minutes to ensure that the primary

antibody was present at the desired concentration.

Unbound primary antibodies were removed by gently rinsing the sections with PBS using a pasteur pipette. The slides were returned to a horizontal rack and the sections were washed further by three 10 minute immersions in approximately 250ml of PBS. The slides were then placed on paper towels and blotted dry in preparation for the secondary incubation (the wax reservoir was again kept filled with PBS). For each slide, polyclonal goat anti-rabbit antibody conjugated to 1nm colloidal gold (British BioCell, c/o Cedarlane Laboratories, Hornby, ON) was used as a secondary antibody at a dilution of 1:150 in incubation buffer. After 1 hour, a pasteur pipette was used to rinse the sections with water. Rinsing was continued in a horizontal slide rack in running distilled water for 5 minutes followed by two 5 minute immersions in DIW.

The location of the secondary antibody was visualized by silver intensification using a silver staining kit (British Biocell). The slides were removed from the water wash and blotted dry, taking care to keep the wax rings filled with water. At one minute intervals, the water was blotted from a slide's reservoir and replaced by one drop of initiator and one drop of enhancer. An additional drop of each was added and the solution was mixed by gently moving the slide in a circular motion. The silver enhancement process was monitored for several of the slides using a Zeiss Standard 25 binocular microscope. When sufficiently stained, the reaction was terminated by carefully rinsing the slides under a stream of distilled water. Slides were rinsed in the same order that the silver enhancement was commenced. Rinses were initiated at one minute intervals to ensure that each slide was enhanced for an equal period of time (typically about 20 minutes). The wax rings were removed under the flowing water with a razor and the slides were again placed in a horizontal rack. After rinsing for an additional 5 minutes under flowing distilled water, the slides were

dehydrated and brought into Histo-Clear™ as previously described. Coverslips were mounted with Permount™ and the sections were viewed and photographed using a Zeiss Axiophot™ photomicroscope. Photographs were taken using 100 ASA 35mm colour film (Quality Film, Toronto, ON).

VI Characterization of the LIM9 Maturation Pathway:

A Anther Protein Preparations:

Lilium anthers at specific stages of development (as determined by the squash technique, see above) were used in the production of four different types of protein preparations for use in immunoblotting and zymogram experiments. "Whole anther protein preparations" contained proteins from all tissues of the anther. "Whole locule protein preparations" contained proteins from the entire contents of the anther locules. From the contents of the locules, "intracellular protein preparations" and "extracellular protein preparations" were also prepared. The intracellular extracts should contain only those proteins contained within the microsporocytes, while extracellular extracts should be dominated by soluble proteins of the locular fluid. In addition, protein preparations were made from mature pollen extracted from dehisced anthers. Prior to their use in experiments, the integrity of each preparation was assessed by SDS-PAGE. Protein concentrations were determined for each extract by the micro-Lowry technique (see above).

i) Whole Anther Protein Preparations:

Several whole anthers of the appropriate developmental stage were cooled in liquid nitrogen and ground to a fine powder with a mortar and pestle. The powder was transferred to a mini-homogenizer and homogenized in 1ml of hot denaturation buffer. The sample was then placed in a boiling water bath for

5 minutes to completely denature the protein. Insoluble debris was pelleted by a spin at 12 000rpm for 2 minutes in a Sorvall MC12V centrifuge. The clear supernatant was extracted with a pipette and stored at -20°C.

ii) Whole Locule Protein Preparations:

A razor was used to cut the tips from anthers of the appropriate developmental stage and the contents of the locule were extracted by gentle squeezing. The extract was homogenized in hot denaturation buffer using a mini-homogenizer. The sample was then placed in a boiling water bath for 5 minutes and then stored at -20°C.

iii) Intracellular and Extracellular Protein Preparations:

Anthers of the appropriate developmental stage were cut and gently squeezed to extract the contents of their locules. The strings of microsporocytes were placed into a mini-homogenizer containing 250µl of 4°C White's microsporocyte culture medium (White, 1963) and gently vortexed. The tube was then centrifuged at 12 000rpm for 2 minutes at 4°C. Intracellular proteins should have been largely confined to the pellet of intact cells while the supernatant should have contained extracellular proteins of the locule. The supernatant was carefully extracted with a pipette and the extracellular proteins were acetone precipitated. The dried pellet was resuspended in 250µl of non-reducing denaturation buffer (1% SDS, 20mM Tris pH 8.6, 8.3% glycerol). The cell pellet was homogenized in 1ml of nonreducing denaturation buffer. Intracellular and extracellular preparations were not heated during preparation. The samples were stored at -20°C.

iv) Pollen Protein Preparations:

Several dehisced anthers were collected from opened flowers and gently vortexed in an Eppendorf tube to extract the pollen. The pollen formed clumps which were removed from the tube, cooled in liquid nitrogen, and ground to a

fine powder with a mortar and pestle. The powder was then homogenized in 1ml of hot denaturation buffer using a mini-homgenizer. The homogenized sample was placed in a boiling water bath and then spun at 12 000rpm for 2 minutes in a Sorvall MC12V centrifuge to pellet insoluble debris. The supernatant was recovered and stored at -20°C.

B Endo H Treatment of Protein Preparations:

Endoglycosidase H digests were performed on whole locule protein preparations from anthers possessing microspores at the tetrad stage of development. For each digest, 1µl (7.5µg) of the protein preparation was combined with 7µl of water and 1µl of 10x denaturation buffer in an Eppendorf tube and heated. After 5 minutes at 95°C, 1µl of G5 buffer (0.5M sodium citrate, pH 5.5) was added followed by 1.5µl (750 units) of Endo H (New England BioLabs, Beverly, MA). (The solution was mixed by gentle vortexing and pooled by a 10 second spin at 12 000rpm following the addition of each reagent). The solution was then incubated at 37°C for 3 hours. Negative control samples were prepared identically with the exception that 1.5µl of DIW was substituted for the Endo H. Samples were run on a 10% polyacrylamide gel (as previously described) and immunoblotted (see below).

C Immunoblotting of Protein Preparations:

Immunoblots were performed on 7.5-15µg aliquots of anther protein preparations. Samples and marker proteins were run on a 12.5% polyacrylamide gel in SDS buffer as previously described. Proteins were transferred to Trans-Blot™ nitrocellulose membrane (Bio-Rad) in cold transfer buffer (25mM Tris pH 8.3, 192mM glycine, 15% methanol). The transfers were performed in a Bio-Rad mini Protean™ II system at a voltage of 100V for approximately 60 minutes.

Nonspecific IgG binding was minimized by blocking the membranes in 3% gelatin in Tween/Tris-buffered saline (TTBS) [20mM Tris pH 7.5, 500mM NaCl, 0.1% Polyoxyethylenesorbitan Monolaurate (Tween 20) (Sigma)] for 60 minutes at room temperature with gentle rocking (alternatively, the membranes were rocked at room temperature for 20 minutes and then left in blocking solution overnight at 4°C).

All immunoblotting incubations were performed at room temperature with gentle rocking. Membranes were incubated first in a dilution of the primary antibody in 1% gelatin in TTBS for 90 minutes. The LIM9 antiserum was used at a dilution of 1:20 000. Xylose residues were identified on complex glycoproteins using a 1:2 500 dilution of 949 polyclonal antiserum (see Lauriere *et al.*, 1989). Following the primary incubation, unbound immunoglobulins (IgGs) were removed by rocking the membrane in TTBS for approximately 25 minutes (TTBS was changed 5 times). The membrane was then incubated in a 1:3 000 dilution of affinity purified goat anti-rabbit IgGs conjugated to alkaline phosphatase (GAR-AP) (Bio-Rad, supplied in 1% BSA, 0.01% NaN_3) in 1% gelatin in TTBS for 60 minutes. The membrane was again rinsed in TTBS as before. The membrane was then incubated in 20ml of substrate solution [3.3µl/ml of 5-Bromo-4-chloro-3-indolylphosphate p-Toluidine salt (BCIP)(Gibco-BRL, supplied @ 50mg/ml), 4.4µl/ml of Nitroblue Tetrazolium chloride (NBT) (Gibco-BRL, supplied @ 75mg/ml), 50mM $MgCl_2$, 0.1M NaCl, 0.1M Tris, pH 9.5]. Removal of a phosphate group from the BCIP by the alkaline phosphatase and reduction of the NBT produced a purple-blue precipitate marking the position of the bound secondary antibody. Once the reaction had proceeded sufficiently (usually less than 15 minutes), the blot was rinsed in DIW and the reaction was terminated by incubating the blot in 0.1M Ethylenediaminetetraacetic Acid (EDTA) pH 8.0 for at least 1 hour.

VII Electrophoretic Assay of LIM9 Protease Activity:

Protein extracts containing the LIM9 protein were assessed for protease activity by an electrophoretic protease assay. In this technique, proteins are mildly denatured and separated by SDS-PAGE on a resolving gel containing a suitable substrate protein. The proteins are then renatured within the gel and the gel is incubated in a buffer appropriate for the protease activity of interest. Active proteases should degrade the substrate protein *in situ*. When stained with Coomassie Brilliant Blue R250, regions in which protease activity has occurred (and hence the substrate protein is absent) remain unstained. The resulting gel is termed a zymogram.

Zymograms were prepared using gelatin as a substrate by a modified version of the technique of Michaud *et al.* (1993). A gelatin-containing polyacrylamide resolving gel [7.5-10% acrylamide, 0.3-0.4% bis acrylamide, 0.10-0.15% gelatin (from a 0.75% boiled stock solution), 0.1% SDS, 375mM Tris pH8.8] and a 4.5% polyacrylamide stacking gel were polymerized and cast as previously described. Samples to be run on a zymogram were prepared in nonreducing denaturation buffer (i.e. without β-SH) and were not heated. Aliquots of intracellular and extracellular locule extracts containing 10µg of protein were brought up to a volume of 12µl with nonreducing denaturation buffer, mixed with 1/3 volume of protein dye and loaded into the wells of the stacking gel as described previously. Electrophoresis was performed at a voltage of 100V for approximately 3.5 hours. To prevent overheating of the SDS running buffer, the process was performed at 4°C.

Following electrophoresis, SDS was removed from the gel by rocking it gently in 100ml of 2.5% Triton X-100 for 30 minutes at room temperature (solution was changed after 15 minutes). The gel was then placed in 100ml of

activation buffer [1% Triton X-100, 50mM N-Hydroxyethylpiperazine-N^1-2-Ethane Sulfonic Acid (HEPES) buffer (USB, Cleveland, OH), 5mM L-Cysteine (Sigma), pH 8.0] and allowed to equilibrate at room temperature for 15 minutes with gentle rocking. The activation buffer was replaced and the gel was incubated at 37°C overnight (approximately 15 hours). The following day, the gel was fixed for 15 minutes in 25% methanol/9% acetic acid and stained in 0.5% Coomassie Brilliant Blue R250 in 25% methanol/9% acetic acid. Next, the gel was destained in 25% methanol/9% acetic acid for several hours. Completed zymograms were washed and dried as described previously for SDS-polyacrylamide gels.

Results:

I LIM9 Expression in the Lily Anther:

A The Morphology and Immunoreactivity of Anther Tissues:

The microsporocytes of *Lilium longiflorum* undergo meiosis synchronously throughout the six tetrasporangiate anthers of a flower. The five thousand or more microsporocytes of a single locule (Taylor and McMaster, 1954) are surrounded by a prominent glandular tapetum and 3-4 middle wall layers. The middle wall layers remain intact at anther dehiscence despite being compressed by surrounding tissues. Outward from the middle wall layers are the endothecium and epidermis. Although initially the same width, the endothecium expands to form the majority of the anther wall at dehiscence while the epidermis largely degenerates.

Paraffin embedded thin sections were prepared from *Lilium* anthers fixed by two protocols. The large vacuolate cells of the tapetum were particularly susceptible to damage during fixation. Tapetal morphology was preserved most faithfully in anthers fixed with 4% paraformaldehyde followed by modified Carnoy's solution. In these anthers, the tapetal cells remained intact and in contact with the middle wall layers. In contrast, anthers fixed only with unmodified Carnoy's often possessed prematurely disrupted tapetal layers which had detached from the remainder of the anther wall.

Despite contrasting preservation of the tapetum, anthers prepared by both fixation treatments displayed identical temporal and spatial patterns of immunoreactivity. An anti-histone H1 antibody identified cell nuclei from each tissue, independent of the anther's fixation or developmental stage (see Figure 6).

The fixation protocols thus appear to have preserved the accessibility and immunoreactivity of proteins throughout the anther. Although each of the anther tissues reacted to the histone H1 antiserum, LIM9 immunostaining appeared to be restricted to the tapetum and locule. With the exception of dehiscent anthers (see below), immunostaining was completely absent from negative control sections in which LIM9 preimmune serum was used as the primary antibody. These observations indicate that neither the LIM9 antiserum nor the secondary antibody generate nonspecific signals.

B LIM9 Expression in the Developing Anther:

The spatial and temporal patterns of LIM9 immunostaining are presented in a composite photograph from a developmental series of anther sections (Figure 6). For each of these sections, the bound primary antibody was labelled using a secondary antibody conjugated to colloidal gold. The presence of the secondary antibody was visualized by a silver intensification process which generates a grey to brown to black gradation of colour. For each anther, immunoblotting experiments (complete with positive and negative controls) were repeated a minimum of five times; typical results are shown.

i) Interphase:

Anthers containing premeiotic (interphase) microsporocytes (PMCs) were the youngest examined by immunocytochemistry. The dense cytoplasm of these closely packed cells was intensely stained by Toluidine Blue. Anther histogenesis had been completed by this stage. The tapetal cells had enlarged and elongated radially, making them easily discernable from the adjacent microsporocytes and cells of the middle wall layers. The LIM9 antiserum consistently failed to generate immunostaining within these early anthers.

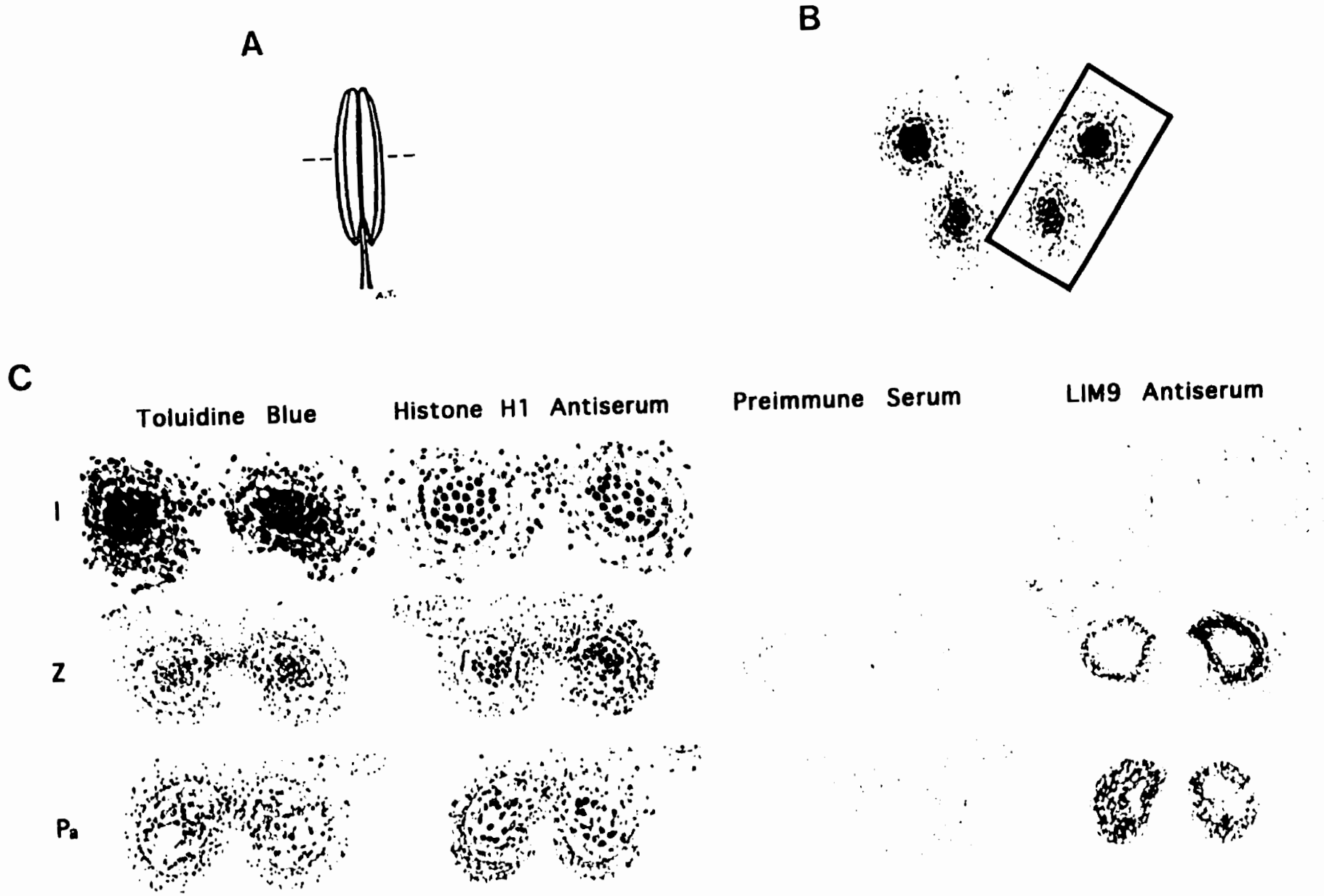
A
B
C
Toluidine Blue
Histone H1 Antiserum
Preimmune Serum
LIM9 Antiserum
I
Z
Pa

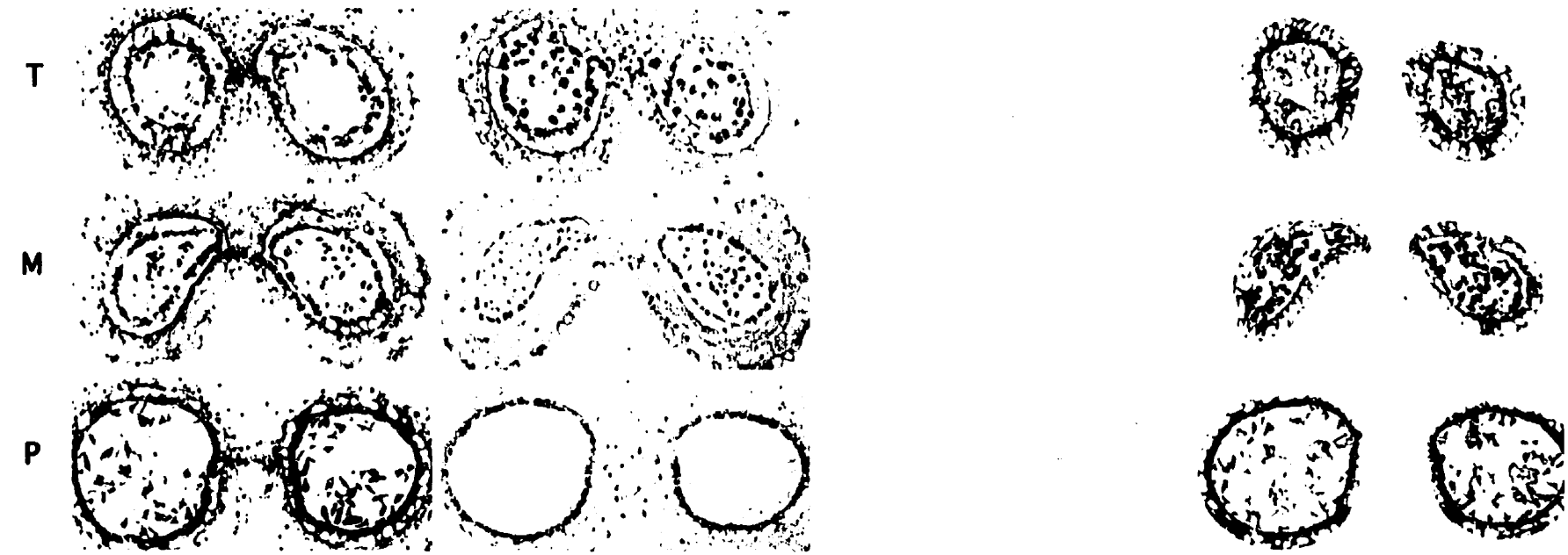

Figure 6 **Silver intensified immunogold labelling of the LIM9 protein in the developing anther.** Immunocytochemistry experiments were performed using transverse sections of *Lilium longiflorum* (var. Enchantment) anthers (**A**). Two complete pollen sacs (**B**) are displayed for sections of anthers from six developmental stages (**C**). For each anther, serial sections were incubated with histone H1 antiserum (positive control), LIM9 preimmune serum (negative control), and LIM9 antiserum. Bound primary antibody was labelled using a secondary antibody conjugated to colloidal gold and visualized by silver enhancement (see Materials and Methods). LIM9 immunostaining was first observed at the late zygotene stage and remained restricted to the tapetum and locule (see text for details). **I**, interphase; **Z**, late zygotene; **Pa**, late pachytene; **T**, tetrad stage; **M**, free microspore stage; **P**, microspore/pollen transition. (Interphase sections are magnified approximately 100X, all other sections are magnified approximately 50X).

ii) Zygotene:

The microsporocytes maintained close contact with one another as meiosis commenced. The tapetal cells continued to enlarge and by the zygotene phase of microsporogenesis had become highly vacuolate. In late zygotene sections immunostained for the LIM9 protein, the tapetal cytoplasm was dark brown to black while the cytoplasm of the microsporocytes was grey to light brown. Each microsporocyte was encircled by a ring of more darkly stained material.

iii) Pachytene:

Intercellular spaces formed within the mass of microsporocytes as these cells progressed through pachytene. (The growth and fusion of these spaces completely isolated the microsporocytes from one another prior to their first division). The tapetal cells continued to elongate into the locule. A single vacuole occupied the majority of the volume of each tapetal cell, causing the cytoplasm to migrate towards the innermost (locular) walls.

Within the locule, amorphous clumps of extracellular material were intensely stained by the LIM9 antiserum at the late pachytene stage. Immunostaining was also generated within the cytoplasm of the microsporocytes. The strongest signal, however, was generated within the cytoplasm of the tapetal cells, adjacent to the locular walls (presumably due to the accumulation of secretory vesicles).

iv) Tetrads:

Following prophase I, the microsporocytes separated completely from one another and underwent two rounds of cytokinesis to yield tetrads of microspores encased within callose. The tapetal cells attained their maximum volume at this stage. Continued growth of the tapetal cell vacuoles had pressed the entire cytoplasm of each cell tightly against the interior of the locular walls.

LIM9 immunostaining of sections from tetrad stage anthers generated a strong signal within the cytoplasm of the tapetal cells and revealed a large quantity of darkly staining extracellular material scattered throughout the locule. Stained extracellular material also coated the surface of each tetrad. Higher magnification (Figure 7) clearly shows that, although the cytoplasm of the microspores was stained by the LIM9 antiserum, the nuclei and the interior of the callose walls were not.

v) Free Microspores:

The period of pollen development following tetrad dissolution but prior to microspore mitosis is termed the free microspore stage. The degeneration of specific anther wall layers was apparent by this stage. The cells of the inter-sporangial septum had shrunken significantly as had most of the cells of the epidermis. In contrast, the endothecium had developed its characteristic wall thickenings and had expanded in width to become the prominent layer of the anther wall. The tapetal cells were highly active and their cytoplasm was darkly stained by Toluidine Blue. The innermost tangential walls of the tapetal cells were thin or absent, presumably to facilitate secretion.

Staining of the microspores by the LIM9 antiserum peaked immediately following their release from the tetrads. The single nucleus of each microspore appeared as an unstained region (data not shown), suggesting that the LIM9 protein within the protoplast was restricted to the cytoplasm. Intensely stained material occurred abundantly in the locular fluid. The cytoplasm of the tapetal cells continued to be stained by the LIM9 antiserum, but this staining was weaker and more diffuse than it had been during the tetrad stage.

vi) Microspore/Pollen Transition:

Although the walls of the tapetal cells were extremely thin or absent by this stage, the tapetal layer remained intact. A layer of yellow sporopollenin

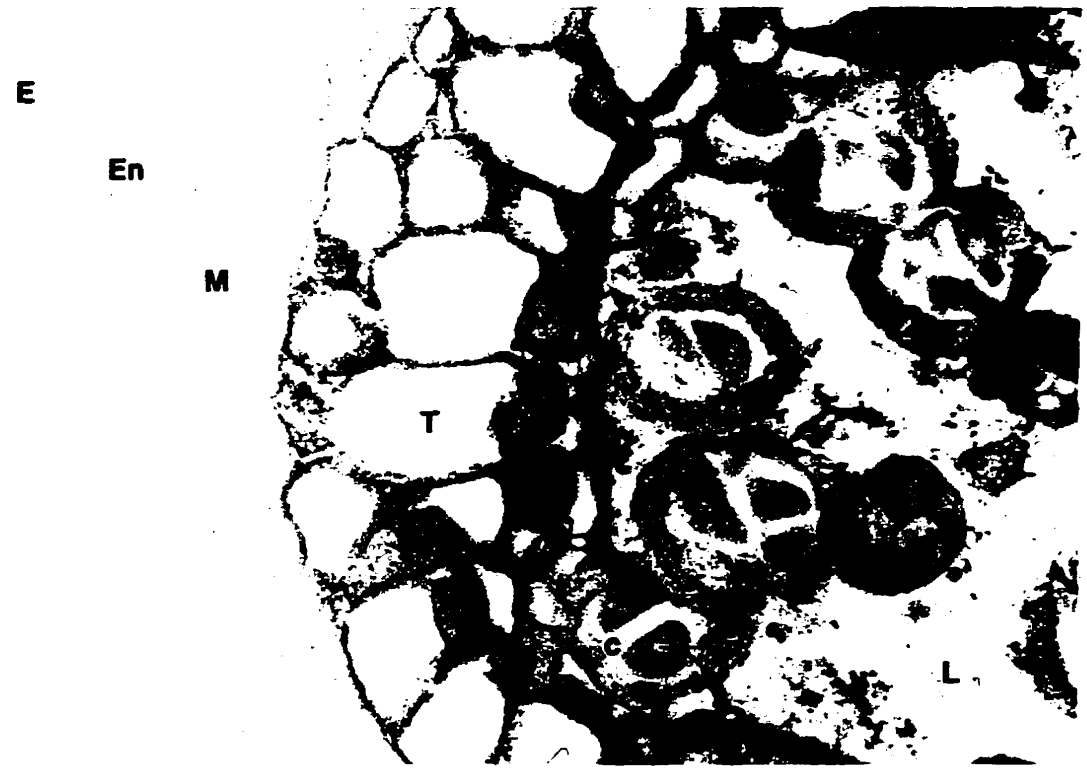

Figure 7 **Silver Intensified Immunogold labelling of the LIM9 protein within the tapetum and locule of a tetrad stage anther section.** Immunocytochemistry using the LIM9 antiserum stained the cytoplasm of the large vacuolate tapetal cells but failed to stain the surrounding wall layers. Extracellular material was identified within the locule where it formed amorphous deposits and coated each microspore tetrad. Staining of the microspore protoplast was restricted to the cytoplasm: the nuclei and callose walls remained unstained. **c**, callose; **E**, epidermis; **En**, endothecium; **L**, locule; **n**, microspore nucleus; **M**, middle wall layers; **T**, tapetum (Magnified approximately 600X).

(rendered green by Toluidine Blue) lined the locule and formed a nearly completed sculpted exine on the surface of the microspores. The shrunken microspores had collapsed inwardly along a longitudinal groove on their surface and become U-shaped in cross-section. As the pollen contained very little cytoplasm, it could not be ascertained whether a mitotic division had occurred. The small volume of cytoplasm was pressed tightly against the pollen wall and was darkly stained by the LIM9 antiserum. Surprisingly, the cytoplasm of the tapetal cells also bound the histone H1 antiserum at this stage. Nonspecific binding does not appear to have occurred, however, as the cytoplasm was not immunostained by the LIM9 preimmune serum or secondary antibody. Instead, histone H1 may have been released into the cytoplasm of the tapetal cells by the breakdown of their nuclear envelopes. Degeneration of the tapetal cell nuclei has been observed during the later stages of microsporogenesis in *Lilium* by several researchers (e.g. Herich and Lux, 1984).

vii) Pollen:

Dehiscent anthers contained large circular pollen grains in which the vegetative and generative cells could be easily discerned (see Figure 1). The tapetum had degenerated completely in these anthers, leaving only a thin layer of cellular debris and sporopollenin-containing orbicules. When sections from these anthers were subjected to immunocytochemistry the mature pollen grains bound antibodies indiscriminately. Sections stained with the LIM9 antibody could not be distinguished from the negative control sections for the same anther (data not shown). Perhaps, among its large store of diverse molecules, the mature pollen grain contains compounds with a high (nonspecific) affinity for immunoglobulins.

From the immunocytochemistry experiments it was unclear whether the LIM9 protein was present within mature pollen grains (and thus might play a

role in pollen germination or pollen tube growth). Total protein extracts were therefore prepared from the mature pollen of dehisced anthers and immunoblotted using the LIM9 antiserum (Figure 8). Despite being several fold more sensitive than immunogold localization (Balsamo *et al.*, 1995), immunoblotting failed to identify the LIM9 protein in these extracts.

viii) Summary:

The LIM9 protein first appears in the anther at the late zygotene stage of microsporogenesis and reaches peak levels during tetrad dissolution. The LIM9 protein appears to be expressed predominantly by the tapetum and is secreted into the locule where it coats the callose walls of the microsporocytes and microspore tetrads. The protein also occurs within the cytoplasm of the microsporocytes and microspores. Immunoblotting experiments suggest that the LIM9 protein is not present as an easily extracted component of mature pollen.

II The LIM9 Product is Posttranslationally Modified:

A LIM9 is Predicted to Encode a Preproprotein with Glycan Acceptor Sites:

The predicted translation product of the LIM9 cDNA (Figure 9) is comprised of 787 amino acid residues and is estimated to have a molecular weight of 84kDa. The mature amino terminus (as determined by N-terminal sequencing of the native LIM9 protein) does not immediately follow the putative initiator methionine, but instead is preceded by 149 amino acid residues. The first 22 of these residues (approximately 2.3kDa) are predominantly hydrophobic and likely constitute a signal peptide (preregion) lost during the protein's entry into the endomembrane system. The following 127 residues are thought to form a proregion which is cleaved from the mature amino acid terminus within the endomembrane system. The remaining 638 amino acid residues (approximately

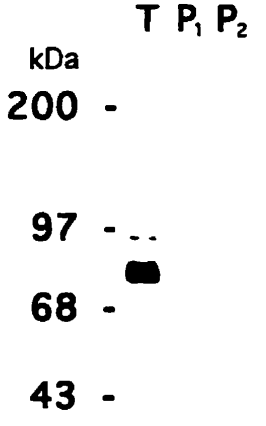

Figure 8 **The LIM9 protein is not a readily extracted component of mature pollen.** Total protein extracts were prepared from whole tetrad-stage anthers and mature pollen, subjected to SDS-PAGE, and immunoblotted with LIM9 antiserum as described in Materials and Methods. Despite a prolonged incubation in the substrate solution and an intense signal in the tetrads lane, signal was not generated within the pollen samples. **T**, 15μg of tetrad stage anther extract; P_1, 15μg of pollen extract; P_2, 30μg of pollen extract.

```
  1  MAFSIALQLITLLAYLNAFVLGGKFMVLMEEDPVITYKIKNSDDAQKYKQRVIS
 55  QHDIFLESLLPIGSYKKLYSYTHLLNGFAIHATSDEAVEILRDAHGVRVVQEDV
109  KMMKMTTHHTPDYLGLQIGVWPELGGAERSGDGVVIGMIDTGINPNHPSFMN
160  PWSREVADLKRFKGRCVPGDQFPLTSCNGKIVGAQYFAHGAIAVGEFNATRDYA
214  SPFDADGHGSHTASTAAGNYRYAVLSNGYNFGYASGMAPGAWIAVYKALYSFGG
268  YMSDVVAAVDKAVEDGVDIISLSVGPSAVPSGPTAFLDILEVELLFATKAGVTV
322  VQAIGNGGPSSSSILSFSPWIMSVAASTIDRQYNNTIILSNGHSISGIGLSPPT
376  PERELIPIAAAEDVCSRNITSFVVLRSCQSPDPFISSLVRGKLIICILTTDSSSP
430  MSIEAILSTIQKIGAVGVIITMDHDIEPEPPSGGASAFPVPGIVLINSDASEAL
481  WEYYSGHTLRGRNGAVISFGATGRILDGRRAIYTGQSPMVARYSSRGPDVNNAL
538  LQTADVLKPNILAPGTSIWAAWSSNSTEGENFALQSGTSMATPHVAGIAALIKQ
592  MHPNWSPAAIASAIMTTAQVVDSYDHALLAQGATTDPSTATPFDYGAGAINPAQ
646  AINPGLIFDADFKNYIQFLCAVPGVDEESVRAAVGVGCPSQHTDWCSDLNTPSV
700  TVANLVGSRRVLRKVMSVGDEQETYKAMVKSPSGVSVIVTPSAFTINPNITSKGL
754  AILLDAVEVTNAYTFGEVVLNGDKKHVVRIPLVVFVSSTLN
```

Figure 9 **The predicted amino acid sequence of the LIM9 translation product.** The LIM9 gene is predicted to encode an 84kDa preproprotein. Following the initiator methionine (outlined at position 1) is a putative 2.3kDa signal peptide of 22 amino acid residues (underlined) and a 10kDa proregion of 93 residues. The mature amino terminus was identified by N-terminal sequencing as the outlined sequence TTHPDYLG. The mature 678 amino acid (72kDa) sequence contains six consensus sites for the addition of glycans (doubly underlined) and four residues which are highly conserved among subtilisin-like serine proteases (bold and underlined).

72kDa of sequence) constitute the mature LIM9 protein. The presence of six consensus sites for the addition of glycans indicate that the mature product of the LIM9 gene may be a glycoprotein.

B The Maturation of the LIM9 Protein: The Empirical Evidence:

i) The LIM9 Antibody Identifies Three Polypeptides:

Immunoblotting experiments presented a temporal pattern of LIM9 expression similar to that observed within the intact anther by immunocytochemistry. The LIM9 antiserum failed to generate a signal on immunoblots prepared using total protein extracts from the locules of premeiotic anthers and anthers at the early zygotene stage of microsporogenesis. However, when locule protein extracts from anthers at the tetrad stage of microsporogenesis were immunoblotted, the LIM9 antiserum consistently identified three distinct bands: a faint 92kDa band; a faint 84kDa band and an intense 82kDa band (Figure 10). Additional immunoblotting experiments (see below), support the hypothesis that the 84kDa band contains the initial LIM9 gene product, the 92kDa band contains a modified transitional polypeptide, while the 82kDa band contains the mature form of the LIM9 protein.

ii) The LIM9 Protein Acquires High-Mannose Glycans:

The glycosylation of proteins begins within the lumen of the ER with the acquisition of high-mannose glycans (see Figure 19). The presence of these glycans on a precursor of the mature LIM9 protein was demonstrated using Endoglycosidase H (Endo H), an enzyme which specifically cleaves the chitobiose core of high-mannose glycans but is incapable of cleaving complex glycans (Tarentino *et al.*, 1974). Total protein extracts prepared from the locules of tetrad stage anthers were incubated with Endo H. On immunoblots of these digested

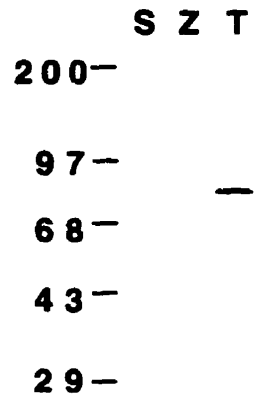

Figure 10 **The LIM9 antiserum recognizes three polypeptides from the locules of tetrad stage anthers.** Total protein extracts were prepared from the locule contents of *Lilium* anthers at the premeiotic S-phase (**S**), early zygotene (**Z**), and tetrad (**T**) stages of microsporogenesis. 10μg aliquots of each were subjected to SDS-PAGE and immunoblotted with LIM9 antiserum. The antiserum failed to generate signal within the S-phase and zygotene lanes. Within the tetrads lane, however, three immunoreactive bands are visible: a dark 82kDa band, and much fainter 84kDa and 92kDa bands.

samples (Figure 11), the LIM9 antiserum identified the 82kDa and 84kDa bands and a new 72kDa band but failed to recognize the 92kDa band.

The susceptibility of the 92kDa polypeptide to Endo H digestion suggests that it may result from the 82kDa proprotein's acquisition of 10kDa of high-mannose glycans. The loss of the proregion from this polypeptide would result in an 82kDa glycoprotein, the Endo H digestion of which may have yielded the faint 72kDa immunoreactive band. The 82kDa band, however, remained after Endo H digestion indicating that it is not comprised solely of a high-mannose glycoprotein. Evidence is presented below that the majority of the 82kDa immunoreactive band is comprised of the mature form of the LIM9 protein which possesses Endo H resistant complex glycans.

iii) The Mature LIM9 Protein Possesses Complex Glycans:

High-mannose glycans can be modified to complex glycans only within the Golgi apparatus. In plants, this occurs by the addition of xylose and/or other sugars to the chitobiose core and renders the glycans resistant to Endo H. To determine if any of the LIM9 polypeptides possessed complex glycans, total protein extracts from the locules of premeiotic, early zygotene stage, and tetrad stage anthers were immunoblotted with a xylose antiserum (949 antiserum; see Lauriere *et al.*, 1989). The antiserum failed to identify the 84kDa and 92kDa polypeptides in each of the samples but did recognize an 82kDa glycoprotein in the tetrad stage sample (Figure 12).

That the 84kDa polypeptide is unaffected by Endo H and is not recognized by the 949 antiserum suggests that it lacks both high-mannose and complex glycans. Together with its apparent molecular weight, these observations strongly implicate it as the initial translation product of the LIM9 gene. The 82kDa polypeptide identified by the xylose antiserum possessed a temporal pattern of expression similar to that of the LIM9 protein. The 82kDa LIM9

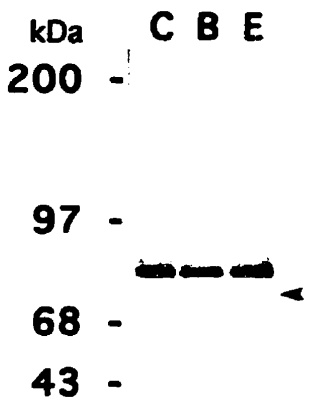

Figure 11 **Endo H treatment reveals the presence of high-mannose glycans on the 92kDa LIM9 protein.** A 7.5µg aliquot of a total protein extract from the locules of tetrad stage anthers was incubated with Endoglycosidase H (see Materials and Methods). Additional tetrad stage 7.5µg aliquots were incubated in buffer solution alone (buffer control) or remained untreated (control). Samples were subjected to SDS-Page and immunoblotted with LIM9 antiserum. The antiserum identified an 82kDa band, an 84kDa band and a 92kDa band in both control samples. Following Endo H treatment, the 92kDa band was no longer identified and a new 72kDa immunoreactive band (arrow) was present. **C**, control (untreated); **B**, buffer control; **E**, Endo H-treated.

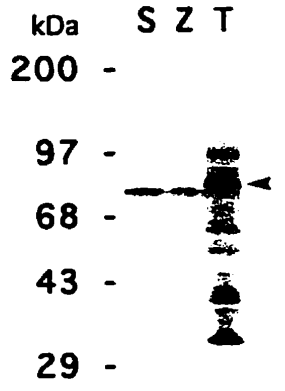

Figure 12 **A xylose antiserum identifies an 82 kDa glycoprotein from tetrad stage anthers.** Total protein extracts were prepared from the locule contents of anthers at the premeiotic S-phase (**S**), early zygotene (**Z**), and tetrad (**T**) stages of microsporogenesis. 10μg aliquots of each were subjected to SDS-PAGE and immunoblotted with 949 anti-serum. An 82kDa band (arrow) is identified only in the tetrads lane.

protein thus appears to possess Endo H resistant complex glycans. As complex glycans are generated only within the Golgi apparatus, this 82kDa glycoprotein is likely the mature modified product of the LIM9 gene. An additional immunoblotting experiment (see below and Figure 13) strengthens this conclusion by indicating that it is the 82kDa protein which is secreted into the anther locule.

iv) The Mature LIM9 Protein Occurs Extracellularly:

Immunocytochemistry experiments provided evidence that the mature LIM9 protein is secreted into the anther locule. To further test this finding, the locule contents of late anthers (zygotene to tetrad stage) were separated into intracellular and extracellular fractions by centrifugation and subjected to immunoblotting with the LIM9 antiserum. Although the LIM9 antiserum identified all three protein bands in the intracellular fraction, only the 82kDa band was identified in the extracellular fraction (Figure 13). Together with the results of the immunoblotting experiments described above, this observation provides strong evidence that the 82kDa polypeptide is the mature secreted form of the LIM9 protein while the 84kDa and 92kDa polypeptides are intracellular precursors.

C Summary of LIM9 Protein Maturation:

The LIM9 protein is thought to be synthesized in the cytoplasm as an 84kDa precursor (Figure 14). A 2.3kDa signal peptide allows the protein to enter the endomembrane system. The signal peptide is cleaved off and high-mannose glycans are added in the endoplasmic reticulum to yield a 92kDa glycoprotein. A proregion of approximately 10kDa is then cleaved off and the protein is transferred to the Golgi apparatus where some or all of the high-mannose glycans are modified to complex glycans. The resulting 82kDa mature glycoprotein exits the Golgi apparatus and is secreted into the anther locule.

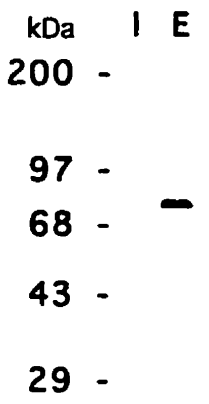

Figure 13 **The 82kDa LIM9 protein is an extracellular component of the locule.** Locule contents were collected from late anthers (zygotene to tetrad stages). Whole cells were pelleted and homogenized to generate an intracellular total protein extract. An extracellular total protein extract was obtained by precipitating soluble proteins from the locular fluid. 10μg aliquots of each extract were subjected to SDS-PAGE and immunoblotted with LIM9 antiserum. The antiserum recognized 82kDa, 84kDa, and 92kDa bands within the intracellular lane but identified only the 82kDa band within the extracellular lane. **I**, intracellular extract; **E**, extracellular extract .

Figure 14 **A putative maturation pathway for the LIM9 protein.** The LIM9 protein is translated within the cytosol as an 84 kDa preproprotein (**a**). Cleavage of the 2.3kDa signal peptide as the protein enters the ER results in an 82kDa polypeptide (**b**). Within the ER, the proprotein acquires 10kDa of high-mannose glycans (**c**). The 10kDa proregion is cleaved off and the glycoprotein is transferred to the Golgi apparatus where its high mannose glycans are converted to complex glycans (**d**). The resulting 82kDa mature glycoprotein is secreted into the anther locule. (● glycan core, ● mannose sugar residues, o xylose and other sugar residues).

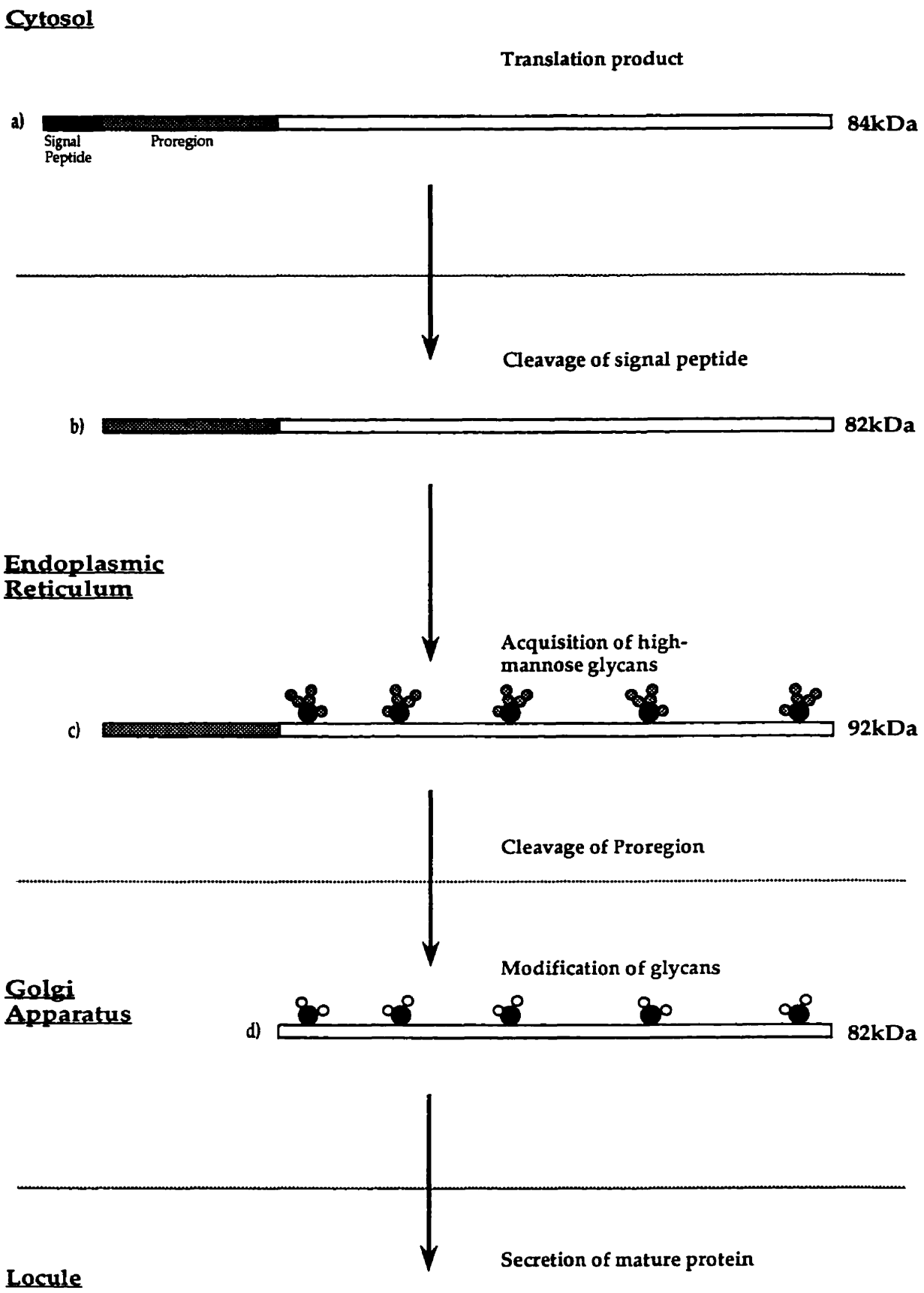
Cytosol
Translation product
a)
Signal Peptide
Proregion
84kDa
Cleavage of signal peptide
b)
82kDa
Endoplasmic Reticulum
Acquisition of high-mannose glycans
c)
92kDa
Cleavage of Proregion
Golgi Apparatus
Modification of glycans
d)
82kDa
Secretion of mature protein
Locule

III Is the LIM9 Protein a Protease?:

The predicted sequence of the LIM9 protein contains four regions (see Figure 9 and Figure 17) which are highly conserved among the subtilisin-like family of serine proteases (see Discussion). To provide empirical evidence that the LIM9 protein exhibits proteolytic activity, an electrophoretic protease assay was performed using *Lilium* anther protein extracts. Proteases, separated by size through a gelatin-containing polyacrylamide gel, were renatured and activated *in situ*. Staining the gel yielded a zymogram on which the locations of proteases were revealed as unstained regions where the gelatin had been degraded.

Zymograms were generated using intracellular and extracellular protein extracts from *Lilium* anther locules containing microsporocytes at the premeiotic, zygotene, and tetrad stages of development (Figure 15 and Figure 16). Each of the lanes containing intracellular protein preparations contained a single weak band which migrated with an apparent molecular weight greater than 200kDa (Figure 15). As the protease responsible for this activity is not observed within the extracellular fraction and its expression is stage-independent, it likely performs a `housekeeping' role essential to the general metabolism of the microsporocytes and microspores. Extensive proteolytic activity occurred only within the extracellular samples where it peaked in intensity at the tetrads stage. The majority of this activity occurred within a diffuse band with an apparent molecular weight of approximately 60kDa. Narrower bands of higher molecular weight were also present; one of which migrated with an apparent molecular weight of 82kDa (Figure 16). The occurrence of the 82kDa band only within the lane containing extracellular proteins of the tetrad stage provides strong evidence that it was generated by the mature LIM9 protein.

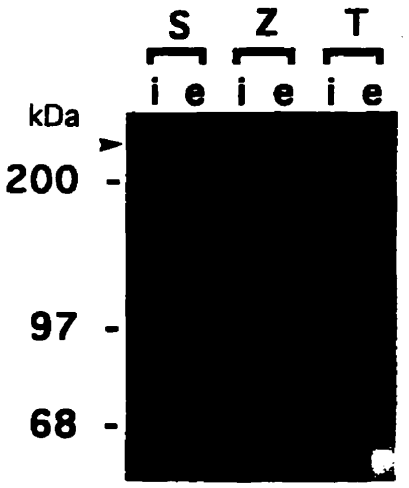

Figure 15 **Zymogram of intra- and extracellular locule extracts.** Intracellular (i) and extracellular (e) samples were prepared from the locule contents of *Lilium* anthers at the premeiotic S-phase (**S**), zygotene (**Z**), and tetrad (**T**) stages of microsporogenesis. Electrophoresis was performed with 10μg aliquots of each sample using a 7% polyacrylamide gel containing 0.10% gelatin. Proteins were renatured *in situ* as described in Materials and Methods. Proteolytic activity was observed in each of the intracellular extracts at a molecular weight greater than 200kDa (arrow). The extracellular fraction exhibited intense proteolytic activity at the tetrad stage (at approximately 60kDa, bottom of lane).

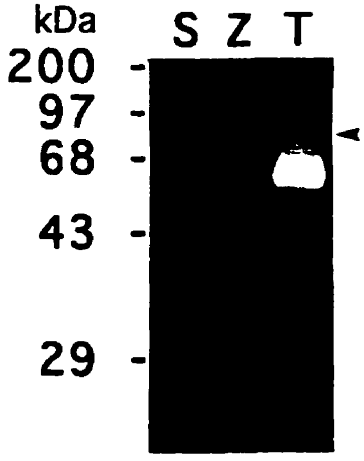

Figure 16 **Zymogram of extracellular locule extracts.** Extracellular samples were prepared from the locule contents of anthers at the premeiotic S-phase (**S**), zygotene (**Z**), and tetrad (**T**) stages of microsporogenesis. Electrophoresis was performed with 10μg aliquots of each sample using a 10% polyacrylamide gel containing 0.15% gelatin. Proteins were renatured *in situ* as described in Materials and Methods. Low levels of proteolytic activity were observed within the S-phase and zygotene lanes. Intense proteolytic activity was observed within the tetrad lane (the majority of which occurred at approximately 60kDa). A well-defined 82kDa band of protease activity (arrow) was present only within the tetrad lane.

The LIM9 protein might also be responsible for some of the protease activity observed at 60kDa. Within the anther locule, a portion of the C-terminus may be cleaved from the putative 82kDa protease by autoproteolysis. Such a cleavage occurs in the closely related serine protease cucumisin, resulting in a significantly shortened enzyme which retains its proteolytic activity (see Discussion).

Discussion

I Similarities Between the LIM9 Protein and Known Serine Proteases:

The predicted product of the LIM9 gene possesses three amino acid residues (aspartic acid, histidine, and serine) which are highly conserved among serine proteases where they form a "catalytic triad" or "charge relay system" essential for endopeptidase activity (Polgar, 1989; Fersht, 1985). The most extensively studied of the proteolytic enzymes (Polgar, 1989), serine proteases take their name from the uniquely reactive serine residue which, acting as an electron acceptor, participates directly in the hydrolysis of a peptide bond. This residue also reacts irreversibly with organophosphates such as the inhibitor diisopropyl fluorophosphate (DFP) (Walsh and Wilcox, 1970; Fersht, 1985). The reactivity of the serine residue is enhanced by the imidazole ring of the histidine which is held in position by a hydrogen bond to the aspartic acid residue. The mature protease is folded such that these three residues are brought together within a hydrophobic pocket, forming the active site of the enzyme (Fersht, 1985).

A The LIM9 Protein Shares Homology with the Serine Protease Subtilisin:

Although comprised of many distinct families, the (chymo)trypsin and subtilisin families are the most thoroughly studied of the serine proteases (Siezen *et al.*, 1991). The members of these two families are widespread and serve diverse functions in both prokaryotes and eukaryotes. Despite operating by an analogous catalytic mechanism, the (chymo)trypsins and subtilisins lack sequence homology and even differ in their secondary structure (Siezen *et al.*, 1991) and the linear arrangement of their reactive residues (see Figure 17 and

Figure 18). In addition to the catalytic residues common to both families, the subtilisins also possess a highly conserved asparagine residue which appears to be an essential stabilizing component of the substrate binding site (Robertus *et al.*, 1972). These striking differences have prompted several researchers to suggest that the two families arose through convergent evolution (e.g. Julius *et al.*, 1984).

It is to the subtilisins that the LIM9 protein exhibits greatest homology. Subtilisins are alkaline endoproteases produced by species of the genus *Bacillus*, where they are linked with the onset of sporulation (Wells *et al.*, 1983). The subtilisins have considerable industrial importance (Siezen *et al.*, 1991) and, through extensive enzymatic studies and x-ray crystallographic studies, have become one of the most thoroughly characterized families of bacterial proteases (Ikemura *et al.*, 1987; Wells *et al.*, 1983). All subtilisins appear to be generated as preproproteins. Subtilisin BPN' from *B. amyloliquefaciens*, for example, is originally translated as a 377 amino acid polypeptide containing a putative signal peptide (preregion) of 27 amino acid residues and a proregion of 75 residues (Wells *et al.*, 1983). The mature 275 amino acid (27.5kDa) protease is a roughly spherical molecule comprised of a single polypeptide folded into three structurally distinct parts, with its active site at their conjunction (Wright *et al.*, 1969). Mature subtilisins are secreted into the extracellular medium where they likely scavenge extracellular proteins and may assist cell lysis and subsequent spore release (Wells *et al.*, 1983; Power *et al.*, 1986). These proteolytic enzymes possess a broad substrate-specificity and have been shown to attack the bonds between a variety of amino acids (Walsh and Wilcox, 1970).

B The LIM9 Protein is One of Several Recently Described Subtilisin-Like Proteins:

Although once thought to be restricted to the prokaryotes, subtilisin-like proteases have recently been identified in a number of eukaryotic organisms, including: fungi (e.g. St. Leger *et al.*, 1992; Joshi, 1995); yeast (e.g. Mizuno *et al.*, 1988); nematodes (e.g. Yang and Kramer, 1994; Thacker *et al.*, 1995); insects (e.g. Roebroek *et al.*, 1991; Chen and Raikhel, 1996); mammals (e.g. Wise *et al.*, 1990); and higher plants (see below). In total, more than 70 subtilisin-like proteases or "subtilases" are currently known (Siezen, 1996; Siezen *et al.*, 1991). Each of these share sequence homology to the subtilisins within the vicinity of their conserved residues (Figure 17). Nearly all subtilisin-like proteases are generated as preproproteins (Siezen *et al.*, 1991) and, although larger than the subtilisins, each shares a similar arrangement of the four characteristic residues of the subtilisin active site (Figure 18). An increased linear displacement of the stabilizing asparagine residue and reactive serine residue, however, appears to be characteristic of the plant members (Tornero *et al.*, 1996). In addition to the LIM9 protein and its tomato cognate TMP (tomato meiotic proteinase; Riggs and Horsch, 1995), these plant proteases include the PR-P69 protein from tomato (Tornero *et al.*, 1996), cucumisin from melon fruits (Yamagata *et al.*, 1994), and the products of the ag12 gene in *Alnus glutinosa* and the ara12 gene in *Arabidopsis* (Ribeiro *et al.*, 1995).

Tomato (*Lycopersicon esculentum*) PR-P69 is a pathogenous related (PR) protein expressed within the leaves and stems of viroid-infected plants (Vera and Conejero, 1988; Tornero *et al.*, 1996). Immunocytochemistry experiments suggest that the protease is secreted into extracellular spaces and is also sequestered within vacuoles where it associates with inclusion bodies (Vera *et al.*, 1989). The 745 amino acid product of the PR-P69 gene contains a putative 22 amino acid

		D-Region	H-Region
1)	LIM9	..(139)DGVVIGMI**D**TGI(150)...(217)DADG**H**GSHTASTAAG(231)..
2)	TMP	..(140)AGVVIGMI**D**TGI(151)...(223)DADG**H**GSHTASTAAG(237)..
3)	PR-P69	..(138)KGVIIGVI**D**TGI(149)...(199)DDDG**H**GTHTASTAAG(213)..
4)	Cucumisin	..(132)SNIVVGVL**D**TGI(143)...(200)DTNG**H**GTHTASTAAG(214)..
5)	Ag12	..(137)EDVIIGVI**D**SGV(148)...(212)DTLG**H**GTHTASTAAG(226)..
6)	Aral2	..(122)SDVVVGVL**D**TGV(133)...(199)DDDG**H**GTHTSSTAAG(213)..
7)	Subtilisin BPN'	..(024)SNVKVAVI**D**SGI(035)...(060)DNNS**H**GTHVAGTVAA(074)..
8)	KEX2	..(167)AGVVAAIV**D**DGL(178)...(209)YDDY**H**GTRCAGEIAA(223)..
9)	Furin/PACE	..(145)HGIVVSIL**D**DGI(156)...(190)NDNR**H**GTRCAGEVAA(204)..
10)	Trypsin	(082)FNGNYLDN**D**IML(093) (042)VSAA**H**CYKSRIQVRL(056)

		N-Region	S-Region
1)	LIM9	..(325)IG**N**GGPSS(332)...(571)SGT**S**MATPHVAGIA(584)..
2)	TMP	..(331)AG**N**GGPSS(338)...(579)SGT**S**MATPHIAGIA(592)..
3)	PR-P69	..(304)AG**N**NGPST(311)...(529)SGT**S**MSCPHLSGVR(542)..
4)	Cucumisin	..(305)AG**N**GGPNF(312)...(522)SGT**S**MSCPHITGIA(535)..
5)	Ag12	..(316)AG**N**AGPFF(323)...(534)SGT**S**MACPHASGVA(547)..
6)	Aral2	..(301)AG**N**AGPSS(308)...(528)SGT**S**MSCPHVSGLA(531)..
7)	Subtilisin BPN'	..(153)AG**N**EGTSG(160)...(525)NGT**S**MASPHVAGAA(538)..
8)	KEX2	..(312)SG**N**GGTRG(319)...(382)GGT**S**AAAPLAAGVY(395)..
9)	Furin/PACE	..(293)SG**N**GGREH(300)...(365)TGT**S**ASAPLAAGII(378)..
10)	Trypsin	(180)QGD**S**GGPVVCNGQL(193)

Figure 17 **Sequence alignment of the LIM9 protein with other subtilisin-like proteases.** Sequences are shown surrounding the conserved aspartic acid (D), histidine (H), asparagine (N), and serine (S) residues of the active site. The LIM9 protein (1) exhibits high sequence homology with the tomato cognate TMP (2) and other plant proteases (3-6). To a lesser extent, homology is exhibited to subtilisin BPN' from *Bacillus amyloliquefaciens* (7), the yeast KEX2 gene product (8), and human furin/PACE (9). Trypsin (10), an unrelated serine protease, shares very little sequence homology with the LIM9 protein, its catalytic residues are arranged in the order his-asp-ser, and it lacks the conserved asparagine residue of the subtilisins and subtilisin-like proteases. [References: (1): Kobayashi *et al*, 1994; (2): Riggs and Horsch, 1995; (3): Tornero *et al.*, 1996; (4): Yamagata *et al.*, 1994; (5,6): Ribeiro *et al.*, 1995; (7): Wells *et al.*, 1983; (8) Mizuno *et al.*, 1988; (9): Wise *et al.*, 1990; (10): Hermodson *et al.*, 1973].

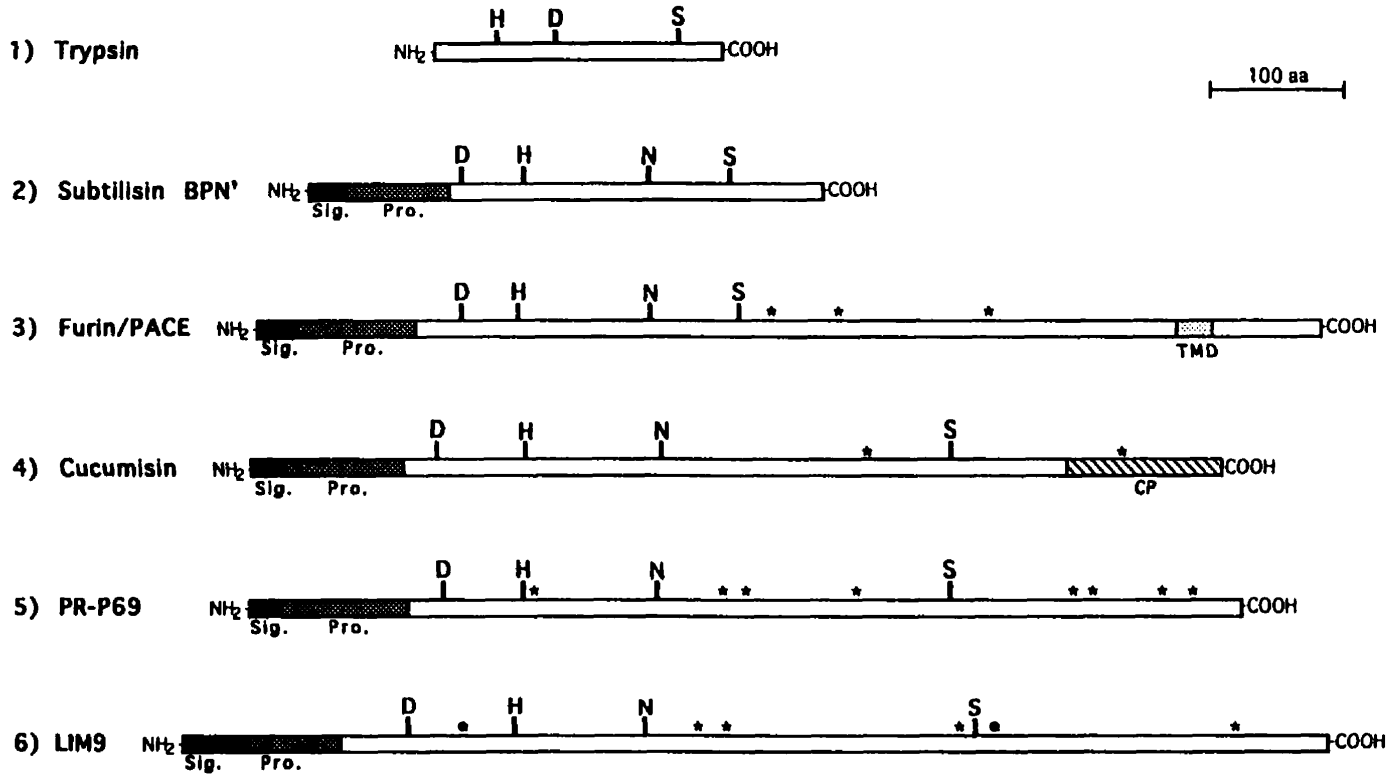

Figure 18 **Schematic representations of subtilisin and four subtilisin-like proteases.** The positions of the conserved aspartic acid (D), histidine (H), asparagine (N), and serine (S) residues are shown. Signal peptides (Sig.), proregions (Pro.), and potential glycan acceptor sites (*) are also included. Trypsin (1), differs from the subtilisins in the linear arrangement of its catalytic residues and lacks a conserved asparagine residue. The linear displacement of the serine residue from the asparagine residue is characteristically large in the plant subtilisin-like proteases (3-6). Furin/PACE (3) possesses a transmembrane domain (TMD) which likely anchors it within the Golgi apparatus. Cucumisin (4) possesses a 14kDa carboxyl peptide (CP) which is cleaved from the mature protease following its secretion from the cell. [References: (1): Hermodson *et al.*, 1973; (2): Wells *et al.*, 1983; (3): Wise *et al.*, 1990; (4): Yamagata *et al.*, 1994; (5): Tornero *et al.*, 1996; (6): Kobayashi *et al.*, 1994].

signal peptide and a 92 amino acid proregion (Figure 18). The remaining 631 amino acid sequence of the mature 69kDa proteinase contains seven potential N-linked glycosylation sites (Tornero *et al.*, 1996). Through *in vitro* assays, Vera and Conejero (1988; 1990), demonstrated that the PR-P69 protease is capable of degrading fibrinogen and fluorescein thiocarbanoyl derivative (FTC)-casein (at an optimum pH of 8.5-9.0) and can also cleave the large subunit of ribulose 1,5-bisphosphate carboxylase/oxygenase (Rubisco) into several smaller polypeptides. Despite its broad substrate-specificity, Tornero *et al.* (1996) speculate that PR-P69 does not degrade the proteins of invading pathogens directly, but instead participates in the post-translational modification of additional proteins involved in the defense response (see below).

Cucumisin accumulates within the extracellular juices of melon fruits (Yamagata *et al.*, 1989). Originally isolated from the fruit of *Cucumis melo* (musk melon: Kaneda and Tominaga, 1975), similar enzymes have since been discovered in the fruits of *Benincasa cerifera* (white gourd: Kaneda and Tominaga, 1977) and *Trichosanthes cucumeroides* (snake gourd: Kaneda *et al.*, 1986). Mature cucumisin is a glycoprotein with a carbohydrate content of approximately 1.4% (w/w) (Yamagata *et al.*, 1994). The prepro-form of cucumisin has a molecular weight of nearly 79kDa and is predicted to contain 731 amino acid residues. The 22 amino acid residues of the putative signal peptide are followed by a prosequence of 88 residues (see Figure 18). The remaining 621 residues comprise a 67kDa extracellular protein which exhibits proteolytic activity *in vitro* when supplied with a broad range of substrates (Yamagata *et al.*, 1994). The 67kDa protease is processed further by an autolytic cleavage which removes 116 non-essential amino acids from the carboxyl terminus, generating a 54kDa form of cucumisin in which proteolytic activity is undiminished (Yamagata *et al.*, 1989; see below). Cucumisin is exceptionally stable and remains

active over a wide range of pH (4-11) and temperatures. Even after 20 minutes at a temperature of 60°C and a pH of 11.1, cucumisin retains 80% of its optimum proteolytic activity (Kaneda *et al.*, 1995).

The ag12 gene was identified in *Alnus glutinosa* root nodules where it was shown by RNA blot hybridization and *in situ* hybridization to be expressed predominantly within actinorhizal-infected cells during early nodule development (Ribeiro *et al.*,1995). Apart from very low levels of expression within the shoot tips, the gene does not appear to be expressed within other organs of *A. glutinosa*. Using the amino acid sequence of the predicted translation product of ag12 to perform a database search, Ribeiro *et al.* (1995) identified a highly homologous *Arabidopsis* cDNA clone which they designated ara12. Two additional *Arabidopsis* sequences with 65% homology to ara12 were also identified. RNA blot hybridization suggests that the ara12 gene is transcribed in all organs of *Arabidopsis* with the highest levels of transcription occurring during early silique development (Ribeiro *et al.*, 1995).

C Subtilisin-Like Proteases May Function as Protein Convertases:

The KEX2 gene product of the yeast *Saccharomyces cerevisiae* is perhaps the best characterized member of the eukaryotic subtilisin-like proteases. Unlike the plant subtilisin-like proteases, the 135kDa enzyme is not secreted but instead appears to be retained within the Golgi apparatus where it is involved in the posttranscriptional modification of prohormones (Fuller *et al.*, 1989a). The protease is likely anchored within the membrane by a transmembrane domain (TMD) with its proteolytic NH_2-terminal domain extending into the lumen of the Golgi apparatus and its carboxyl terminus extending into the cytosol (Fuller *et al.*, 1989a). The Ca^{2+}-dependent (Fuller *et al.*, 1989b) activity of the protease is responsible for the cleavage of proregions from pro-α-factor and pro-killer toxin

(Julius *et al.*, 1984). The cleavages occur following pairs of basic amino acid residues (most commonly lysine-arginine and arginine-arginine: Wise *et al.*, 1990). These simple dibasic sites have been conserved during evolution, making it possible for the KEX2 protease to process mammalian proproteins such as proalbumin (Bathurst *et al.*, 1987) and proinsulin (Thim *et al.*, 1986).

The proregion is assumed to maintain hormone precursors in an inactive state during transport; its removal then allows the protein to attain its mature conformation. The enzymes responsible for the precise cleavage of proregions from the prohormones of higher animals have long eluded researchers (Barr, 1991). Subtilisin-like proteases, however, have recently been implicated in the proregion cleavage of several hormone and pheromone precursors in nematodes, insects, and mammals (Denault and Leduc, 1996). (This has prompted their alternate name of subtilisin-related proprotein convertases or SPCs). Seven such proteases have been discovered in mammals alone (Denault and Leduc, 1996). For example, the mammalian subtilisin-like proteases furin (or PACE: paired basic amino acid cleaving enzyme) and PC2/PC3 (protein convertase 2 and 3) have been shown to cleave the proregions from pro-von Wilebrand factor (Wise *et al.*, 1990), and proglucagon (Rouille *et al.*, 1995) respectively. With the exception of furin/PACE, mammalian subtilisin-like proteases appear to be secreted (Steiner *et al.*, 1992). Perhaps they function at specific extracellular sites in a manner similar to that of urokinase-type plasminogen activator (U-PA), a serine protease which cleaves the proregion from inactive blood plasminogen to yield active plasmin at wounds and other sites of tissue remodeling (Alberts *et al.*, 1994). Many of the mammalian subtilisin-like proteases have been implicated in the processing of viral glycoproteins, including the human immunodeficiency virus (HIV-1) envelop glycoprotein gp160 (e.g. Vey, 1995; Vollenweider *et al.*, 1996; Miranda *et al.*, 1996). As the production of infectious

HIV-1 virions is dependent upon the processing of gp160 by these host cell proteases, mammalian subtilisin-like proteases have rapidly become an area of intense study.

All plant subtilisin-like proteases appear to be secreted and, while not involved in intracellular proprotein processing, may be responsible for the precise modification of extracellular proteins or cell-surface proteins. The expression of ag12 and ara12 peaks during the early stages of root nodule development and silique development respectively. It therefore seems likely that these proteases play a role in protein processing rather than protein degradation (Ribeiro *et al.*, 1995). Tornero *et al.* (1996) have recently implicated the tomato PR-P69 protein in the cleavage of an extracellular matrix protein. These researchers propose that such an interaction may mediate signalling processes and modulate interactions of the cell surface with the extracellular environment.

II The Maturation of Preproproteins and Protein Secretion:

In eukaryotic cells, the endoplasmic reticulum, Golgi apparatus, and the vesicles, vacuoles and other organelles derived from them form a structurally and functionally connected system termed the endomembrane system. Within this system, proteins are posttranslationally modified and sorted to non-cytoplasmic compartments of the cell or the cell exterior (for review see Harris, 1986). Proteins enter the endomembrane system through the endoplasmic reticulum and are shuttled by vesicles to the Golgi apparatus and between its numerous cisternae. As proteins move unidirectionally through the system many are sequentially modified, each modification catalyzed by an enzyme localized to a compartment or sub-compartment. Specific sequences target some

proteins to be retained within a particular compartment. Proteins lacking such sequences flow passively through the system and are ultimately packaged into vesicles which fuse with the cell surface. Secretion is thus the "bulk flow" or "default" pathway through the endomembrane system (Jones and Robinson, 1989).

A Entering the ER Lumen: the Role of the Signal Peptide:

The translation of mRNAs encoded by nuclear genes occurs within the cytosol of the eukaryotic cell. Proteins destined for the lumina of eukaryotic organelles or for secretion must first cross the barrier imposed by the ER membrane. Similarly in prokaryotes, proteins destined for secretion must cross the cell membrane. In all cells, proteins appear to be targeted for translocation across lipid bilayers by a hydrophobic amino-terminal sequence termed the signal peptide (Briggs and Gierasch, 1986). A putative signal peptide of 22 amino acids is thought to mediate the LIM9 protein's entrance into the endomembrane system and its subsequent secretion into the anther locule.

The translation of a secretory protein is initiated within the cytosol as its mRNA is bound by a ribosome. Once the signal peptide protrudes sufficiently from the ribosome, it is recognized and bound by a ribonucleoprotein termed the signal recognition particle (SRP). The SRP also binds to the ribosome, temporarily arresting translation (Rapoport, 1991). The SRP then binds to an integral ER membrane protein, the SRP receptor or "docking protein". Additional proteins within the membrane may anchor the ribosome and form a hydrophilic protein-conducting channel through the membrane (Simon and Blobel, 1991).

Translation competence is restored as the binding of a guanosine triphosphate (GTP) to the SRP causes it to disassociate from the signal peptide

and ribosome (Rapoport, 1991). Hydrolysis of the GTP actuates the SRP's release from its receptor. Freed from the SRP, the signal peptide is bound by the lipid bilayer, perhaps directly (von Heijne, 1986; see below), or through interactions with integral membrane proteins (Rapoport, 1991). As the translation product elongates, it protrudes as a loop through the newly-formed membrane pore and into the lumen of the ER. During or after translation, signal peptidase catalyses the cleavage and digestion of the signal sequence, freeing the amino terminus of the new protein and making the translocation across the membrane irreversible (Rapoport, 1991).

With the exception of mitochondrial and chloroplast proteins, signal sequences range from 13 to 36 amino acid residues in length (von Heijne, 1986). Despite a lack of sequence homology, signal peptides function properly when interchanged between different proteins, even when these proteins are from evolutionarily distant organisms. One of the few characteristic features of signal peptides is a central region of uncharged hydrophobic residues known as the hydrophobic core (Walter and Lingappa, 1986). (Of the 22 amino acids of the LIM9 protein's putative signal peptide, 17 are hydrophobic and likely constitute this region). The hydrophobic core may take the form of an α-helix or β-strand capable of partitioning into and spanning the lipid bilayer, thereby anchoring the nascent protein to the membrane (Bedouelle and Hofnug, 1981). The core region may also interact with a hydrophobic pocket of the signal recognition particle (Finklestein *et al.*, 1983).

B The Proregion: an Intramolecular Chaperone?:

Proregions appear to be common to the precursors of all plant proteases (Yamagata *et al.*, 1994). In mammals, proregions are known to maintain enzymes in an inactive state until they are secreted from the expressing cell or

reach their target location. Several serine proteases, for example, are stored within the mammalian pancreas as inactive proproteins termed zymogens. These protease precursors are unable to attain a mature conformation until the proregion is removed (Fersht, 1985). While an inhibitory role also seems likely for the proregions of the subtilisins and subtilisin-like proteases, these sequences also appear to participate directly in protein maturation and are a prerequisite for the generation of active proteases.

i) The proregion plays an essential role in subtilisin maturation:

Several experiments suggest that the proregions of subtilisins act as "intramolecular chaperones" which guide the proper folding of the proteases during their maturation (Ohta *et al.*, 1991). Ikemura *et al.* (1987) ligated portions of the subtilisin E gene into an *E. coli* expression vector containing the *E. coli* OmpA signal peptide and expressed them in *B. subtilus*. When the entire coding region for prosubtilisin was expressed, proteolytic subtilisin was detected in the periplasmic space. However, if the proregion sequence was omitted, the mature subtilisin which was secreted was incapable of proteolytic activity. Although both mature polypeptides were shown to possess the same primary structure, subtilisin expressed without the prosequence probably lacked the secondary structure required for enzymatic activity. This hypothesis is further supported by the findings of Ikemura and Inouye (1988). These researchers observed that prosubtilisin E expressed in *E. coli* and denatured with 6M guanidine-HCL was self-processed into mature active subtilisin when dialysed in a Na-phosphate renaturing solution. However, when the mature form of subtilisin (i.e. lacking the proregion) was similarly expressed and denatured, renaturation was unsuccessful. The exogenous addition of a synthetic subtilisin E propeptide *in vitro* permitted the successful renaturation of mature subtilisin E and other

mature subtilisins expressed without their proregions (Ohta *et al.* 1991; Zhu *et al.*, 1989).

Autoproteolysis appears to effect the final step in the maturation of subtilisin, the removal of the proregion. Power *et al.* (1986) found that preprosubtilisin expressed *in vivo* did not undergo proregion cleavage if it possessed a mutation of one its catalytic residues. The proregion of this inactive protease was, however, cleaved *in vitro* by the addition of functional subtilisin.

ii) The structure of the subtilisin proregion:

Although sequence homology is not observed among the proregions of subtilisins and subtilisin-like proteases, the proregions may share a common overall structure which facilitates their functioning. Using localized polymerase chain reaction (PCR) random mutagenesis, Lerner *et al.* (1990) identified several single residue mutations within the prosequence of subtilisin E which effected the protease's activity. The majority of these mutations were found to occur within clusters of hydrophobic residues. (A similar clustering of hydrophobic residues occurs within the proregion of the LIM9 protein). Kobayashi and Inouye (1992) hypothesize that the proregion may interact directly with the mature portion of the protease through these hydrophobic regions. Alternatively, the folding may be facilitated by electrostatic interactions between the proregion and the mature polypeptide. The proregion of subtilisin E has an abundance of charged residues: of the 77 residues comprising the proregion, 23 (30%) are charged (Ikemura *et al.*, 1987). Similarly, nearly 31% (21 out of 77) of the residues in the putative proregion of the LIM9 protein are charged.

C Protein Glycosylation

The majority of secreted eukaryotic enzymes contain asparagine (N)-linked oligosaccharides or glycans (Jones and Robinson, 1989). N-linked glycans

are grouped into two major categories. High-mannose glycans possess 6-9 mannose (Man) residues and two N-acetylglucosamine (GlcNAc) residues. Complex or modified glycans are derived from high-mannose glycans with which they share a common pentasaccharide core structure (Kornfeld and Kornfeld, 1985):

In addition to this core structure, complex glycans contain one or more other sugar residues (fucose, xylose and arabinose in plants).

i) The assembly of plant glycoproteins:

The assembly of high-mannose glycans and their modification to complex glycans is achieved through a cascade of enzyme-catalyzed events (Figure 19). Immunocytochemical techniques have allowed most of the enzymes responsible for glycosylation to be localized to compartments or even sub-compartments of the endomembrane system (for review see Jones and Robinson, 1989). The glycosylation process begins in the ER where the glycan precursor $Glc_3Man_9(GlcNAc)_2$ is assembled by the sequential addition of N-acetylglucosamine, mannose and glucose (Glc) to the integral ER membrane protein dolichol-phosphate (Elbein, 1988). Within the ER lumen, oligosaccharyl-transferase catalyses the cotranslational transfer of this precursor to an asparagine residue within an acceptor site on the nascent protein (Kornfeld and Kornfeld, 1985). Acceptor sites consist of the amino acid sequence Asparagine-X-Serine/Threonine, where X is any amino acid except proline or aspartic acid (Marshall, 1972). The rate at which the nascent protein assumes it proper folding and the acceptor sites become inaccessible to oligosaccharyltransferase may determine how many of these sites are actually glycosylated (Kornfeld and

Figure 19 **The Processing pathway of plant complex glycans.** The transfer of $(Glc)_3Man_9(GlcNAc)_2$ from dolichyl-phosphate (Dol-P-P) to the asparagine residue (N) of a nascent polypeptide is catalyzed by oligosaccharyl-transferase (**a**). Glucose residues (▶) are removed by α-glucosidases I and II (**b, c**). The glycoprotein is transported to the Golgi apparatus where three mannose residues (□) are cleaved from the high-mannose glycan by α-mannosidase I (**d**). A GlcNAc residue (○) is added by GlcNAc-transferase (**e**) and two additional mannose residues are cleaved by α-mannosidase II (**f**). A fucose residue (F) is added by fucosyl-transferase (**g**) and an additional GlcNAc is added by GlcNAc-transferase (**h**). Xylose (X) is added by xylosyl-transferase (**i**) and the two GlcNAc residues added in the Golgi apparatus are removed by N-acetylglucosaminidase (j) to yield a mature complex glycan $[Xyl(Man)_3Fuc(GlcNAc)_2]$ (modified from Chrispeels and Tague, 1991; Kornfeld and Kornfeld, 1985).

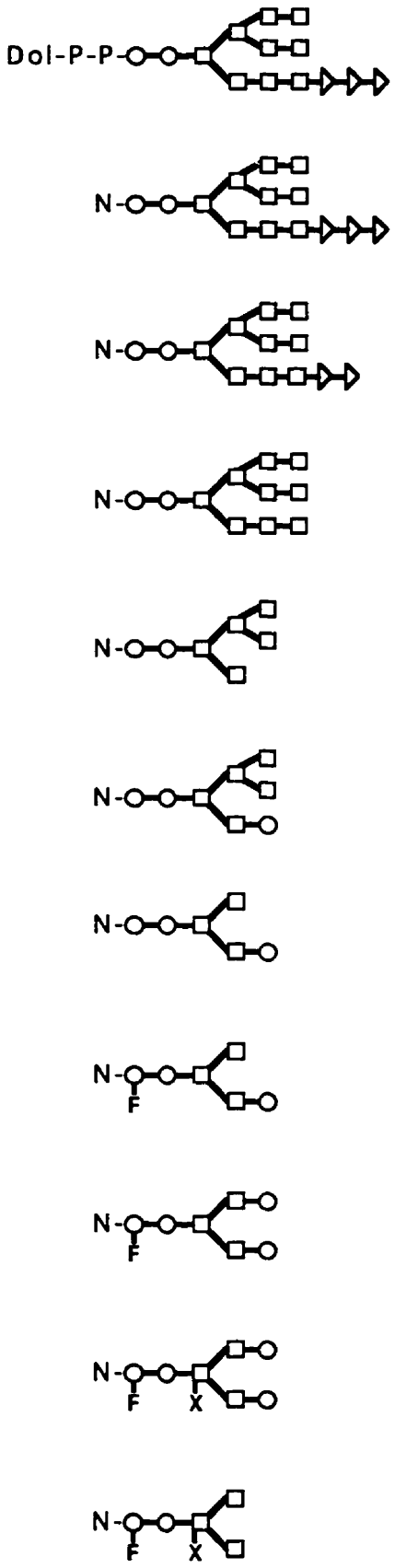
Dol-P-P
N
N
N
N
N
N
N
F
N
F
N
F
X
N
F
X
a) oligosaccharyl-transferase
b) α-glucosidase I
c) α-glucosidase II
d) α-mannosidase I
e) GlcNAc-transferase I
f) α-mannosidase II
g) fucosyl-transferase
h) GlcNAc-transferase II
i) xylosyl-transferase
j) N-acetylglucosaminidase
Endoplasmic Reticulum
Golgi Apparatus

Kornfeld, 1985). Immediately following the transfer of the oligosaccharide precursor to the nascent polypeptide, glucosidases I and II cleave the three glucose residues, generating a typical high-mannose glycan [$Man_9(GlcNAc)_2$].

Glycoproteins not targeted to remain within the ER are transported within vesicles to the cis face of the Golgi apparatus. Within the cis- and medial-cisternae, mannose residues are trimmed from the glycans by α-mannosidases I and II, leaving only the pentasaccharide core [$Man_3(GlcNAc)_2$]. In plants, transferases within the medial- and trans-cisternae then add one or more of the following sugar residues: N-acetylglucosamine, fucose, galactose, arabinose, and xylose (Xyl) (Chrispeels and Tague, 1991; Gleeson and Clarke, 1980). These additions typically yield plant complex glycans with the formula $Xyl(Man)_3$ $Fuc(GlcNAc)_2$ (Driouich *et al.*, 1989; Lauriere *et al.*, 1989). [The majority of antibodies raised to these glycans (e.g. the 949 antiserum) recognize the xylose residues; as this sugar does not occur in mammals it is probably highly immunogenic (Driouich *et al.*, 1989)]. Glycoproteins targeted for secretion are then packaged into vesicles which fuse with the plasma membrane and empty their contents through exocytosis.

High-mannose glycans can pass through the Golgi apparatus without being modified to complex glycans. Vitale *et al.* (1984), for example, identified glycans of both types on mature phytohemagglutinin from *Phaseolus vulgaris*. The complex glycans of this plant glycoprotein were also found to vary in composition, with some modified by the addition of a single fucose residue and others by the addition of a single xylose residue. As in this study of the LIM9 protein, the nature of the glycans on phytohemagglutinin was revealed by their susceptibility to the enzyme endoglycosidase H (Vitale *et al.*, 1984). As previously described, Endo H cleaves high-mannose glycans between the GlcNAc residues of

the core structure (Tarentino *et al.*, 1974). In complex glycans, the binding of additional sugar residues to the core likely prevents the binding of Endo H.

ii) The role of glycosylation:

Glycans do not appear to play a specific role in protein sorting or targeting for secretion as was once thought (Driouich *et al.*, 1989); many secreted proteins occur which are not glycosylated (e.g. barley aleurone α-amylase: Jones *et al.*, 1987). Glycosylation, however, may affect the efficiency of a protein's transport within the endomembrane system. For example, the glycosylation inhibitor tunacamycin greatly diminishes the transport of proconcanavalin A (pro-Con A) to protein bodies (Faye and Chrispeels, 1987). Perhaps glycoproteins alter the physiochemical properties of the protein, thereby making it more soluble or allowing it to fold correctly (Gibson *et al.*, 1981). Incorrectly folded proteins appear to be inefficiently transported to the Golgi apparatus and may be selectively retained within the endoplasmic reticulum (Lodish, 1988). Alternatively, glycosylation may make proteins more hydrophilic and prevent interactions with hydrophobic domains of the ER which would retard their transport (Jones and Robinson, 1989). The glycans of glycoproteins may also provide protection against proteolytic degradation (Driouich *et al.*, 1989). Finally, glycans may play a role in post-translational proteolytic processing (Faye and Chrispeels, 1987) or the biological activity of the mature protein (Tsaftari *et al.*, 1980).

D Extracellular Protein Modification: The Autolysis of Cucumisin:

As the fruit of *Cucumis melo* matures, the concentration of 67kDa cucumisin decreases with a concurrent increase in the concentration of the mature 54kDa form of cucumisin. Similarly, the concentration of 67kDa cucumisin diminishes *in vitro* with a parallel increase in the concentrations of

54kDa cucumisin and a 14kDa polypeptide (Yamagata *et al*, 1989). If, however, serine protease inhibitors are included in the incubations, this transition does not occur. It therefore seems likely that the 54kDa and 14kDa proteins arise from the limited autolysis of 67kDa cucumisin. The conversion of cucumisin from its 67kDa form to its 54kDa form *in vitro* or *in vivo* is not accompanied by a decrease in proteolytic activity. The 54kDa cucumisin, however, is less stable than 67kDa cucumisin at acidic pH and high temperatures (Yamagata *et al.*, 1989).

The LIM9 protein is closely related to cucumisin and thus may be modified in a similar fashion. When zymograms were prepared using samples containing the LIM9 protein, a major band of proteolytic activity was observed at approximately 60kDa. Perhaps a 60kDa protease is generated by an extracellular autolytic cleavage of the LIM9 protein in a manner similar to that observed for cucumisin.

III Possible Functions of the LIM9 Protein:

The LIM9 protein occurs within the tapetum, locular fluid and, to a lesser extent, within the microsporocytes and microspores. Immunoblotting experiments indicate that the 82kDa LIM9 protein and its 84kDa and 92kDa precursors occur within the microsporocytes (i.e. the intracellular fraction of the locule) after their cytoplasmic connections to the tapetal cells have been severed (see Figure 13). This strongly suggests that, rather than being transferred symplastically or apoplastically from the tapetum to the microspores, the LIM9 protein is simultaneously expressed in both cell types. If verified by *in situ* hybridization experiments, LIM9 would become one of very few cloned anther-specific genes known to be expressed by both the sporophyte and the gametophyte (Roberts *et al.*, 1993).

Microsporogenesis and the onset of dehiscence appear to require the transcriptional activation of numerous tissue-specific gene sets that are inactive during anther histogenesis (Goldberg *et al.*, 1993). Although the LIM9 protein was recognized by an antiserum to proteins which bound DNA cellulose (Riggs and Horsch, 1995), it certainly does not appear to be among the transcription factors involved in this transformation. (More likely, it merely shares epitopes with one or more DNA-binding proteins). Immunolocalization studies failed to identify any association between the LIM9 protein and the nuclei of either the tapetal cells or the microsporocytes and microspores. Instead, the protein is modified within the endomembrane system of the cytoplasm and secreted into the anther locule. A strong sequence homology to subtilisin-like enzymes and the preliminary results of SDS-PAGE functional assays implicate the LIM9 protein as an extracellular serine protease.

Serine proteases serve several functions in biological systems, from the precise cleavage and modification of protein precursors to the complete proteolytic degradation of proteins into their constituent amino acids. While *in vivo* studies have indicated that some subtilisin-like serine proteases act as protein convertases, *in vitro* studies suggest that others (e.g. cucumisin and PR-P69) are capable of extensive non-specific proteolysis. At present, neither activity can be ruled out for the LIM9 protein. Microsporogenesis and dehiscence are complex processes requiring the coordinated turnover of a large population of enzymes, metabolites and structural proteins. As the LIM9 protein is present within the locule for an extensive period of microsporogenesis and pollen development, it could be responsible for the modification or degradation of any of a large number of proteins. Perhaps the timing of the LIM9 protein's activity is more precisely constrained by the pH of the locule (as has been observed for

callases; Izhar and Frankel, 1971) or by Ca^{+2} concentration (as has been observed for other plant subtilisin-like proteases; e.g. Vera and Conejero, 1988).

The apparent restriction of the LIM9 protein to the tapetum and locule suggests that it plays a role in pollen development and not dehiscence. Extensive enzymatic activity occurs within the cytoplasm of the microsporocytes and microspores. During meiosis, numerous enzyme-catalyzed events coordinate chromosome segregation and cell division, while proteases and RNAses likely purge the microspore of the sporophytic transcription and translation machinery. Additional enzymes must catalyze two major episodes of amlyogenesis and amlyolysis and the recycling of the microspore cytoplasm (Pacini, 1990). It seems unlikely, however, that the LIM9 protein plays a direct role in these cytoplasmic events. The presence of a putative signal peptide and the results of immuno-blotting and immunocytochemistry experiments indicate that the mature LIM9 protein is secreted; zymogram experiments suggest that it remains inactive within the cell. The LIM9 protein could, however, coordinate events within the microspore indirectly through the degradation or modification of receptors on its surface, thereby providing a means of communication between sporophyte and gametophyte. This role, however, is also unlikely due to the apparent impermeability of the callose wall to polypeptides (Heslop-Harrison, 1966a).

It has been suggested that the callose wall of the developing microspores and the sporopollenin lining of the tapetum serve to prevent the transfer of pathogens from the sporophyte to the gametophyte. Perhaps the accumulation of the LIM9 protein in the locule plays a similar role. The highly homologous plant subtilisin-like protease PR-P69 plays a role in the pathogen defense response of tomato (Tornero *et al.*, 1996). Likewise the Ag12 gene product of *A. glutinosa* likely moderates the activities of infectious actinormycetes (Ribeiro *et al.*, 1995). By activating PR proteins, or by degrading foreign proteins directly, the

LIM9 protein might constitute an early defence against the establishment of pathogens within the locule.

The locular fluid in which the microsporocytes are suspended is a complex solution of metabolites, enzymes and precursors of the pollen wall and pollen coat. Perhaps the LIM9 protein maintains the composition of the locular fluid by acting as an extracellular scavenger in a manner similar to that suggested for the bacterial subtilisin proteases. The putative protease may facilitate the turnover of enzymes or degrade other complex molecules within the locule, making the simple subunits (metabolites) available to the developing microspores. Alternatively, the LIM9 protein may play a role in the breakdown of the tapetum and the subsequent release of pollenkitt and tryphine. The temporal patterns of the protein's expression and the spatial patterns of its accumulation, however, suggest that the protein is most likely involved in the processing of enzymes and precursor molecules required for the assembly of the pollen wall.

The pollen wall is unique to the male gametophyte and its construction is likely catalyzed by several enzymes that are encoded by microspore- and tapetum-specific genes. Several anther-specific genes possessing a temporal pattern of expression similar to that of LIM9 have been implicated in the construction of the pollen wall. Only the products of the satap35 and satap44 genes from mustard, however, have been shown by immunocytochemistry to interact directly with pollen wall components (Staiger and Apel, 1993; Staiger *et al.*, 1994). The expression of these genes appears to occur exclusively within the tapetum, beginning during prophase I of microsporocyte meiosis. The proteins are secreted into the locule where they reach peak levels as the microspores are released from the tetrads. The proteins are initially associated with globules presumed to contain sporopollenin and may act as carriers, directing precursor molecules from the tapetal cells to the pollen wall. The satap proteins appear to

be ultimately incorporated into the exine of the developing pollen grains, although it is uncertain whether the satap proteins form a structural component of the pollen wall or are involved in the *in situ* polymerization of exine precursors (Staiger *et al.*, 1994).

Immunocytochemisty experiments revealed that the LIM9 protein accumulates around the microspores while they are encased within callose. In this location, the LIM9 protein might modify wall precursor molecules or cleave them from the carrier molecules that directed them to the microspore. As a protein convertase, the LIM9 protein might activate callase, or enzymes involved in the polymerization of wall precursors. As the callose wall appears to act as a barrier to proteins, the LIM9 protein coating its outer surface likely originates solely within the tapetum. This protein could assist in the elaboration of the exine only after the dissolution of the callose wall. The primexine would thus be constructed with the assistance of LIM9 protein expressed within the microspore. The distribution of this protein on the surface of the microspore plasma membrane might ultimately effect the species-specific patterning of the pollen wall.

Immunoblotting experiments failed to identify the LIM9 protein in pollen extracts. It is therefore unlikely that this protein is a component of the protoplast or an easily extracted component of the germinal apertures or sexine cavities which could be solubilized upon germination. Thus, although the LIM9 protein may be present within mature pollen as an inextractable component of the wall matrix, it does not appear to play a role in incompatibility responses, pollen germination, or the conductance of the pollen tube through the tissues of the style.

IV Future Goals and Prospects of LIM9/TMP Research:

Definitive proof that the LIM9 protein is capable of proteolysis requires that functional assays be performed using an extract free of contaminating proteins. Attempts to purify the LIM9 protein from anther extracts by immunoprecipitation have proved unsuccessful. (As the LIM9 antiserum was raised to a denatured polypeptide, it may not recognize the LIM9 protein in its native state). Work is currently underway to express the entire LIM9 coding region in *E. coli*. This strategy should provide a functional protease, providing that glycosylation is not a prerequisite for the protein's biological activity. If an active protease is obtained, its substrate specificity, optimal pH range, susceptibility to class-specific protease inhibitors, and capacity for self-processing could be assessed. Functional assays could also be designed to determine if the protease is Ca^{2+}-dependent, while cross-linking assays might also be performed to determine if the protease interacts with (and modifies) other anther proteins.

Zymogram experiments with the LIM9 protein suggest that it may incur an additional cleavage to generate a 60kDa polypeptide. Such a protein has not been identified by immunoblotting experiments. The LIM9 antiserum used in this study was generated toward the carboxyl terminus of the recombinant protein. The cleavage (and degradation) of the C-terminus from the LIM9 protein (as occurs in cucumisin) would thus remove most or all of the antigenic determinants (epitopes) recognized by the LIM9 antibody. Work is currently underway to generate an antiserum to the NH_2-terminus of the protein. If this new antiserum identifies an additional LIM9 product, immunocytochemistry experiments should be repeated to determine if this protein is incorporated into the mature pollen or is transported outside of the locule.

Mutagenesis and transgenic technologies offer a means by which the function of genes can be assessed *in vivo*. Unfortunately, due to its large genome and the lack of an appropriate transformation/regeneration system, *Lilium* is not amenable to this sort of study. A tomato cognate to the LIM9 gene (TMP) has, however, been isolated and shown by DNA gel blot hybridization to exist at a single locus within the tomato genome (Riggs and Horsch, 1995). Tomato is amenable to transgenic studies and work is currently underway to generate transgenic tomato plants expressing antisense TMP. The function of the TMP protein could then be inferred cytologically from developmental abnormalties observed within the microspores and anther tissues. (For example, the absence of the TMP protein might result in a thin or malformed pollen exine layer). The evolutionary conservation of the LIM9 and TMP proteins in two distantly related plants (a monocotyledon and a dicotyledon respectively) suggests that these proteins perform a role which is essential to the process of microsporogenesis.

References:

Alberts, B., Bray, D., Lewis, J., Raff, M., Roberts, K., and Watson, J. D. 1994. Molecular biology of the cell, third edition. Garland Publishing, Inc., New York.

Balsamo, R. A., Wang, J. -L., Ekard, K. J., Wang, C. -S., and Lord, E. M. 1995. Immunogold localization of a developmentally regulated, tapetal specific, 15kDa lily anther protein. Protoplasma, **189**: 17-25.

Barr, P. J. 1991. Mammalian subtilisins: the long-sought dibasic processing endoproteases. Cell, **66**: 1-3.

Bathurst, I. C., Brennan, O. S., Carrell, R. W., Cousens, L. S., Brake, A. J., and Barr, P. J. 1987. Yeast KEX2 protease has the properties of a human proalbumin converting enzyme. Science, **235**: 348-350.

Bedinger, P. 1992. The remarkable biology of pollen. Plant Cell, **4**: 879-887.

Bedouelle, H. and Hofnug, M. 1981. *In* Membrane transport and neuroreceptors. *Edited by* D. Oxender. Alan R. Liss Incorporated, New York, pp. 399-403.

Bennett, M. D., Rao, M. K., Smith, J. B., and Bayliss, M. W. 1973. Cell development in the anther, the ovule, and the young seed of *Triticum aestivum* L. *var.* Chinese Spring. Phil. Trans. Roy. Soc. London Ser. B, **226**: 39-81.

Bhandari, N. N. 1984. The microsporangium. *In* Embryology of angiosperms. *Edited by* B. M. Johri. Springer-Verlag, London, pp. 53-121.

Blackmore, S. and Barnes, S. H. 1990. Pollen wall development in angiosperms. *In* Microspores: evolution and ontogeny. *Edited by* S. Blackmore and R. B. Knox. Academic Press, London, pp. 173-192.

Blackmore, S. and Knox, R. B. 1990. Microsporogenesis: the male programme of development. *In* Microspores: development and ontogeny. *Edited by* S. Blackmore and R. B. Knox. Academic Press, New York, pp. 1-10.

Blomstedt, C. K., Knox, R. B., and Singh, M. B. 1996. Generative cells of *Lilium longiflorum* possess translatable mRNA and functional protein synthesis machinery. Plant Mol. Biol., **31**: 1083-1086.

Bold, H. C., Alexopoulos, C. J., and Delevoryas, T. 1987. Morphology of plants and fungi: fifth edition. Harper and Row, Publishers, New York.

Bonner, L. J. and Dickinson, H. G. 1989. Anther dehiscence in *Lycopersicon esculentum* Mill. I. structural aspects. New Phytol., **113**: 97-115.

Brewbaker, J. L. 1967. The distribution and phylogenetic significance of binucleate and trinucleate pollen grains in the angiosperms. Am. J. Bot., **54**: 1069-1083.

Briggs, M. S. and Gierasch, L. M. 1986. Molecular mechanisms of protein secretion: the role of the signal sequence. Advan. Protein Chem., **38**: 109-179.

Chapman, G. P. 1987. The tapetum. Internat. Rev. Cytol., **107**: 111-125.

Chen, J. -S. and Raikhel, A. S. 1996. Subunit cleavage of mosquito pro-vitellogenin by a subtilisin-like convertase. Proc. Nat. Acad. Sci. USA, **93**(12): 6186-6190.

Chrispeels, M. J. and Tague, B. W. 1991. Protein sorting in the secretory system of plant cells. Internat. Rev. Cytol., **125**: 1-45.

Clement, C. and Audran, J. C. 1995. Anther wall layers control sugar nutrition in *Lilium*. Protoplasma, **187**: 172-181.

Clement, C., Burrus, M., and Audran, J. C. 1996. Floral organ growth and carbohydrate content during pollen development in *Lilium*. Am. J. Bot., **83**(4): 459-469.

Clement, C., Chavant, L., Burrus, M., and Audran, J. C. 1994. Anther starch variations in *Lilium* during pollen development. Sex. Plant Reprod., **7**: 347-356.

Darwin, C. 1877. The different forms of flowers on plants of the same species. John Murray, London.

Davis, G. L. 1966. Systematic embryology of the angiosperms. John Wiley & Sons, New York.

Denault, J. B. and Leduc, R. 1996. Furin/PACE/SPC1: A convertase involved in exocytic and endocytic processing of precursor proteins. FEBS Letters, **379**(2): 113-116.

Dickinson, H. G. 1987. The physiology and biochemistry of meiosis in the anther. Int. Rev. Cytol., **107**: 79-109.

Driouich, A., Gonnet, P., Makkie, M., Laine, A., and Faye, L. 1989. The role of high-mannose and complex asparagine-linked glycans in the secretion and stability of glycoproteins. Planta, **180**: 96-104.

Elbein, A. D. 1988. Glycoprotein processing and glycoprotein processing inhibitors. Plant Physiol., **87**: 291-295.

Esau, K. 1977. Anatomy of seed plants. John Wiley & Sons, New York.

Faye, L. and Chrispeels, M. J. 1987. Transport and processing of the glycosylated precursor of concanavalin A in jack-bean. Planta, **170**: 217-224.

Fersht, A. 1985. Enzyme structure and mechanism: second edition. W. H. Freeman and Company, New York.

Finkelstein, A. V., Bendzko, P., and Rapoport, T. A. 1983. Recognition of signal sequences. FEBS Lett., **161**: 176-179.

Frankis, R. C. and Mascarenhas, J. P. 1980. Messenger RNA in the ungerminated pollen grain: a direct demonstration of its presence. Ann. Bot., **45**: 595-599.

Fuller, R. S., Brake, A., and Thorner, J. 1989a. Intracellular targeting and structural conservation of a prohormone-processing endopeptide. Science, **246**: 482-486.

Fuller, R. S., Brake, A., and Thorner, J. 1989b. Yeast prohormone processing enzyme (KEX2 gene product) is a Ca^{2+}-dependent serine protease. Proc. Nat. Acad. Sci. USA, **86**: 1434-1438.

Gibson, R., Kornfeld, S., and Schlesinger, S. 1981. The effect of oligosaccharide chains of different sizes on the maturation and physical properties of vesicular stomatitis virus. J. Biol. Chem., **256**: 456-462.

Gleeson, P. A. and Clarke, A. E. 1980. Antigenic determinants of a plant proteoglycan, the Gladiolus style arabinogalactan-protein. Biochem. J., **191**: 437-447.

Goldberg, R. B. 1988. Plants: novel developmental processes. Science, **240**: 1460-1467.

Goldberg, R. B., Beals, T. P., and Sanders, P. M. 1993. Anther development: basic principles and practical applications. Plant Cell, **5**: 1217-1229.

Graybosch R. A. and Palmer, R. G. 1988. Male sterility in soybean: an overview. Am. J. Bot., **75**: 144-156.

Greyson, R. I. 1994. The development of flowers. Oxford University Press. Oxford.

Hanson, D. D., Hamilton, D. A., Travis, J. L., Bashe, D. M., and Mascarenhas, J. P. 1989. Characterization of a pollen-specific cDNA from *Zeas mays* and its expression. Plant Cell, **1**: 173-179.

Harris, N. 1986. Organization of the endomembrane system. Ann. Rev. Plant Physiol., **37**: 73-92.

Hasenkampf, C., Qureshi, M., Horsch, A., and Riggs, C. D. 1992. Temporal and spatial distribution of meiotin-1 in anthers of *Lilium longiflorum*. Dev. Gen., **13**: 425-434.

Herich, R. and Lux, A. 1984. Electron microscope study of tapetal cell nuclei degradation of *Lilium henryi*. Physiol. Plant, **20**: 1-5.

Hermodson, M. A., Ericsson, L. H., Neurath, H., and Walsh, K. A. 1973. Determination of the amino acid sequence of porcine trypsin by sequenator analysis. Biochem., **12**(17): 3146-3153.

Heslop-Harrison, J. 1966a. Cytoplasmic continuities during spore formation in flowering plants. Endeavor, **25**: 65-72.

Heslop-Harrison, J. 1966b. Cytoplasmic connections between angiosperm meiocytes. Ann. Bot., **30**: 221-230.

Heslop-Harrison, J. 1968. Tapetal origin of pollen-coat substances in *Lilium*. New Phytol., **67**: 779-786.

Heslop-Harrison, J. 1971. The pollen wall: structure and development. *In* Pollen: development and physiology. *Edited by* J. Heslop-Harrison. Butterworth, London, pp. 75-98.

Heslop-Harrison, J. 1980. Compartmentation in anther development and pollen wall morphogenesis. *In* Cell compartmentation and metabolic channelling.

Edited by L. Nover, F. Lynen, and K. Mothes. Elsevier/North/Holland Biomedical Press., New York, pp 471-493.

Heslop-Harrison, J. 1987. Pollen germination and pollen-tube growth. *In* Pollen: cytology and development. *Edited by* K. L. Giles and J. Prakash. Int. Rev. Cytol., **107**: 1-78.

Heslop-Harrison, J., Knox, R. B., and Heslop-Harrison, Y. 1974. Pollen wall proteins: exine-held fraction associated with the incompatibility response in *Cruciferae*. Theoret. Appl. Genet., **44**: 133-137.

Hird, D. L., Worrall, D., Hodge, R., Smartt, S., Paul, W., and Scott, R. 1993. The anther-specific protein encoded by the *Brassica napus* and *Arabidopsis thaliana* A6 gene displays similarity to β-1,3-glucanases. Plant J., **4**(6): 1023-1033.

Horvitz, H. R. and Herskowitz, I. 1992. Mechanisms of asymmetric cell division: two Bs or not two Bs, that is the question. Cell, **68**: 237-255.

Ikemura, H. and Inouye, M. 1988. *In vitro* processing of pro-subtilisin produced in *Escherichia coli*. J. Biol. Chem., **263**(26): 12959-12963.

Ikemura, H., Takagi, H., and Inouye, M. 1987. Requirement of pro-sequence for the production of active subtilisin E in *Escherichia coli*. J. Biol. Chem., **262**(16): 7859-7864.

Ito, M. and Takegami, M. H. 1982. Commitment of mitotic cells to meiosis during the G_2 phase of premeiosis. Plant & Cell Physiol., **23**(6): 943-952.

Izhar, S. and Frankel, R. 1971. Mechanism of male sterility in *Petunia*: the relationship between pH, callase activity in the anthers, and the breakdown of microsporogenesis. Theor. App. Genet., **41**: 104-108.

Jensen, W. A. 1973. Fertilization in flowering plants. BioScience, **23**(1): 21-27.

Jones, R. L., Bush, D. S., Sticher, L., Simon, P., and Jacobsen, J. V. 1987. Intracellular transport and secretion of barley aleurone α-amylase. *In* Plant membranes: structure, function, biogenesis. *Edited by* Leaver, C. and Sze, H. Liss, New York, pp. 325-340.

Jones, R. L. and Robinson, D. G. 1989. Transley review no. 17: protein secretion in plants. New Phytol., **111**: 567-597.

Joshi, L. 1995. Cloning of a cuticle-degrading protease from the entomopathogenic fungus, *Beauveria bassiana*. FEMS Microbiol. Lett., **125**: 211-218.

Julius, D., Brake, A., Blair, L., Kunisawa, R., and Thorner, J. 1984. Isolation of the putative structural gene for the lysine-arginine-cleaving endopeptidase required for processing of yeast prepro-α-factor. Cell, **37**: 1075-1089.

Kamalay, J. C. and Goldberg, R. B. 1980. Regulation of structural gene expression in tobacco. Cell, **19**: 935-946.

Kamalay, J. C. and Goldberg, R. B. 1984. Organ-specific nuclear RNAs in tobacco. Proc. Nat. Acad. Sci. USA, **81**: 2801-2805.

Kaneda, M., Sobue, A., and Tominaga, N. 1986. Isolation and characterization of proteinases from the sarcocarp of snake gourd (*Trichosanthes cucumeroides*) fruit. J. Biochem., **99**(2): 569-578.

Kaneda, M. and Tominaga, N. 1975. Isolation and characterization of a protease from the sarcocarp of melon fruit. J. Biochem., **78**: 1287-1296.

Kaneda, M. and Tominaga, N. 1977. Isolation and characterization of a proteinase from white gourd. Phytochem., **16**: 345-346.

Kaneda, M., Yonezawa, H., and Uchikoba, T. 1995. Improved isolation, stability and substrate specificity of cucumisin, a plant serine protease. Biotechnol. Appl. Biochem., **22**: 215-222.

Kaul, M. L. K. 1988. Male sterility in higher plants. *In* Monographs on theoretical and applied genetics, Vol. 10. *Edited by* R. Frankel, M. Grossman, H. Linskens, P. Maliga, and R. Ripley. Springer Verlag, Berlin. pp. 15-95.

Keijzer, C. J. 1987a. The process of anther dehiscence and pollen dispersal. I. the opening mechanism of longitudinally dehiscing anthers. New Phytol., **105**: 487-498.

Keijzer, C. J. 1987b. The process of anther dehiscence and pollen dispersal. II. the formation and the transfer mechanism of pollenkitt, cell-wall development of the loculus tissues and a function of orbicules in pollen dispersal. New Phytol., **105**: 499-507.

Knox, R. B. 1984. The pollen grain. *In* Embryology of angiosperms. *Edited by* B. M. Johri. Springer-Verlag, New York, pp. 197-271.

Knox, R. B. and Heslop-Harrison, J. 1970. Pollen wall proteins: localization and enzymatic activity. J. Cell Sci., 6: 1-27.

Kobayashi, T. and Inouye, M. 1992. Functional analysis of the intramolecular chaperone: mutational hot spots in the subtilisin pro-peptide and a second-site suppressor mutation within the subtilisin molecule. J. Mol. Biol., **226**: 931-933.

Kobayashi, T., Kobayashi, E., Sato, S., Hotta, Y., Miyajima, N., Tanaka, A., and Tabata, S. 1994. Characterization of cDNAs induced in meiotic prophase in lily microsporocytes. DNA Res., **1**: 15-26.

Koltunow, A. M., Truettner, J., Cox, K. H., Wallroth, M., and Goldberg, R. B. 1990. Different temporal and spatial gene expression patterns occur during anther development. Plant Cell, **2**: 1201-1224.

Kornfeld, R. and Kornfeld, S. 1985. Assembly of asparagine-linked oligosaccharides. Ann. Rev. Biochem., **54**: 631-664.

Laemmli, U. K. 1970. Cleavage of structural proteins during the assembly of the head of bacteriophage T4. Nature, **227**: 680-685.

Larson, A., Lewis, C. W. 1962. Pollen wall development in *Parkinsonia aculeata*. Grana Palynol., **3**: 21-27.

Lauriere, M., Lauriere, C., Chrispeels, M. J., Johnson, K. D., and Sturm, A. 1989. Characterization of a xylose-specific antiserum that reacts with the complex asparagine-linked glycans of extracellular and vacuolar glycoproteins. Plant Physiol., **90**: 1182-1188.

Lerner, C. G., Kobayashi, T., and Inouye, M. 1990. Isolation of subtilisin pro-sequence mutations that affect formation of active protease by localized random polymerase chain reaction mutagenesis. J. Biol. Chem., **265**(33): 20085-20086.

Lodish, H. F. 1988. Transport of secretory and membrane glycoproteins from the rough endoplasmic reticulum to the Golgi. J. Biol. Chem., **263**(5): 2107-2110.

Lowry, O. H., Rosebrough, N. J., Farr, A. L., and Randall, R. J. 1951. Protein measurement with the folin phenol reagent. J. Biol. Chem., **193**: 265-275.

Mackenzie, A., Heslop-Harrison, J., and Dickinson, H. G. 1967. Elimination of ribosomes during meiotic prophase. Nature, **215**: 997-999.

Maheshwari, P. 1950. An introduction to the angiosperms. McGraw-Hill, New York.

Mariani, C., DeBeuckeleer, M., Truettner, J., Leemans, J., and Goldberg, R. B. 1990. Induction of male sterility in plants by a chimaeric ribonuclease gene. Nature, **347**: 737-741.

Marshall, R. D. 1972. Glycoproteins. Ann. Rev. Biochem., **41**: 673-702.

Mascarenhas, J. P. 1975. The biochemistry of angiosperm pollen development. Bot. Rev., **41**(3): 259-314.

Mascarenhas, J. P. 1989. The male gametophyte of flowering plants. Plant Cell, **1**: 657-664.

Mascarenhas, J. P. 1990a. Gene activity during pollen development. Ann. Rev. Plant Physiol. Plant Mol. Biol., **41**: 317-338.

Mascarenhas, J. P. 1990b. Gene expression in the angiosperm male gametophyte. *In* Microspores: development and ontogeny. *Edited by* S. Blackmore and R. B. Knox. Academic Press, London, pp. 267-280.

McCormick, S. 1991. Molecular analysis of male gametogenesis in plants. Trends Genet., **7**(9): 298-303.

McCormick, S. 1993. Male gametophyte development. Plant Cell, **5**: 1265-1275.

Michaud, D., Faye, L., and Yelle, S. 1993. Electrophoretic analysis of plant cysteine and serine proteinases using gelatin-containing polyacrylamide gels and class specific proteinase inhibitors. Electrophoresis, **14**: 94-98.

Miranda, L., Wolf, J., Pichuantes, S., Duke, R., and Franzusoff, A. 1996. Isolation of the human PC6 gene encoding the putative host protease for HIV-1 gp160 processing in CD4+ T lymphocytes. Proc. Nat. Acad. Sci. USA, **93**(15): 7695-7700.

Mizuno, K., Nakamura, T., Oshima, T., Tanaka, S., and Matsuo, H. 1988. Yeast KEX2 gene encodes an endopeptidase homologous to subtilisin-like serine proteases. Biochem. Biophys. Res. Commun., **156**: 264-254.

Mulcahy, D. L. and Mulcahy, G. B. 1987. The effects of pollen competition. Am. Scientist, **75**: 44-50.

Nacken, W. K. F., Huijzer, P., Beltram, N. -P., Saedler, H., and Sommer, H. 1991. Molecular characterization of two stamen-specific genes, tap1 and fil1, that are expressed in the wild type but not in the *deficiens* mutant of *Antirrhinum majus*. Mol. Gen. Genet., **229**: 129-136.

Nasrallah, J. B. and Nasrallah, M. E. 1993. Pollen-stigma signalling in the sporophytic self-incompatibility response. Plant Cell, **5**: 1325-1335.

Newbigin, E., Anderson, M. A., and Clarke, A. E. 1993. Gametophytic self-incompatibility systems. Plant Cell, **5**: 1315-1324.

Ohta, Y., Hojo, H., Aimoto, S., Kobayashi, T., Zhu, X., Jordan, F., and Inouye, M. 1991. Pro-peptide as an intramolecular chaperone: renaturation of denatured subtilisin E with a synthetic pro-peptide. Mol. Microbiol., **5**: 1507-1510.

Olden, K., Parent, J. B., and White, S. L. 1982. Carbohydrate moieties of glycoproteins. a re-evaluation of their function. Biochim. Biophysic. Acta, **650**: 209-232.

Pacini, E. 1990. Tapetum and microspore function. *In* Microspores: ontogeny and development. *Edited by* S. Blackmore and R. B. Knox. Academic Press, London, pp. 213-237.

Pacini, E. and Franchi, G. G. 1983. Pollen grain development in *Smilax aspersa* L. and possible functions of the loculus. *In* Pollen: biology and implications for plant breeding. *Edited by* D. L. Mulcahy and E. Ottavino. Elsevier, New York, pp. 183-190.

Pandey, K. K. 1958. Time of S-allele action. Nature, **181**: 1220-1221.

Peddada, L. and Mascarenhas, J. P. 1975. 5S ribosomal RNA synthesis during pollen development. Dev. Growth. Diff., **17**: 1-8.

Polgar, L. 1989. Mechanisms of protease action. CRC Press, Boca Raton, Florida.

Polowick, P. L., and Sawhney, V. K. 1992. Ultrastructural changes in the cell wall, nucleus and cytoplasm of pollen mother cells during meiotic prophase I in *Lycopersicon esculentum* (Mill.). Protoplasma, **169**: 139-147.

Polowick, P. L. and Sawhney, V. K. 1993. Differentiation of the tapetum during microsporogenesis in tomato (*Lycopersicon esculentum* Mill.), with special reference to the tapetal cell wall. Ann. Bot., **72**: 595-605.

Power, S. D., Adams, R. M., and Wells, J. A. 1986. Secretion and autoproteolytic maturation of subtilisin. Proc. Nat. Acad. Sci. USA, **83**: 3096-3100.

Raghavan, V. 1988. Anther and pollen development in rice (*Oryza sativa*). Amer. J. Bot., **75**(2): 183-196.

Rapoport, T. A. 1991. Protein transport across the endoplasmic reticulum membrane: facts, models, mysteries. FASEB J., **5**: 2792-2798.

Raven, P. H., Evert, R. F., and Eichorn, S. E. 1986. Biology of Plants. Worth, New York.

Raven, J. A. and Smith F. A., 1976. Nitrogen assimilation and transport in vascular land plants in relation to intracellular pH regulation. New Phytol., **76**: 415-431.

Reznickova, S. A. and Dickinson, H. G. 1982. Ultrastructural aspects of storage lipid mobilization in the tapetum of *Lilium hybrida* var. enchantment. Planta, **155**: 400-408.

Ribeiro, A., Akkermans, A. D. L., van Kammen, A., Bisseling, T., and Pawlowski, K. 1995. A nodule-specific gene encoding a subtilisin-like protease is expressed in early stages of actinorhizal nodule development. Plant Cell, **7**: 785-794.

Riggs, C. D. 1994. Purification and characterization of histone H1 from meiotic cells of a monocotyledonous plant, *Lilium longiflorum*. Genome, **37**(5): 736-741.

Riggs, C. D. and Horsch, A. P. 1995. Molecular cloning of an anther specific gene from tomato. Plant Physiol [Suppl.], **108**: 117.

Roberts, M. R., Foster, G. D., Blundell, R. P., Robinson, S. W., Kumar, A., Draper, J., and Scott, R. 1993. Gametophytic and sporophytic expression of an anther specific *Arabidopsis thaliana* gene. Plant J., **3**(1): 111-120.

Robertus, J. D., Kraut, J., Alden, R. A., and Birktoft, J. 1972. Subtilisin; a stereochemical mechanism involving transition-state stabilization. Biochem., **11**(23): 4293-4303.

Roebroek, A. J. M., Pauli, I. G. L., Zhang, Y., and van de Ven, W. J. M. 1991. cDNA sequence of a *Drosophila melanogaster* gene, D*fur*1, encoding a protein

structurally related to the subtilisin-like proprotein processing enzyme furin. FEBS, **289**(2): 133-137.

Rouille, Y., Martin, S., and Steiner, D. F. 1995. Differential processing of proglucagon by the subtilisin-like prohormone convertases PC2 and PC3 to generate either glucagon or a glucagon-like peptide. J. Biol. Chem., **270**(44): 26488-26496.

Rowley, J. R. 1973. Formation of pollen exine bacules and microchannels on a glycocalyx. Grana, **13**: 129-138.

Rowley, J. R. 1993. Cycle of hyperactivity in tapetal cells. Plant Syst. Evol. [Suppl.], **7**: 23-37.

Satina, S. and Blakeslee, A. F. 1941. Periclinal chimeras in *Datura stramonium* in relation to the development of leaf and flower. Am. J. Bot., **28**: 862-871.

Satina, S., Blakeslee, A. F., and Avery, A. G. 1940. Demonstration of the three germ layers in the shoot apex of *Datura* by means of induced polyploidy in periclinal chimeras. Am. J. Bot., **44**: 311-317.

Schrauwen, J. A., Mettenmeyer, T., Croes, A. F., and Wullems, G. J. 1996. Tapetum-specific genes: what role do they play in male gametophyte development? Acta. Bot. Neerl., **45**(1): 1-15.

Scott, R. 1993. Anther development: a molecular perspective. *In* The molecular biology of flowering. CAB International, Wallingford, U. K., pp. 141-184.

Scott, R., Hodge, R., Paul, W., and Draper, J. 1991. The molecular biology of anther differentiation. Plant Science, **80**: 167-191.

Shaw, G. 1971. The chemistry of sporopollenin. *In* Sporopollenin. *Edited by* J. Grant, P. R. Muir, M. Gijzel, P. Van, and G. Shaw. Academic Press, London, pp. 305-350.

Sheffield, E., Cawood, A., Bell, P. R., and Dickinson, H. G. 1979. The development of nuclear vacuoles during meiosis in plants. Planta, **146**: 597-601

Siezen, R. J. 1996. Modelling and engineering of enzyme/substrate interactions in subtilisin-like enzymes of unknown 3-dimensional structure. *In* Subtilisin enzymes, practical protein engineering. *Edited by* R. Bott and C. Betzel. Plenum Press, New York/London, pp. 63-93.

Siezen, R. J., de Vos, W. M., Leunissen, J. A. M., and Dijkstra, B. W. 1991. Homology modelling and protein engineering strategy of subtilases, the family of subtilisin-like serine proteases. Protein Eng., **4**(7): 719-737.

Simon, S. M. and Blobel, G. 1991. A protein-conducting channel in the endoplasmic reticulum. Cell, **65**: 371-380.

Smith, A. G., Gasser, C. S., Budelier, K. A., and Fraley, R. T. 1990. Identification and characterization of stamen- and anther-specific genes from tomato. Mol. Gen. Genet., **222**: 9-16.

Spitzer, N. C. 1970. Low resistance connections between cells in the developing anther of the Lily. J. Cell Biol., **45**: 565-575.

Staiger, D. and Apel, K. 1993. Molecular characterization of two cDNAs from *Sinapis alba* L. expressed specifically at an early stage of tapetum development. Plant J., **4**(4): 697-703.

Staiger, D., Krappeler, S., Muller, M., and Apel, K. 1994. The proteins encoded by the two tapetum-specific transcripts Satap35 and Satap44, from *Sinapis alba* L., are localized in the exine cell wall layer of developing microspores. Planta, **192**: 221-231.

Steiglitz, H. 1977. Role of β-1,3-glucanase in postmeiotic microspore release. Dev. Biol., **57**: 87-97.

Steiglitz, H. and Stern, H. 1973. Regulation of β(1,3)-glucanase activity in developing anthers of *Lilium*. Dev. Biol., **34**: 169-173.

Steiner, D. F., Smeekens, S. P., Ohagi, S., and Chan, S. J. 1992. The new enzymology of precursor processing endoproteases. J. Biol. Chem., **267**(33): 23435-23438.

Stern, H. and Hotta, Y. 1967. Chromosome behavior during development of meiotic tissue. *In* The control of nuclear activity. *Edited by* L. Golstein. Prentice Hall, Inc., Englewood Cliffs, New Jersey, pp. 47-76.

Stinson, J. R., Eisenberg, A. J., Willing, R. P., Pe, M. E., Hanson, D. D., and Mascarenhas, J. P. 1987. Genes expressed in the male gametophyte of flowering plants and their isolation. Plant Physiol., **83**: 442-447.

St. Leger, R. J. 1995. The role of cuticle-degrading proteases in fungal pathogenesis of insects. Can. J. Bot. [Suppl.], **73**: S1119-S1125.

Sussex, I. M. 1989. Developmental programming of the shoot meristem. Cell, **56**: 225-229.

Takegami, M. H., Yoshioka, M., Tanaka, I., and Ito, M. 1981. Characteristics of isolated microsporocytes from liliaceous plants for studies of the meiotic cell cycle *in vitro*. Plant Cell Physiol., **22**: 1-10.

Tanksley, S. D., Zamir, D., and Rick, C. M. 1981. Evidence for extensive overlap of sporophytic and gametophytic gene expression in *Lycopersicon esculentum*. Science, **213**: 453-455.

Tarentino, A. L., Plummer, T. H. and Maley, F. 1974. The release of intact oligosaccharides from specific glycoproteins by Endo-β-N-acetyl-glucosaminidase H. J. Biol. Chem., **249**(3): 818-824.

Taylor, J. H. and McMaster, R. 1954. Autoradiographic and microphotometric studies of deoxyribose nucleic acid during microgametogenesis in *Lilium longiflorum*. Chromosoma, **6**: 489-521.

Thacker, C., Peters, K., Srako, M., and Rose, A. M. 1995. The bli-4 locus of *Caenorhabditis elegans* encodes structurally distinct KEX2/subtilisin-like endoproteases essential for early development and adult morphology. Genes Dev., **9**(8): 956-971.

Thim, L., Hansen, M. T., Norris, K., Hoegh, I., Boel, E., Forstrom, J., Ammerer, G., and Fiil, N. P. 1986. Secretion and processing of insulin precursors in yeast. Proc. Nat. Acad. Sci. USA, **83**: 6766-6770.

Tornero, P., Conejero, V., and Vera, P. 1996. Primary structure and expression of a pathogen-induced protease (PR-P69) in tomato plants: similarity of functional domains to subtilisin-like endoproteases. Proc. Nat. Acad. Sci. USA, **93**(13): 6332-6337.

Tsaftari, A. S., Sorenson, J. C., and Scandalios, J. C. 1980. Glycosylation of catalase inhibitor is necessary for activity. Biochem. Biophys. Res., Commun., **92**: 889-895.

Tupy, J., Suss, J., Hrabetova, E., and Rihova, L. 1983. Developmental changes in gene expresion during pollen differentiation and maturation in *Nicotiana tobacum* L. Biologia Plantarum, **25**: 231-237.

Twell, D. 1992. Use of a nuclear-targeted β-glucuronidase fusion protein to demonstrate vegetative cell-specific gene expression in developing pollen. Plant J., **2**(6): 887-892.

Ursin, V. M., Yamaguchi, J., and McCormick, S. 1989. Gametophytic and sporophytic expression of anther-specific genes in developing tomato anthers. Plant Cell, **1**: 727-736.

Vera, P. and Conejero, V. 1988. Pathogenesis-related proteins of tomato. Plant Physiol., **87**: 58-63.

Vera, P. and Conejero, V. 1990. Effect of ethephon on protein degradation and the accumulation of 'pathogenesis-related' (PR) proteins in tomato leaf discs. Plant Physiol., **92**: 227-233.

Vera, P., Hernandez, J., and Conejero, V. 1989. Immunogold localization of the citrus exocortis viroid-induced pathogenesis-related proteinase P69 in tomato leaves. Plant Physiol., **91**: 119-123.

Vey, M. 1995. Proteolytic processing of human cytomegalo virus glycoprotein B (gpUL55) is mediated by the human endoprotease furin. Virology, **206**(1): 746-749.

Vitale, A., Warner, T. G., and Chrispeels, M. J. 1984. *Phaseolus vulgaris* phytohemagglutinin contains high-mannose and modified oligosaccharide chains. Planta, **160**: 256-263.

Vollenweider, F., Benjamet, S., Decroly, E., Savaria, D., Lazure, C., Thomas, G., Chretien, M., and Seidah, N. G. 1996. Comparative cellular processing of the human immunodeficiency virus (HIV-1) envelope glycoprotein gp160 by the mammalian subtilisin/Kexin-like convertases. Biochem. J., **314**(2): 521-532.

von Heijne, G. 1986. A new method for predicting signal sequence cleavage sites. Nucleic Acids Res., **14**(11): 4683-4690.

Wagner, V. T., Cresti, M., Salvatici, P., and Tiezzi, A. 1990. Changes in volume, surface area, and frequency of nuclear pores on the vegetative nucleus of tobacco pollen in fresh, hydrated, and activated conditions. Planta, **181**: 304-309.

Walker, J. W. 1974. Aperture evolution in the pollen of primitive angiosperms. Am. J. Bot., **61**: 1112-1137.

Walsh, K. A. and Wilcox, P. E. 1970. Serine proteases. Methods Enzymol., **19**: 31-41.

Walter, P. and Lingappa, V. R. 1986. Mechanism of protein translocation across the endoplasmic reticulum membrane. Ann. Rev. Cell Biol., **2**: 499-516.

Wang, C. -S., Walling, L. L., Eckard, K. J., and Lord, E. M. 1992a. Patterns of protein accumulation in developing anthers of *Lilium longiflorum* correlate with histological events. Am. J. Bot., **79**(2): 118-127.

Wang, C. -S., Walling, L. L., Eckard, K. J., and Lord, E. M. 1992b. Immunological characterization of a tapetal protein in developing anthers of *Lilium longiflorum*. Plant Physiol., **99**: 822-829.

Weberling, F. 1989. Morphology of Flowers and Inflorescences. Cambridge University Press, Cambridge, U. K.

Wells, J. A., Ferrari, E., Henner, D., Estell, D. A., and Chen, E. Y. 1983. Cloning, sequencing, and secretion of *Bacillus amyloliquefaciens* subtilisin in *Bacillus subtilis*. Nucleic Acids Res., **22**(11): 7911-7925.

White, P. R. 1963. The cultivation of animal and plant cells, second edition. Ronald Press, New York.

Whitehouse, H. L. K. 1951. Multiple-allelomorph incompatibility of pollen and style in the evolution of the angiosperms. Ann. Bot. New Series, **14**: 198-216.

Willing, R. P. and Mascarenhas, J. P. 1984. Analysis of the complexity and diversity of mRNAs from pollen and shoots of *Tradescantia*. Plant Physiol., **75**: 865-868.

Wise, R. J., Barr, P. J., Wong, P. A., Kiefer, M. C., Brake, A. J., and Kaufman, R. J. 1990. Expression of a human proprotein processing enzyme: correct cleavage of the von Willebrand factor precursor at a paired basic amino acid site. Proc. Natl. Acad. Sci. USA, **87**: 9378-9382.

Worral, D., Hird, D., Hodge, R., Wyatt, P., Draper, J., and Scott, R. 1992. Premature dissolution of the microsporocyte callose wall causes male sterility in transgenic tobacco. Plant Cell, **4**: 759-771.

Wright, C. S., Alden, R. A., and Kraut, J. 1969. Structure of subtilisin BPN' at 2.5 A resolution. Nature, **221**: 235-242.

Yamagata, H., Masuzawa, T., Nagaoka, Y., Ohnishi, T., and Iwasaki, T. 1994. Cucumisin, a serine protease from melon fruits, shares structural homology with subtilisin and is generated from a large precursor. J. Biol. Chem., **269**(52): 32725-32731.

Yamagata, H., Ueno, S., and Iwasaki, T. 1989. Isolation and characterization of a possible native cucumisin from developing melon fruits and its limited autolysis to cucumisin. Agric. Biol. Chem., **53**(4): 1009-1017.

Yang, J. and Kramer, J. M. 1994. *In vitro* mutagenesis of *Caenorhabditis elegans* cuticle collagens identifies a potential subtilisin-like protease cleavage site and demonstrates that carboxyl domain disulfide bonding is required for normal function but not assembly. Mol. Cell Biol., **14**: 2722-2730.

Zang, G., Gifford, D. J., and Cass, D. D. 1993. RNA and protein synthesis in sperm cells isolated from *Zea mays* L. pollen. Sex. Plant Reprod., **6**: 239-243.

Zhu, X., Ohta, Y., Jordan, F., and Inouye, M. 1989. Pro-sequence of subtilisin can guide the refolding of denatured subtilisin in an intermolecular process. Nature, **339**: 483-484.

IMAGE EVALUATION
TEST TARGET (QA-3)

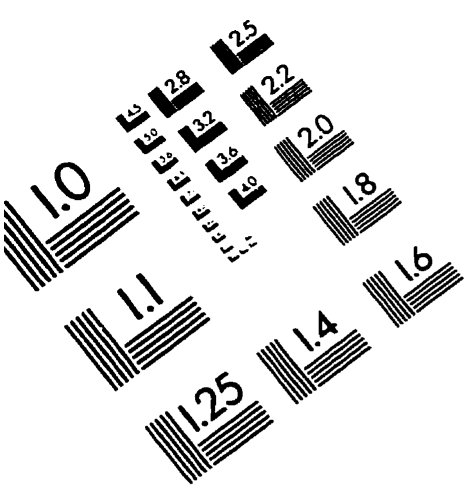

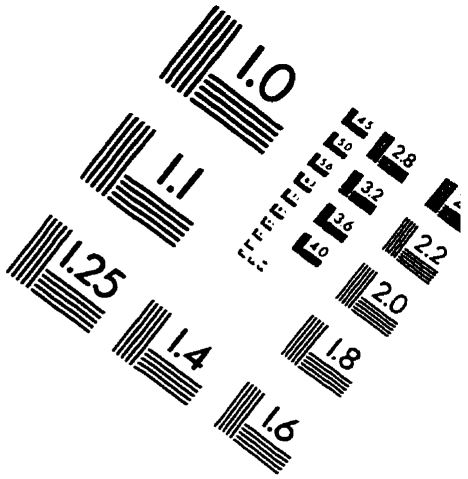

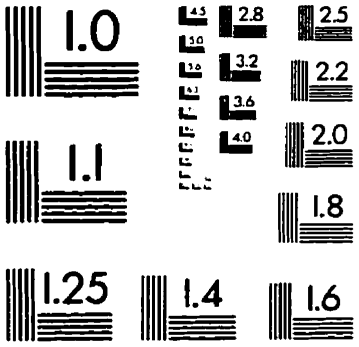

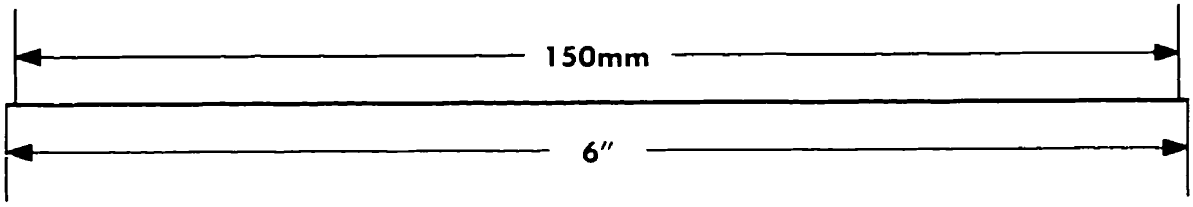

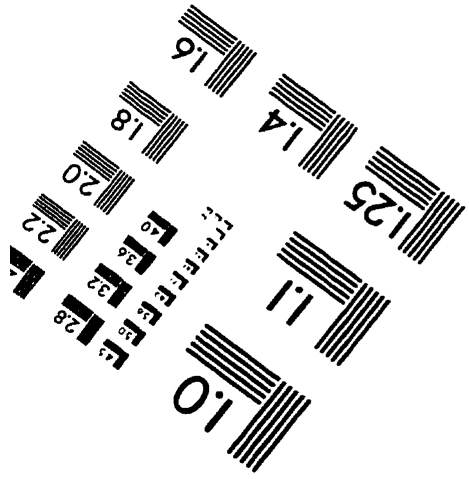

APPLIED IMAGE, Inc
1653 East Main Street
Rochester, NY 14609 USA
Phone: 716/482-0300
Fax: 716/288-5989

© 1993, Applied Image, Inc., All Rights Reserved